New perspectives on solitons and instantons in the Standard Model and beyond

Thomas Steingasser

München 2022

New perspectives on solitons and instantons in the Standard Model and beyond

Thomas Steingasser

Dissertation
an der
der Ludwig–Maximilians–Universität
München

vorgelegt von
Thomas Steingasser
aus Neuburg a.d. Donau

München, den 01.04.2022

Erstgutachter: Prof. Dr. Stefan J. Hofmann
Zweitgutachter: Prof. Dr. Justin Khoury
Tag der mündlichen Prüfung: 07.06.2022

Contents

List of Figures

Zusammenfassung

In der ersten Hälfte dieser Arbeit entwickle ich eine neuartige Perspektive auf die Dynamik topologischer Solitone. Die Grundlage dieser Betrachtungsweise ist eine neue Art von Feldern, die eine größtenteils von den Eigenschaften der zugrundeliegenden Theorie unabhängige Parametrisierung gewisser Anregungen beliebiger Solitone ermöglichen. Durch deren Eigenschaften ist es möglich universelle Wirkungen zu konstruieren, in denen sich verschiedene Theorien und Solitone ausschließlich über eine endliche Anzahl von Hintergrundfunktionen manifestieren.

Diese Beschreibung lässt sich durch eine Verallgemeinerung der kollektiven Koordinaten des Solitons konstruieren. Hieraus lässt sich ebenfalls eine physikalische Interpretation der involvierten Felder ableiten, die ich ausführlich darlege. Dieser Diskussion folgt eine detaillierte Analyse ihrer klassischen Dynamik in einer räumlichen Dimension, insbesondere im Hinblick auf die genannte Interpretation. Ein besonderer Fokus liegt hierbei auf der Frage der Anwendbarkeit der Beschreibung, für die sich ebenfalls eine klare physikalische Interpretation finden lässt. Anschließend erläutere ich die Verallgemeinerung des Formalismus auf Theorien in beliebig vielen räumlichen Dimensionen und veranschauliche sie an besonders instruktiven Beispielen. Anhand dieser untersuche ich auch den Zusammenhang zwischen der neuen Parametrisierung mit einer möglichen Eichinvarianz der zugrundeliegenden Theorie. Dieser erste Teil wird abgerundet von einem Überblick über die Grundlagen der Quantisierung der Theorie in diesem Rahmen.

Der zweite Teil dieser Arbeit befasst sich mit Instantonen und dem Zerfall des elektroschwachen Vakuums. Die Grundlage meiner Arbeit zu diesem Thema bildet eine ausführliche Analyse des Zusammenspiels der Skalenabhängigkeit der Higgs-Kopplung durch ihren Renormalierungsgruppenfluss mit Korrekturen des Higgs-Potentials durch Physik jenseits des Standardmodells. Das Ergebnis ist eine einfache Relation für die Renormierungs-Skala des Tunnelprozesses und die damit zusammenhängende Größe des Instantons. Diese ist essentiell für eine verlässliche Berechnung der Zerfallsrate des Vakuums, und damit auch seiner Lebenszeit, im Standardmodell und typischen Erweiterungen. Zur Veranschaulichung präsentiere ich die zur Zeit genausten und aktuellsten Werte für die Lebenszeit im Standardmodell sowie seiner Erweiterung um die minimalen Realisierungen von Neutrinomassen und der Idee des Higgs als Pseudo-Nambu-Goldstone-Boson eines stark gekoppelten Technifermionenkondensats. Sowohl die genauen Werte für die Lebenszeiten und deren

Abhängigkeit von den Parametern der Erweiterungen als auch das präzise Verständnis der Skalenabhängigkeit bilden die Grundlage für das nächste Ergebnis, nämlich einen bisher unbekannten Zusammenhang zwischen der Metastabilität des elektroschwachen Vakuums mit der unnatürlichen Kleinheit der Higgsmasse, die sich im sogenannten Hierarchieproblem manifestiert. Ich lege dar dass beide Eigenschaften nicht unabhängig voneinander sind, da Metastabilität eine Higgsmasse mehrere Größenordnungen kleiner als ihren natürlichen Wert voraussetzt. Ich zeige dies zunächst durch einige analytische Abschätzungen, die eine obere Schranke an die Higgs-Masse als Funktion der Lebenszeit des Vakuums liefern. Diese Relation gilt sowohl im Standardmodell als auch in allen generischen Erweiterungen, was ich anhand der bereits etablierten Beispiele numerisch veranschauliche. Den Abschluss dieser Arbeit bildet ein Ausblick auf eine potentielle Vertiefung dieses Ergebnisses.

Introduction

One of the most remarkable properties of the laws of nature is that they manifest in vastly different forms at different scales. At the largest scales, the universe appears homogeneous and isotropic, and all familiar structures are entirely negligible. This allows for the description of all matter and energy as a fluid, while spacetime can be characterized by a single function, the scale factor. Meanwhile, at the smallest scales, no classical description of matter is possible, and it can be expected that the same is true for spacetime. While gravity is the dominant interaction at galactic scales, it is entirely negligible in the context of most particle physics. And although electromagnetism is the dominant force at the level of atomic physics, it is easily overtaken at the nuclear level by the weak and strong interactions.

While the dominance of gravity at large scales is easily understood as a consequence of its purely additive properties, the apparent scale dependence of the remaining interactions appears to be a fundamental property of quantum field theory, linked to the *renormalization group* and giving rise to the idea of *effective field theories*, from which the concept of *naturalness* arises.

Although these ideas have proven themselves a powerful tool in the understanding of fundamental physics, they are arguably most significant in situations in which they fail, thus offering a starting point for the development of new physics. One of their most prominent failures is their inability to explain a large number of apparent fine-tunings in the parameters of the universe. This famously includes the hierarchy between the electroweak and the Planck scale, $\frac{v}{M_{\mathrm{Pl}}} \sim 10^{-17}$, but also the matter-antimatter-asymmetry manifesting in the tiny baryon-to-photon-ratio $\frac{n_b}{n_\gamma} \sim 10^{-10}$, the CP problem, $\theta \lesssim 10^{-10}$, the flavor problem, $\frac{m_Q}{m_t} = 10^{-5} - 10^{-2}$ and the smallness of the Hubble constant relative to the Planck mass, $\frac{H_0}{M_{\mathrm{Pl}}} \sim 10^{-63}$. While some of these on the first look unnatural values can be explained by replacing the notion of naturalness by the more general *technical naturalness*, doing so fails to address other apparent fine-tunings of nature, most importantly the metastability of the electroweak vacuum, which is the result of an extremely delicate balancing of several Standard Model couplings and the Hubble constant.

One famous example for which the emergence of a tiny scale is well-understood is the QCD scale Λ_{QCD}, which is discussed in chapter 1. The QCD scale is linked to the strong

coupling becoming non-perturbative due to its RG running. As it depends on the scale only logarithmically, it is clear that for all generic cases there exists a large hierarchy between Λ_{QCD} and the scale at which the value of the QCD coupling is fixed through some high energy mechanism, e.g., the GUT or the Planck scale. This mechanism inspired the idea of *Higgs compositeness*, in which the Higgs is understood as a pseudo-Nambu-Goldstone boson of a fermion condensate that forms as a result of some gauge coupling becoming strong at a scale Λ_f. In the simplest such models, generic parameters of the UV theory lead to a value of the Higgs mass and vacuum expectation value of roughly the same order as Λ_f, but far below the Planck scale. The absence of any signs of compositeness in experiments can therefore, in the simplest composite models, only be explained through yet another fine-tuning in the UV theory. This problem is, however, not specific to these models, as something similar happens, e.g., for supersymmetry.

The first main result at the center of this thesis bears the potential to explain this remaining hierarchy for a wide class of Standard Model extensions, in particular Higgs compositeness and supersymmetry, and in parts also the Standard Model with gravity. In chapter 5 it is argued that a mechanism very similar to that responsible for the QCD scale causes a hierarchy of several orders of magnitude between the Higgs mass and its natural value in all metastable vacua. Such a line of reasoning might seem unusual from the perspective of the mentioned Standard Model extensions, as they are usually understood to stabilize the electroweak vacuum. The situation is, however, more subtle. This will become clear throughout chapter 4, which provides an in-depth analysis of the calculation of decay rates in quantum field theory, combining results from the literature with new results concerning technical aspects as well as numerical results. These new results, their discussion and its implications for the concrete example of compositeness represent the second central result of this thesis.

The arguments at the heart of chapter 5 add to the plausibility that the Standard Model is indeed only an effective field theory of some strongly coupled sector, suggesting that the study of such theories might offer a path towards a better understanding of the Standard Model itself. While metastability is closely linked to the existence of instantons, these theories often give rise to solitons, to which the third and final central result of this thesis is related. Chapter 3 presents a new approach towards the construction of an effective description of the fluctuations around topological solitons, which generalizes the idea of collective coordinates in a way that allows to describe a wide range of models and configurations within one unified framework.

The foundation for these results is laid in chapter 1, which reviews some features of the Standard Model's vacuum and some of its most important properties, in particular the condensation of the QCD sector at low energies as well as the origin of its instability at large energies. Chapter 2 prepares the discussion of the effective description of the dynamics of topological solitons in chapter 3.

Chapter 1

The vacuum in the Standard Model of particle physics and beyond

The most successful quantum field theory is without a doubt the Standard Model of particle physics (SM) [3]. It describes all known interactions with unprecedented accuracy and is able to explain most of their underlying mathematical structure through one simple principle, *gauge invariance* under the SM gauge group

$$SU(3) \otimes SU(2)_L \otimes U(1)_Y.$$

From this simple structure - together with the Higgs potential - arises a remarkably complex theory. One of the arguably most fascinating and important examples of this is its vacuum. Both the QCD sector, represented by the $SU(3)$ subgroup, as well as the electroweak sector, represented by the $SU(2)_L \otimes U(1)_Y$ subgroup, can be related to non-trivial properties of the vacuum from the scale dependence of the relevant couplings. The QCD sector gives rise to a rich vacuum topology and thus allows for the formation of topological solitons. Meanwhile, the electroweak sector contains a mechanism rendering the Higgs vacuum unstable, thus allowing for the therefore false vacuum to decay through an instanton.

Despite its great successes, there are strong reasons to believe that the Standard Model is incomplete. On the observational side, the SM offers no explanations for dark energy and dark matter, neutrino masses and B-anomalies. On the theoretical side, especially the Higgs sector remains poorly understood: The shape of its potential needs to be included by hand, and both of its parameters appear to be strongly fine-tuned to simultaneously allow for a non-stable vacuum and a small Higgs mass.

1.1 Overview

Neglecting generation indices, the full Lagrangian of the SM is given by

$$\mathcal{L} = -\frac{1}{4}B_{\mu\nu}B^{\mu\nu} - \frac{1}{8}\mathrm{tr}\left(\mathbf{W}_{\mu\nu}\mathbf{W}^{\mu\nu}\right) - \frac{1}{2}\mathrm{tr}\left(\mathbf{G}_{\mu\nu}\mathbf{G}^{\mu\nu}\right) +$$

(U(1), SU(2), and SU(3) gauge kinetic terms)

$$+ \left(\bar{\nu}_L, \bar{l}_L\right)\tilde{\sigma}^\mu i D_\mu \begin{pmatrix}\nu_L \\ l_L\end{pmatrix} + \bar{l}_R\sigma^\mu i D_\mu l_R + \bar{\nu}_R\sigma^\mu i D_\mu \nu_R + (\text{h.c.}) -$$

(lepton kinetic terms)

$$- \left[\left(\bar{\nu}_L, \bar{l}_L\right)\mathbf{H}Y^l l_R + \bar{l}_R Y^{l\dagger}\mathbf{H}^\dagger \begin{pmatrix}\nu_L \\ l_L\end{pmatrix}\right] +$$

(lepton Yukawa terms)

$$+ \left(\bar{u}_L, \bar{d}_L\right)\tilde{\sigma}^\mu i D_\mu \begin{pmatrix}u_L \\ d_L\end{pmatrix} + \bar{u}_R\sigma^\mu i D_\mu u_R + \bar{d}_R\sigma^\mu i D_\mu d_R + (\text{h.c.}) -$$

(quark kinetic terms)

$$- \left[\left(\bar{u}_L, \bar{d}_L\right)\mathbf{H}Y^d d_R + \bar{d}_R Y^{d\dagger}\mathbf{H}^\dagger \begin{pmatrix}u_L \\ d_L\end{pmatrix}\right] - \left[\left(-\bar{d}_L, \bar{u}_L\right)\mathbf{H}^* Y^u u_R + \bar{u}_R Y^{u\dagger}\mathbf{H}^T \begin{pmatrix}-d_L \\ u_L\end{pmatrix}\right] +$$

(quark Yukawa terms)

$$+ \left(D_\mu \mathbf{H}\right)^\dagger D^\mu \mathbf{H} + \frac{m^2}{2}\mathbf{H}^\dagger\mathbf{H} - \lambda(\mathbf{H}^\dagger\mathbf{H})^2$$

(Higgs kinetic and potential terms)

From this Lagrangian the beta functions of all running parameters can be derived, leading to the results summarized in section A.2 of the appendix. Matching them with the most recent experimental data, which can be converted to matching conditions for the couplings at the top mass scale [4], integrating the beta functions leads to the RG trajectories of the couplings depicted in Fig. 1.1. For the matters discussed within this thesis, the result contains two potentially consequential observations: At low energies, the strong gauge coupling grows very quickly, while at large energies, the quartic Higgs coupling becomes negative.

1.2 Higgs sector

The crucial term in the SM Lagrangian for the understanding of the electroweak sector's vacuum is the Higgs potential,

$$V(\mathbf{H}) = -\frac{m^2}{2}\mathbf{H}^\dagger\mathbf{H} + \lambda(\mathbf{H}^\dagger\mathbf{H})^2. \tag{1.1}$$

While the potential depends formally on the full SU(2)-doublet Higgs,

$$\mathbf{H} = \frac{1}{\sqrt{2}}\begin{pmatrix}G_1 + iG_2 \\ H + iG_3\end{pmatrix}, \tag{1.2}$$

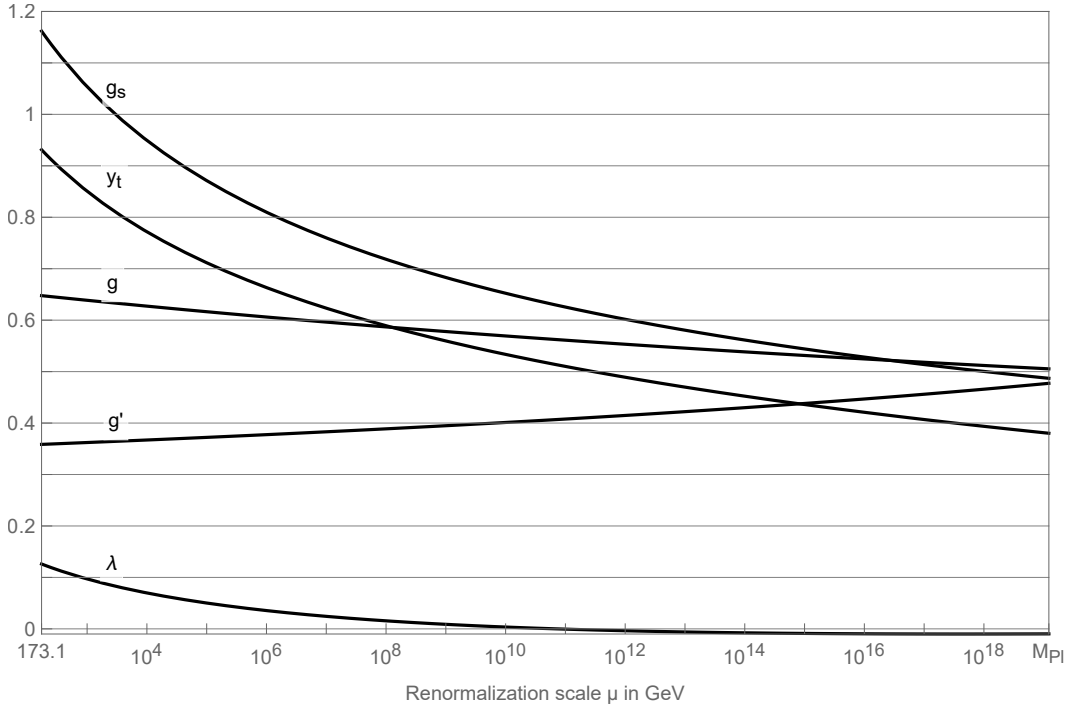

Figure 1.1: The RG trajectories of the most important SM couplings from the top quark mass until the Planck scale.

it is clear from (1.1) that $\mathbf{H}$ contains three Goldstones corresponding to $SU(2)$-rotations of the doublet. As this symmetry is part of the theory's gauge group, they can be eliminated in the so-called *unitary gauge*. In this gauge, the Higgs doublet consequently takes the form

$$\mathbf{H} = \left(0, \frac{H}{\sqrt{2}}\right). \tag{1.3}$$

In terms of the component field H, the Higgs potential is now given by

$$V(H) = \frac{1}{4}(-m^2H^2 + \lambda H^4). \tag{1.4}$$

For $m^2, \lambda > 0$, this potential has an, up to a residual Z_2-symmetry of the theory, unique minimum - the vacuum expectation value (vev) at $H = v := \frac{m}{\sqrt{2\lambda}}$. The properties of the Higgs particle can then be obtained by considering a fluctuation around this minimum, $H = v + h$, which picks up a mass $m_h^2 = m^2 = 2\lambda v^2$. Through the Higgs' interactions, the decomposition also generates mass terms of order v for the fermions and three of the four gauge bosons.

This mechanism relies heavily on the precise shape of the potential, and in particular the signs of the coefficients in the Lagrangian. While the necessary values have been confirmed through measurements near the electroweak scale, their scale dependence opens up the possibility of drastically different physics at higher energies. This can be formalized

through the *RG improved effective potential*, which, for energies well above the electroweak scale, can be approximated by

$$V_{\text{eff}}(h) \simeq \frac{1}{4}\lambda_{\text{eff}}(h)h^4\,, \tag{1.5}$$

where $\lambda_{\text{eff}}(h)$ combines the running quartic coupling, its loop corrections and the Higgs' wave function renormalization factors.

1.2.1 Metastability

Depending on the precise values of the couplings, it is possible for λ to turn negative at high energies [5]. The data compiled at the LHC indicates that this might indeed be the case, as the measured values of the quartic and Yukawa couplings lie just shy of the critical value beyond which λ would remain positive at all scales, leading to the RG trajectory depicted in Figure 1.2. For the most accurate values available for the couplings, λ turns negative at the instability scale $\mu_I \simeq 10^{11}$ GeV, and so does the effective potential, see Figure 1.3. This allows the electroweak vacuum to decay through the nucleation of a bubble, in the center of which the Higgs field takes large values within a small region of space [6, 7]. Consequently, this bubble expands, "pulling" the Higgs field over the potential barrier in a growing part of space.

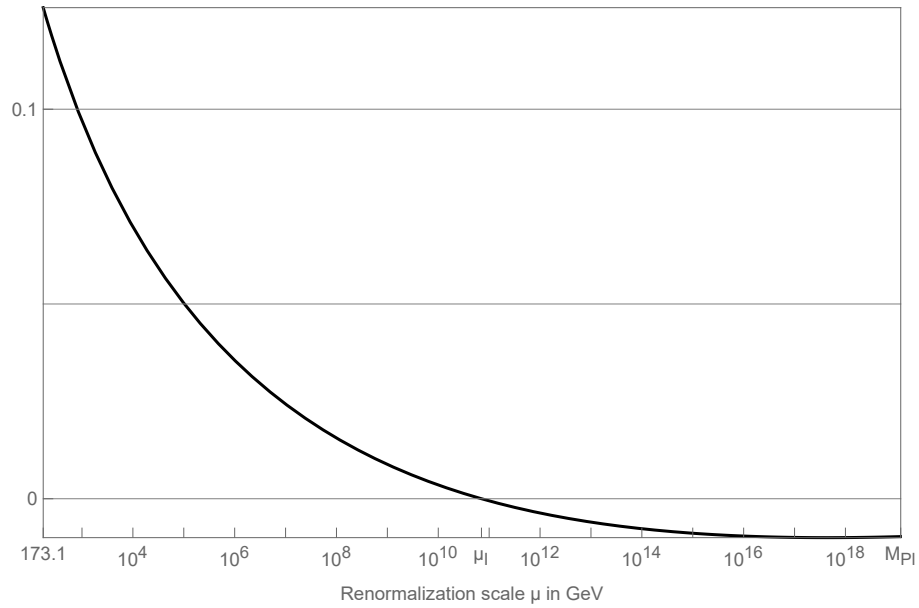

Figure 1.2: The RG trajectory of the Higgs' quartic coupling λ.

A remarkable property of the transition from stable to unstable vacua is its sensitivity to the Higgs' couplings. For most choices of the couplings at any arbitrary matching scale, the vacuum is either stable or highly unstable. Metastability meanwhile occurs only in a thin sliver of the parameter space, seemingly suggesting a strong fine-tuning of the couplings

to achieve it. While this is not only essential for the interpretation of metastability as an example of near-criticality, it has also very practical consequences as it implies that all results are strongly sensitive to potential new physics - and thus, in particular the instability scale as well as the vacuum's lifetime.

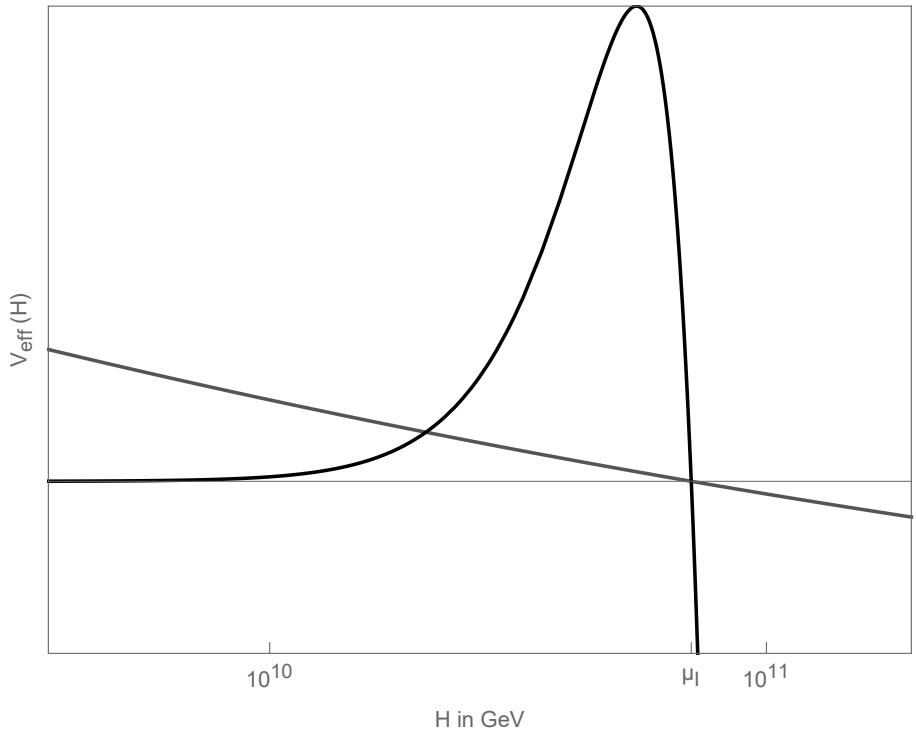

Figure 1.3: The effective potential and the quartic coupling near the instability scale, not to scale.

1.2.2 The hierarchy problem

Having reasonable certainty that the SM should be extended, the next logical question - besides the nature of the extension - is beyond which energy the new physics manifests. The easiest way to find an answer to this question would be through the observation of some new particle. Unfortunately, despite ever increasing energies in colliders, there has to this date been no such observation. Also the SM itself offers no hint where to expect new physics. To the contrary, the couplings of the SM do not only appear to be fine-tuned to allow for metastability, but also to ensure pertubativity until the Planck scale and even beyond.

There are now two possible explanations for such a behavior. Either the SM, and particular its Higgs sector, is indeed a good and, crucially, complete description of nature until and beyond the Planck scale, and the Higgs mass is a fundamental parameter of nature. While this appears consistent, it is also highly unappealing, as it not only suggests that there is no

explanation for the properties of the Higgs, but also that nature contains two fundamental scales 17 orders of magnitude apart from one another [8].

The first alternative to this scenario is that the degrees of freedom of the SM, and in particular the Higgs, offer a good description of their relevant degrees of freedom until large energies, but are coupled to some additional degrees of freedom of mass M. The existence of such new physics clearly cannot be ruled out as long as M is sufficiently large to avoid production of these degrees of freedom in today's accelerators. Direct detection is, however, not the only way such additional particles would manifest themselves, as they would effect the SM observables through loop corrections.

This effect is most consequential for the Higgs mass. Assuming that the Higgs is indeed a fundamental scalar, it is easy to see that each particle interacting with the Higgs through some coupling y induces a correction to its mass term, which should scale as

$$\delta m^2 \sim \pm \frac{M^2 y^2}{(4\pi^2)}, \tag{1.6}$$

with "+" for a boson and "-" for a fermion. Famously, the measured Higgs pole mass is 125 GeV, and thus of order of the electroweak scale. While such a value poses no problem for new particles with a significant coupling of masses of order $1 - 10$ TeV, like light right-handed neutrinos, it becomes increasingly difficult to realize for heavier particles. In fact, the only way to consolidate the observed value with additional particles with masses above the TeV-scale is if the running mass is tuned to cancel the correction up to some tiny remnant of order of the electroweak scale.

An alternative perspective on this issue can be gained from the treatment of the SM as an effective field theory, which would suggest that the heavy particles of interest need to be integrated out at energies below their mass M [9]. One the one hand, this would trivially solve the issue of the pole mass, as the loop correction would disappear from the equation for the pole mass. However, it would simply reappear in the matching condition connecting the SM mass parameter with that of the UV theory,

$$(m^{SM})^2 = (m^{UV})^2 \pm \delta m^2, \tag{1.7}$$

so that once again significant fine-tuning is necessary to allow for a small mass parameter.

An elegant way around this issue is to embed the SM, and in particular the Higgs, into some larger framework in which these loop corrections are absent, naturally leading to the ideas of, e.g., (partial) compositeness or supersymmetry. The - at least temporary - failure of this approach can also be understood efficiently by treating the SM as a low energy effective field theory. Doing so, the value of the mass parameter can be obtained by matching the SM with the Lagrangian of the full theory at the matching scale Λ_{UV}. There, based on dimensional reasons it can be expected that the matching condition is of the form

$$(m^{SM})^2 = \alpha_0 \Lambda_{UV}^2 + \sum_{i \geq 1} \alpha_i M_i^2, \tag{1.8}$$

where the scales $\{M_i\}_{i\geq 1}$ are parameters of dimension (energy) appearing in the UV theory, usually the masses of heavy particles, and the coefficients $\{\alpha_i\}_{i\geq 0}$ are some real numbers whose precise value depends on the chosen UV theory. The absence of new physics in experiments now implies that $m^{SM} \ll \Lambda_{UV} \lesssim M_i$. Thus, a small Higgs mass can only be achieved if the coefficients $\{\alpha_i\}_i$ are tuned to be many orders of magnitude smaller than one, which usually requires cancellations between unrelated terms of the UV theory. A concrete example of this is given in section 1.6.

All these scenarios lead to the same conclusion: On the most simplistic level, consolidating the absence of new physics in flavor, precision and LHC experiments with the 125 GeV Higgs requires a significant amount of tuning. This is the well-known *(weak) hierarchy* or *Higgs naturalness problem.*

1.3 QCD sector

While the electroweak sector is responsible for the non-trivial features of the vacuum at high energies, at low energies this role is taken over by the QCD sector. While the Higgs potential was decisive for the former, in the latter case the relevant dynamics can be linked to the gluon self-interactions contained within the field strength tensor as well as its interactions with the quarks,

$$\mathcal{L} = -\frac{1}{2}\mathrm{tr}\left(\mathbf{G}_{\mu\nu}\mathbf{G}^{\mu\nu}\right) + \left(\bar{u}_L, \bar{d}_L\right)\tilde{\sigma}^\mu i D_\mu \begin{pmatrix} u_L \\ d_L \end{pmatrix} + \bar{u}_R \sigma^\mu i D_\mu u_R + \bar{d}_R \sigma^\mu i D_\mu d_R + (\text{h.c.}). \tag{1.9}$$

The one-loop beta function of the QCD gauge coupling is famously given by

$$\beta_{g_s} = -7\frac{g_s^3}{(4\pi)^2}, \tag{1.10}$$

which can be solved analytically, leading to

$$g_s(\mu) = \frac{4\pi}{\sqrt{14\ln\left(\frac{\mu}{\Lambda_{\mathrm{QCD}}}\right)}}. \tag{1.11}$$

This very simple expression contains the foundations to two of QCD's most essential phenomena: Confinement and asymptotic freedom. *Asymptotic freedom* refers to the coupling becoming weaker for higher energies, while *confinement* can be related to the growth of g_s at small energies. As it is easy to see from relation (1.11), the solution for g_s obtained through the integration of its one-loop beta function appears to have a pole at the *confinement* or *QCD scale* Λ_{QCD}. While the investigation of asymptotic freedom is naturally simplified by its defining feature of a small coupling, the opposite is true for confinement. Thus, the perturbatively determined value of the QCD scale is quite sensitive to higher-order corrections as well as to the chosen renormalization scheme. This is illustrated in Fig. 1.4, using the running of g_s at one- at four-loop in pure QCD, matched to the SM value

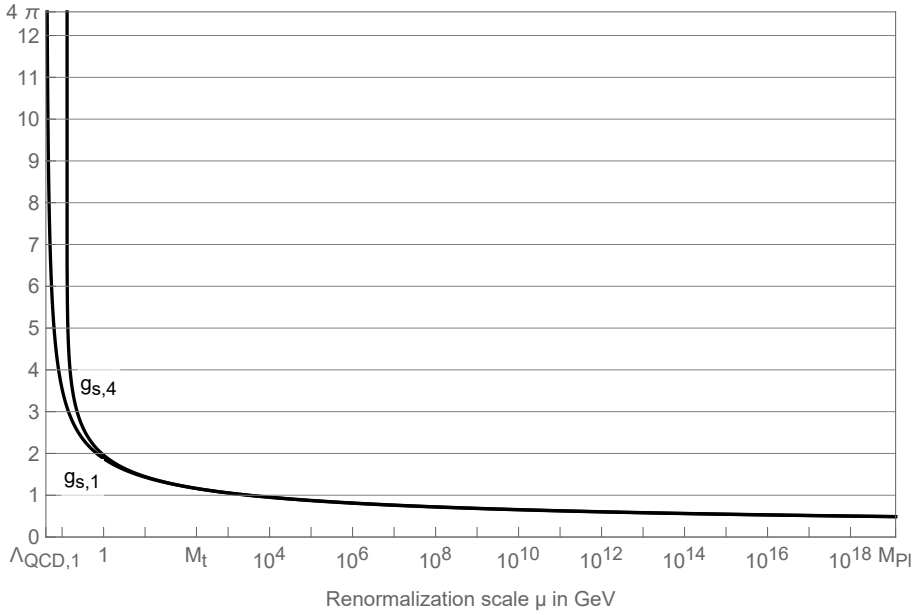

Figure 1.4: The running of g_s in pure QCD at one-loop, $g_{s,1}$, and four-loop, $g_{s,4}$, respectively.

at the top mass. Using high-precision lattice calculations, the up-to-date best theoretical prediction for its value suggests $\Lambda_{\rm QCD}^{\rm lattice} = 332$ MeV [10].

Below this energy, all degrees of freedom transforming under the $SU(3)$, and thus interacting via QCD, are strongly coupled. Thus, to allow for a perturbative description of the dynamics below $\Lambda_{\rm QCD}$, new degrees of freedom need to be defined. Although a rigorous, theoretical derivation remains a matter of active research, it is well-known from observations that at low energies, quarks are *confined* into mesons and baryons, which therefore offer an obvious candidate for these new degrees of freedom. An effective description of their properties can be constructed within the more general framework of *chiral perturbation theory*.

1.4 Below the SM: Chiral perturbation theory and the Skyrme model

A strong hint regarding the structure of the effective field theory describing the degrees of freedom below the QCD scale can be obtained from the (approximate) symmetries of the full theory. In the Standard Model, the quark masses are given by

$$\begin{aligned} m_u &= 2.16 \text{ MeV}, \ m_d = 4.67 \text{ MeV}, \ m_s = 93 \text{ MeV}, \\ m_c &= 1.27 \text{ GeV}, \ m_b = 4.18 \text{ GeV}, \ m_t = 172.76 \text{ GeV}. \end{aligned} \tag{1.12}$$

Thus, compared to the QCD scale $\Lambda_{\rm QCD} \sim 300$ MeV, there are three heavy quarks as well as three light ones, out of which - depending on the level of accuracy - either two

or all three can considered approximately massless, so that their left- and right-handed parts decouple. In the rougher approximation of three massless flavors, which is more appropriate at higher energies, the low-energy theory can thus be constructed around an approximate $SU(3)_L \times SU(3)_R$-symmetry, corresponding to eight would-be-Goldstones. As the flavor symmetry is explicitely broken by the mass terms, also these lightest degrees of freedom can be expected to be massive, with three light excitations - corresponding to the $SU(2)$ subgroup of up-down-rotations - and five more heavy ones. As an immediate consequence, for low enough energies the approximate symmetry group effectively reduces to a $SU(2)_L \times SU(2)_R$, which can be represented on a theory of an $SU(2)$-valued field U. Such a field can be naturally parametrized in terms of three pion fields $\{\pi^a\}_a$ and the $SU(2)$-generators $\{T_a\}_a$,

$$U(x) = \exp\left(i\frac{\pi^a}{f}T_a\right), \tag{1.13}$$

with the pion decay constant $f = 93$ MeV [11]. Under the assumption that the $SU(2)_L \times SU(2)_R$-symmetry is realized exactly, i.e. that the up- and down quark are exactly massless, the pions would be Goldstones, and the most general Lagrangian in accordance with the symmetry would be of the form

$$\mathcal{L} = \mathcal{L}(\partial U) = \frac{f_\pi^2}{4}\mathrm{tr}\left(\partial_\mu U \partial^\mu U^\dagger\right) + ... \tag{1.14}$$

As even the $SU(2)$-symmetry of the UV theory is only approximate, pions are only *pseudo-Nambu Goldstone bosons*, i.e., they should have a small but non-vanishing mass. The simplest suitable term capable of providing such a mass is of the form

$$\mathcal{L}^{m_\pi} = m_\pi^2 f_\pi^2\left(\mathrm{tr}(U) - 2\right). \tag{1.15}$$

A particularly interesting subset of this effective theory is the so-called *Skyrme model*, which is described by the action

$$S[U] = \int d^4x \ \frac{f_\pi^2}{4}\mathrm{tr}\left(\partial_\mu U \partial^\mu U^\dagger\right) + \frac{1}{32e^2}\mathrm{tr}\left([\partial_\mu U, \partial_\nu U^\dagger][\partial^\mu U, \partial^\nu U^\dagger]\right). \tag{1.16}$$

The parameter e is the *Skyrme constant*, which determines the strength of the self-coupling. Through the addition of the self-interaction term, the *Skyrme term*, solitonic solutions become possible [12, 13]. To understand their topological structure the vacuum manifold $\mathcal{V}$ of the this theory is required. It is easy to see that said manifold is nothing else then the space of all constant SU(2)-matrices, i.e. $\mathcal{V} \cong \mathrm{SU}(2)$. For the soliton to have finite energy it must satisfy $U(\boldsymbol{x}) \to U_0$ =const. for $|\boldsymbol{x}| \to \infty$. This implies that from the point of view of the field, all points at spatial infinity can be identified. Doing this the space $\mathbb{R}^3$ becomes homeomorphic to the 3-sphere S^3, which can be shown by the famous stereographic projection.

Hence any static field configuration $U(\boldsymbol{x})$ can be viewed as a map from the spatial S^3 to its vacuum space SU(2). This means that it can be classified by an element of the homotopy

group π_3 (SU(2)), which is indeed nontrivial:

$$\pi_3(\mathrm{SU}(2)) \cong \mathbb{Z} \tag{1.17}$$

To sort a specific configuration $U(\boldsymbol{x})$ into one of these classes, one needs to find its topological charge which is determined by its topological current,

$$J_B^\mu = -\frac{\varepsilon^{\mu\alpha\beta\gamma}}{24\pi^2}\mathrm{tr}\big((U^\dagger\partial_\alpha U)(U^\dagger\partial_\beta U)(U^\dagger\partial_\gamma U)\big). \tag{1.18}$$

Here, the index B means *baryonic current*. Starting from this the topological charge becomes

$$Q_B = \int J_B^0\, d^3\boldsymbol{x} = -\frac{\varepsilon^{ijk}}{24\pi^2}\int \mathrm{tr}\big((U^\dagger\partial_i U)(U^\dagger\partial_j U)(U^\dagger\partial_k U)\big)d^3\boldsymbol{x}. \tag{1.19}$$

1.5 Beyond the SM: The νMSM

In the pure SM, the three left-handed neutrinos are necessarily massless to preserve gauge invariance and renormalizability. Numerous direct observations, together with cosmological constraints, instead suggest neutrino masses at the eV-scale. The required extension of the SM should, in the best case scenario, not only explain their small mass relative to the electroweak scale, but also compared to the lightest leptons. The most popular mechanism to achieve this is the so-called *seesaw-mechanism*, in which integrating out a heavy, right-handed singlet fermion - usually referred to *right-handed neutrino* - leads to a small mass term for the left-handed neutrinos for small energies while restoring gauge invariance at high energies.

The simplest realization of this idea consists of the SM together with three heavy, right-handed singlet neutrinos N_I, $I = 1, 2, 3$. Their Lagrangian is given by

$$\mathcal{L} = \bar{N}_I i\gamma^\mu\partial_\mu N_I - Y_{\alpha I}\bar{\mathbf{L}}_\alpha N_I(\epsilon\mathbf{H}^*) - \frac{1}{2}M_{IJ}\bar{N}_I^c N_J + \mathrm{h.c.}\,, \tag{1.20}$$

where $\bar{\mathbf{L}}_\alpha$ denotes the lepton doublets ($\alpha = e, \mu, \tau$), $Y_{\alpha I}$ is the matrix of Yukawa couplings, and ϵ is the totally anti-symmetric SU(2) matrix. The last term is a Majorana mass matrix for the right-handed neutrinos. This model is usually referred to as the νMSM or type I seesaw [14–20], as the mass matrix of the left-handed neutrinos after symmetry breaking is given by

$$m_\nu = -\frac{v^2}{2}YM^{-1}Y^T\,, \tag{1.21}$$

which is to be understood as a matrix in generation space. This relation implies that, in generic cases, increasing the mass of the right-handed neutrinos decreases the mass of the left-handed ones, and vice versa. In other words, the lightness of the left-handed neutrinos is either the result of the large masses of their right-handed counterparts or tiny Yukawa couplings.

However, there is a subtlety to this argument. As the physical masses of the left-handed neutrinos are the eigenvalues of the mass matrix (1.21), it is possible that cancellations between the different elements of the latter lead to small eigenvalues despite Yukawa couplings of order ~ 1 and right-handed neutrinos with masses in the TeV-range [88]. While the fine-tuning necessary to achieve such cancellations could of course be accidental, it can naturally arise as the result of an additional approximate symmetry protecting the masses of the left-handed neutrinos. One of the most important examples for such a symmetry is related to the preservation of the $B - \tilde{L}$ number, where $\tilde{L}$ denotes an extension of the lepton number by right-handed neutrinos [14], and is given by

$$N_3 \to e^{i\alpha} N_3, \;\; N_2 \to e^{-i\alpha} N_2, \;\; N_1 \to e^{i\beta} N_1. \tag{1.22}$$

Imposing this as an exact symmetry, and taking into account several observational constraints, the Majorana mass matrix and the matrix of Yukawa couplings are restricted to be of the form

$$M = \begin{pmatrix} 0 & 0 & 0 \\ 0 & 0 & M \\ 0 & M & 0 \end{pmatrix} \quad \text{and} \quad Y = \begin{pmatrix} 0 & Y_1 & 0 \\ 0 & Y_2 & 0 \\ 0 & Y_3 & 0 \end{pmatrix}, \tag{1.23}$$

up to rotations of the right-handed neutrinos in flavor space. Inserting this into (1.20), one finds that one of the right-handed neutrinos, N_1, remains massless and sterile. Meanwhile N_2 and N_3 combine into a Dirac spinor of mass M and with a Yukawa coupling to the Higgs and the left-handed spinors. This does, however, not induce a mass for the left-handed neutrinos.

Thus, consistency with observations requires the symmetry (1.22) to be broken, which can be made manifest by introducing symmetry-breaking terms for both the Yukawa coupling as well as the mass term,

$$\Delta M = \begin{pmatrix} m_{11} e^{i\alpha_1} & m_{12} & m_{13} \\ m_{21} & m_{22} e^{i\alpha_2} & 0 \\ m_{31} & 0 & m_{33} e^{i\alpha_3} \end{pmatrix}, \qquad \Delta Y = \begin{pmatrix} y_{11} & 0 & y_{13} \\ y_{21} & 0 & y_{23} \\ y_{31} & 0 & y_{33} \end{pmatrix}. \tag{1.24}$$

Adding these terms generates a mass for the sterile right-handed neutrino,

$$M_1 \simeq m_{11} - 2\cos(\alpha) \cdot \frac{m_{12} m_{13}}{M}. \tag{1.25}$$

Also the masses of the two initially heavy right-handed neutrinos receive corrections, inducing a - phenomenologically relevant - mass difference between them, which is to leading order given by

$$\begin{aligned} M_2^2 - M_3^2 \simeq 2 \cdot \Big[& 4 m_{12} m_{13} \big(m_{12} m_{13} + M m_{22} \cos(\beta) + M m_{33} \cos(\gamma) \big) + \\ & + M^2 \big(m_{22}^2 + m_{33}^2 + 2 m_{22} m_{33} \cos(\beta + \gamma) \big) \Big]^{\frac{1}{2}} \end{aligned} \tag{1.26}$$

Lastly, the combined breaking of the $B-\tilde{L}$ and gauge symmetry also induces a mass matrix for the left-handed neutrinos of the form (1.21), whose eigenvalues are, again to leading order,

$$m_1 \simeq \Big(\sum_{i=1}^{3}|y_{i1}|^2\Big)\frac{v^2}{m_{11}} \tag{1.27}$$

$$m_{2,3} \simeq \left(\Big(\sum_{i=1}^{3}|Y_i|^2\Big)^{\frac{1}{2}}\cdot\Big(\sum_{i=1}^{3}|y_{i3}-\frac{1}{2}\frac{m_{33}}{M}Y_i|^2\Big)^{\frac{1}{2}} \pm |\sum_{i=1}^{3}Y_i^* y_{i3}|\right)\frac{v^2}{M}. \tag{1.28}$$

Despite its simplicity, this model can not only explain neutrino masses, but also offers a mechanism for baryogenesis and might explain dark matter. This can, to some extent, also be realized in generic seesaw models. One advantage of the νMSM and all other low-scale seesaw models compared to these models is that they do not require the introduction of an additional energy scale, as the mass term for the right-handed neutrinos can be of order of the electroweak scale. The existence of an additional scale would not only require explanation, but also worsen the hierarchy problem. Considering an individual neutrino for concreteness, it is easy to see that it induces a correction to the Higgs mass which scales as

$$\delta m_h^2 = \frac{M^2|Y|^2}{(4\pi)^2}. \tag{1.29}$$

Thus, for $M \lesssim 1$ TeV, this correction is small enough to allow for the observed 125 GeV Higgs mass without the need for any further fine-tuning. The smallness of M is also of particular interest from the point of view of the vacuum selection mechanisms reviewed in section 1.7, which require an additional Yukawa coupling of order one which becomes active around the TeV-scale.

1.6 Beyond the SM: Higgs Compositeness

One of the simplest solutions to the hierarchy problem, which at the same time affects the vacuum's metastability, is the idea of Higgs compositeness [21–23]. The hierarchy problem can be traced back to the assumption that the Higgs is a fundamental scalar - thus, it would be trivially solved if the Higgs were not a fundamental scalar, but rather a pseudo-Nambu Goldstone boson of some dynamically broken symmetry. This can be achieved, e.g., through the condensation of additional fermions which couple to an appropriate gauge group. The simplest phenomenologically viable scenario for this is a SU(2) gauge theory with 2 Dirac-, i.e., 4 Weyl-fermions in a fundamental representation. Denoting the two fermions U and D, in analogy with QCD, the corresponding Lagrangian is of the form

$$\mathcal{L} = -\frac{1}{8}\mathrm{tr}(F_{\mu\nu}F^{\mu\nu}) + \bar{U}(i\gamma^\mu D_\mu - m)U + \bar{D}(i\gamma^\mu D_\mu - m)D \tag{1.30}$$

This Lagrangian contains a potential symmetry, which can be seen by decomposing the Dirac fermions into Weyl fermions, $U = U_L \oplus U_R$ and $D = D_L \oplus D_R$ respectively, and then

considering the new quantity

$$F = (U_L, D_L, -i\sigma^2 C\bar{U}_R^T, -i\sigma^2 C\bar{D}_R^T)^T. \tag{1.31}$$

Then, under an infinitesimal SU(4) transformation $F \to \sum_{n=0}^{\infty} \alpha_n T_n$, where $\{T_n\}_n$ denotes an appropriate set of $SU(4)$ generators, the Lagrangian transforms as

$$\mathcal{L} \to \mathcal{L} + \frac{im}{2} \sum_{n=1}^{\infty} \alpha_n F^T (-i\sigma^2) C(\sigma_H T_n + T_n^T \sigma_H) F + h.c., \tag{1.32}$$

with

$$\sigma_H = \begin{pmatrix} 0 & 0 & 1 & 0 \\ 0 & 0 & 0 & 1 \\ -1 & 0 & 0 & 0 \\ 0 & -1 & 0 & 0 \end{pmatrix}. \tag{1.33}$$

Thus, for $m = 0$, the theory contains an additional SU(4) symmetry, which is broken by the mass terms down to the subgroup spanned by the generators T_{nn} satisfying

$$\sigma_H T_n + T_n^T \sigma_H = 0. \tag{1.34}$$

This now just happens to be the defining equation for the symplectic algebra $Sp(4)$, which can be identified with the generators of so(5), the algebra of the Lie group SO(5). Thus, the mass term induces the symmetry breaking $SU(4) \to SO(5) \simeq Sp(4)$. Following Goldstone's theorem, this implies that the theory contains 5 Goldstone bosons, as dim(SU(4))=15 and dim(Sp(4))=10.

The same symmetry breaking pattern can be obtained through condensation of the technifermions, which, as can be shown through lattice simulations [21], leads to a non-vanishing of the vacuum expectation value

$$\Sigma = \langle \bar{U}U + \bar{D}D \rangle. \tag{1.35}$$

Comparing this expression with the mass term, it is clear that they transform in the same way under an SU(4) transformation up to prefactors. Thus, even without a mass term, the condensation through the SU(2) interaction will induce the $SU(4) \to SO(5) \simeq Sp(4)$ symmetry breaking below the condensation scale $\Lambda_f \sim 4\pi f$, with the technipion decay constant defined in analogy to the QCD pion decay constant.

Below Λ_f, the low-energy dynamics of this theory is characterized by the condensate and its five Goldstones. With the SM in mind, three condensates will turn out to be of particular interest:

$$\Sigma_A = \begin{pmatrix} i\sigma^2 & 0 \\ 0 & i\sigma^2 \end{pmatrix}, \ \Sigma_B = \begin{pmatrix} i\sigma^2 & 0 \\ 0 & -i\sigma^2 \end{pmatrix}, \ \Sigma_H = \begin{pmatrix} 0 & \mathbb{1}_{2\times 2} \\ \mathbb{1}_{2\times 2} & 0 \end{pmatrix}. \tag{1.36}$$

Under an SU(4)-transformation R of the underlying fields combined into F, the condensate transforms as

$$\Sigma \to R\Sigma R^T. \tag{1.37}$$

The Goldstone modes can now be identified with perturbations generated by the SU(4) generators broken by the condensate, $\{T_n^\perp\}_n$, so that the full condensate including low-energy perturbations is given by

$$\Sigma = \exp\left(i\frac{\phi_n}{f}T_n^\perp\right)\Sigma_{\text{vac}}, \tag{1.38}$$

where Σ_{vac} is the condensate representing the vacuum.

The first step towards matching these degrees of freedom with their counterparts of the SM is to identify the correct condensate to expand around. One of the most important criteria it has to satisfy is that it has to reproduce the electroweak symmetry group, i.e., $SU(2)_L \otimes U(1)_Y$. The generators of this group can be found within the generators that remain unbroken by Σ_B,

$$T_1^{\parallel\Sigma_B} = \begin{pmatrix} 0 & \mathbb{1}_{2\times2} \\ \mathbb{1}_{2\times2} & 0 \end{pmatrix}, \quad T_2^{\parallel\Sigma_B} = \begin{pmatrix} 0 & i\sigma^1 \\ -i\sigma^1 & 0 \end{pmatrix}, \quad T_3^{\parallel\Sigma_B} = \begin{pmatrix} 0 & i\sigma^2 \\ -i\sigma^2 & -0 \end{pmatrix},$$
$$T_4^{\parallel\Sigma_B} = \begin{pmatrix} 0 & i\sigma^3 \\ -i\sigma^3 & 0 \end{pmatrix}, \quad T_5^{\parallel\Sigma_B} = \begin{pmatrix} \sigma^1 & 0 \\ 0 & -\sigma^1 \end{pmatrix}, \quad T_6^{\parallel\Sigma_B} = \begin{pmatrix} \sigma^1 & 0 \\ 0 & \sigma^1 \end{pmatrix},$$
$$T_7^{\parallel\Sigma_B} = \begin{pmatrix} \sigma^3 & 0 \\ 0 & -\sigma^3 \end{pmatrix}, \quad T_8^{\parallel\Sigma_B} = \begin{pmatrix} \sigma^3 & -0 \\ -0 & \sigma^3 \end{pmatrix}, \quad T_9^{\parallel\Sigma_B} = \begin{pmatrix} \sigma^2 & 0 \\ 0 & -\sigma^2 \end{pmatrix},$$
$$T_{10}^{\parallel\Sigma_B} = \begin{pmatrix} \sigma^2 & 0 \\ 0 & \sigma^2 \end{pmatrix}.$$

The generators of the SM gauge group can now be obtained as linear combinations of a subset of these:

$$S_1 = \frac{1}{4}(T_5^{\parallel\Sigma_B} + T_6^{\parallel\Sigma_B}) = \frac{1}{2}\begin{pmatrix} \sigma_1 & 0 \\ 0 & 0 \end{pmatrix}, \quad S_2 = \frac{1}{4}(T_9^{\parallel\Sigma_B} + T_{10}^{\parallel\Sigma_B}) = \frac{1}{2}\begin{pmatrix} \sigma_2 & 0 \\ 0 & 0 \end{pmatrix},$$
$$S_3 = \frac{1}{4}(T_7^{\parallel\Sigma_B} + T_8^{\parallel\Sigma_B}) = \frac{1}{2}\begin{pmatrix} \sigma_3 & 0 \\ 0 & 0 \end{pmatrix}, \quad S_4 = \frac{1}{4}(-T_5^{\parallel\Sigma_B} + T_6^{\parallel\Sigma_B}) = \frac{1}{2}\begin{pmatrix} 0 & 0 \\ 0 & -\sigma_1^T \end{pmatrix},$$
$$S_5 = \frac{1}{4}(-T_9^{\parallel\Sigma_B} + T_{10}^{\parallel\Sigma_B}) = \frac{1}{2}\begin{pmatrix} 0 & 0 \\ 0 & -\sigma_2^T \end{pmatrix}, \quad S_6 = \frac{1}{4}(-T_7^{\parallel\Sigma_B} + T_8^{\parallel\Sigma_B}) = \frac{1}{2}\begin{pmatrix} 0 & 0 \\ 0 & -\sigma_3^T \end{pmatrix}.$$

Now, using (1.35) and (1.31) while recalling that the Pauli matrices form a set of generators for SU(2), it is straightforward to identify the subgroup generated by S^1, S^2 and S^3 with $SU(2)_L$ and S^4, S^5 and S^6 with $SU(2)_R$, where S^6 takes the role of the hypercharge operator. Thus, Σ_B is suited to reconstruct the electroweak sector of the SM from it[1].

So far, the theory lacks a mechanism to break the electroweak symmetry down in the usual manner. As a side effect, all Goldstones are massless, while at least one of them - the Higgs - should obtain a mass through the symmetry breaking. The reconstruction of these

[1] In principle, this would also be true for Σ_A. The resulting physics is independent of the choice.

properties usually sets out from the consideration of a superposition of the two condensates Σ_B and Σ_H, which is arguably more natural for the case of a natural composite Higgs, i.e., where $f^2 \sim m^2$. However, due to the ongoing absence of any sign of compositeness in experiments, it is reasonable to develop a new perspective on compositeness that goes beyond the idea of naturalness. Given the vanishing masses in Σ_B, it is clear that the limit of small masses corresponds to a condensate that can with good accuracy be approximated by Σ_B, which will serve as an expansion point in the following.

Again keeping the SM in mind, it can be expected that the spontaneous symmetry breaking occurs due to a non-vanishing vev of the Higgs field. Thus, as a first step, the five Goldstone's of the condensate have to be related to the component fields of the SM Higgs. First, the three SM Goldstones responsible for the gauge boson masses need to be determined through the condensate's couplings to the gauge fields. After gauging the electroweak symmetry found within the unbroken part of the SU(4), it is contained in the gauge invariant kinetic term

$$\mathcal{L}_{\text{kin}} = \text{Tr}(D_\mu \Sigma D_\mu \Sigma^\dagger). \tag{1.39}$$

Expanding this expression, the SM Goldstones can be identified with the ones linked to the generators

$$T_1^{\perp\Sigma_B} = \frac{1}{2\sqrt{2}}\begin{pmatrix} 0 & -\sigma^3 \\ -\sigma^3 & 0 \end{pmatrix}, \quad T_2^{\perp\Sigma_B} = \frac{1}{2\sqrt{2}}\begin{pmatrix} 0 & i\mathbb{1}_{2\times 2} \\ -i\mathbb{1}_{2\times 2} & 0 \end{pmatrix} \quad \text{and} \quad T_3^{\perp\Sigma_B} = \frac{1}{2\sqrt{2}}\begin{pmatrix} 0 & \sigma^1 \\ \sigma^1 & 0 \end{pmatrix}.$$

Moving to unitary gauge, these modes are absorbed into gauge bosons. Thus, there remain two Higgs candidates, namely the Goldstones arising from the generators

$$T_4^{\perp\Sigma_B} = \frac{1}{2\sqrt{2}}\begin{pmatrix} 0 & \sigma^2 \\ \sigma^2 & 0 \end{pmatrix} \quad \text{and} \quad T_5^{\perp\Sigma_B} = \frac{1}{2\sqrt{2}}\begin{pmatrix} \mathbb{1}_{2\times 2} & 0 \\ 0 & -\mathbb{1}_{2\times 2} \end{pmatrix}.$$

The dynamical condensate including their corresponding Goldstones is therefore given by

$$\Sigma = \exp\left(i\phi_4 T_4^\perp + i\phi_5 T_5^\perp\right)\Sigma_B. \tag{1.40}$$

Using that $(T_4^\perp)^2 = (T_5^\perp)^2 = \frac{1}{8}$ and $T_4^\perp T_5^\perp = T_5^\perp T_4^\perp = 0$, it is straightforward to see that the exponent can be resummed to yield

$$\Sigma = \left[\cos\left(\frac{\sqrt{\phi_4^2+\phi_5^2}}{2\sqrt{2}f}\right) + i\frac{2\sqrt{2}}{\sqrt{\phi_4^2+\phi_5^2}}\sin\left(\frac{\sqrt{\phi_4^2+\phi_5^2}}{2\sqrt{2}f}\right)(\phi_4 T_4^\perp + \phi_5 T_5^\perp)\right]\Sigma_B. \tag{1.41}$$

Thus, the Goldstones induce a mixing of the condensate Σ_B with the two condensates $T_4^{\perp\Sigma_B}\cdot\Sigma_B$ and $T_5^{\perp\Sigma_B}\cdot\Sigma_B$, which can be identified with the Σ_H and Σ_A vacua:

$$T_4^{\perp\Sigma_B}\Sigma_B = \frac{1}{2\sqrt{2}}\begin{pmatrix} 0 & \sigma^2 \\ \sigma^2 & 0 \end{pmatrix}\cdot\begin{pmatrix} i\sigma^2 & 0 \\ 0 & -i\sigma^2 \end{pmatrix} = \frac{1}{2\sqrt{2}i}\begin{pmatrix} 0 & \mathbb{1}_{2\times 2} \\ \mathbb{1}_{2\times 2} & 0 \end{pmatrix} = \frac{1}{2\sqrt{2}i}\Sigma_H \tag{1.42}$$

$$T_5^{\perp\Sigma_B}\Sigma_B = \frac{1}{2\sqrt{2}}\begin{pmatrix} \mathbb{1}_{2\times 2} & 0 \\ 0 & -\mathbb{1}_{2\times 2} \end{pmatrix}\cdot\begin{pmatrix} i\sigma^2 & 0 \\ 0 & -i\sigma^2 \end{pmatrix} = \frac{1}{2\sqrt{2}}\begin{pmatrix} i\sigma^2 & 0 \\ 0 & i\sigma^2 \end{pmatrix} = \frac{1}{2\sqrt{2}}\Sigma_A. \tag{1.43}$$

Now, as Σ_H breaks the electroweak gauge symmetry, so does a non-vanishing vev of the ϕ_4-field, making it a natural candidate for the Higgs. This conjecture can be verified by observing that the structure of T_5 implies that ϕ_5 is a pseudo-scalar, and thus cannot be the Higgs. To make this connection explicit, the two fields can be renamed as $\phi_4 \to H$ and $\phi_5 \to N$. Thus, the full dynamical condensate can be written as

$$\begin{aligned}\Sigma = &\cos\left(\frac{\sqrt{H^2+N^2}}{2\sqrt{2}f}\right)\Sigma_B + i\frac{N}{\sqrt{H^2+N^2}}\sin\left(\frac{\sqrt{H^2+N^2}}{2\sqrt{2}f}\right)\Sigma_A + \\ &+\frac{H}{\sqrt{H^2+N^2}}\sin\left(\frac{\sqrt{H^2+N^2}}{2\sqrt{2}f}\right)\Sigma_H\end{aligned} \tag{1.44}$$

1.6.1 Recovering the Higgs potential

Having identified a suitable Higgs candidate, it remains to recover its potential. Given that it appears as a Goldstone, the potential can either be generated through loop corrections or through an explicit breaking of its underlying symmetry, e.g., the technifermion's flavor SU(4).

The latter induces a mass term for the technipions, i.e., the Higgs and the N. Asssuming that SM gauge group is only dynamically broken, this mass term can be expected to be linked to the alignment with the gauge invariant Σ_B condensate, and is thus given by

$$V_m = C_m f^4 \mathrm{Tr}(\Sigma_B \Sigma) = 4f^4 \cos\left(\frac{\sqrt{H^2+N^2}}{2\sqrt{2}f}\right), \tag{1.45}$$

where C_m denotes a coefficient encoding details of the precise breaking of the SU(4).

Additional contributions to the potential can be obtained from top-quark and gauge-boson loops, which can be shown to take the form [21]

$$\begin{aligned}V_{SU(2)} &= -C_g g^2 f^4 \sum_{i=1}^{3}\mathrm{Tr}(S^i\Sigma(S_i\Sigma)^*) = \\ &= -C_g g^2 f^4 \cdot \frac{3}{2}\left(\cos^2\left(\frac{\sqrt{H^2+N^2}}{2\sqrt{2}f}\right) + \frac{N^2}{H^2+N^2}\sin^2\left(\frac{\sqrt{H^2+N^2}}{2\sqrt{2}f}\right)\right),\end{aligned} \tag{1.46}$$

$$\begin{aligned}V_{U(1)} &= -C_g g'^2 f^4 \mathrm{Tr}(S^6\Sigma(S_6\Sigma)^*) = \\ &= -C_g g'^2 f^4 \cdot \frac{1}{2}\left(\cos^2\left(\frac{\sqrt{H^2+N^2}}{2\sqrt{2}f}\right) + \frac{N^2}{H^2+N^2}\sin^2\left(\frac{\sqrt{H^2+N^2}}{2\sqrt{2}f}\right)\right),\end{aligned} \tag{1.47}$$

$$V_{\mathrm{top}} = -C_t {y_t}^2 f^4 \sum_{a=1}^{2}\mathrm{Tr}(P^a\Sigma)^2 = -C_t {y_t}^2 f^4 \cdot \frac{H^2}{H^2+N^2}\sin^2\left(\frac{\sqrt{H^2+N^2}}{2\sqrt{2}f}\right), \tag{1.48}$$

where C_g and C_t denote non-perturbatively fixed coefficients which can be expected to be positive.

Defining two new parameters $X_t = C_t y_t^2 - C_g \frac{1}{2}(3g^2 + g'^2)$ and $X_m = C_m$, the above contributions can be combined into the full potential at 1-loop,

$$V_{1-loop}(H,N) = f^4\left[X_t\left(\cos^2\left(\frac{\sqrt{H^2+N^2}}{2\sqrt{2}f}\right) + \frac{N^2}{H^2+N^2}\sin^2\left(\frac{\sqrt{H^2+N^2}}{2\sqrt{2}f}\right)\right) - 4X_m\cos\left(\frac{\sqrt{H^2+N^2}}{2\sqrt{2}f}\right)\right] \tag{1.49}$$

The Higgs potential can now be obtained by setting $N = 0$ and expanding (1.49) as a series in H:

$$\begin{aligned} V_H^{1-loop}(H) =& f^4\left[X_t\cos^2\left(\frac{H}{2\sqrt{2}f}\right) - 4X_m\cos\left(\frac{H}{2\sqrt{2}f}\right)\right] \\ =& -\frac{1}{4}\left(\frac{X_t}{2} - X_m\right)f^2\cdot H^2 + \frac{1}{4}\left(-\frac{X_m}{96} + \frac{X_t}{48}\right)\cdot H^4 + \left(\frac{X_m}{92160} - \frac{X_t}{11520}\right)\cdot\frac{H^6}{f^2} + \dots \end{aligned} \tag{1.50}$$

Comparing this potential with that of the SM, the Higgs parameters can be expressed in terms of X_t and X_m,

$$m^2 = \frac{1}{2}(X_t - 2X_m)f^2, \tag{1.51}$$

$$\lambda = \frac{1}{96}(2X_t - X_m). \tag{1.52}$$

For spontaneous symmetry breaking to occur through the SM pattern, the potential has to satisfy $m^2 < 0$ and $\lambda > 0$ at some small energy. The first condition now implies that $X_t > 2X_m$, while the second seems to suggest that $2X_t - X_m > 0$. The latter is, however not necessary, as relations (1.51) and (1.52) only hold at the matching scale. If this scale lies sufficiently far above the electroweak scale, it is possible to set out from a negative λ and achieve the condition for symmetry breaking at a lower energy through the RG running of λ[2].

Equation (1.51) further illustrates the essence of the hierarchy problem. The natural value of m^2 is of order f^2, and to achieve a value significantly smaller one needs to impose a significant cancelation between the coefficients X_t and X_m. An efficient way of parametrizing this fine-tuning is via the so-called *vacuum alignment angle*

$$\theta_0 = \frac{\bar{H}}{2\sqrt{2}f}\,, \tag{1.53}$$

where $\bar{H}$ is the Higgs vev.[3] Minimizing (1.50), the vacuum alignment angle satisfies

$$\cos\theta_0 \equiv \frac{2X_m}{X_t}\,. \tag{1.54}$$

[2]This will be discussed in greater detail in section 5.2.

[3]In composite Higgs models, the scale v is traditionally used to translate between couplings and masses, for instance $m_W = \frac{1}{2}g^2v^2$. See, e.g., [21]. v coincides with the Higgs vacuum expectation value $\bar{H}$ only in the limit $f \gg \bar{H}$.

In terms of θ_0 the Higgs mass parameter takes the simple form

$$m_h^2 = X_t \sin^2\left(\frac{\theta_0}{2}\right) f^2 \,. \tag{1.55}$$

As θ_0 appears also in the Higgs' couplings to SM gauge bosons, reproducing the pure SM in the limit $\theta_0 \to 0$, it is in principle accessible to experiments. Indeed, the continuing agreement of experimental data with the pure SM can be translated to the upper bound $\sin\theta_0 \lesssim 0.2$ [22, 23]. Evidently, compositeness replaces the fine-tuning underlying the hierarchy problem with another apparent fine-tuning between X_t and X_m.

The smallness of θ_0 allows for an efficient, effective treatment of this model at all scales of interest. In the limit $\theta_0 \ll 1$ the pseudo-Nambu Goldstone boson N decouples, as its couplings to SM particles contain a factor of $\sin\theta_0$. Thus, the relevant particle content reduces to the one of the SM, leaving only higher-order corrections to the potential. These can be further simplified by observing that, in the limit $\theta_0 \ll 1$,

$$2X_m \simeq X_t \,. \tag{1.56}$$

Hence the coefficients of the terms of higher order in H in (1.50) can be brought to a simple form $\sim \lambda/f^{2n}$, and in particular $X_t \simeq 64\lambda$.

Keeping in mind the decoupling of N and the suppression of higher-order terms by powers of Λ_f, it is straightforward to extend this analysis beyond tree level. From the perspective of the pure SM, compositeness manifests itself through higher-dimensional corrections to the potential,

$$V_{\text{eff}}(H) = -\frac{m_h^2}{4}H^2 + \frac{\lambda}{4}H^4 + \frac{C_6}{\Lambda_f^2}H^6 + \dots \tag{1.57}$$

The values of the Wilson coefficients at the matching scale Λ_f can be obtained by matching the potential (1.50) with that of the SM Higgs, (1.4), reproducing to leading order the tree-level relations $C_{2n}(\Lambda_f) \sim \lambda(\Lambda_f)$. For instance, the C_6 coefficient satisfies

$$C_6(\Lambda_f) = -\frac{\pi^2}{12}\lambda(\Lambda_f) \,. \tag{1.58}$$

At lower energies, the coefficients C_n are obtained by integrating their beta functions.

1.7 Beyond the SM: Vacuum selection

An essential question for the understanding of the Universe's apparent fine-tuning is the question to what it is tuned. In the case of the Higgs sector, both metastability as well as the hierarchy problem can be understood as examples of *near-criticality* [6, 24]. Metastability requires the SM parameters to lie close to the critical value marking the transition from stable to non-stable vacuum, and the Higgs mass exactly vanishing would correspond

to a transition from a symmetry breaking to a symmetry preserving potential[4]. While unexpected from the perspective of pure particle physics or cosmology, such behavior is common in the context of dynamical systems. One possible interpretation of this connection is that those parameters of our Universe which appear tuned to criticality underlie some evolution, which naturally leads to universes[5] similar to ours. This idea has recently gained some attention following the development of two concrete realizations of this idea, one based on dynamics in the early Universe [25, 26], and one arising on the larger scales of an inflationary multiverse [27–30].

This approach is closely related to, but independent of, the *anthropic principle*, which is based on the observation that for us to wonder about the laws of nature we need to exist in the first place [24]. In other words, a universe that it not hospitable to intelligent life can not be observed, and any universe that can be observed is automatically suited for life. Following this reasoning, no matter how unlikely a certain observation might seem, it is inevitable if it is necessary for our existence. Unfortunately, this reasoning on its own is incomplete, as it merely breaks up the fundamental question for an explanation of the Universe in two - why we observe the Universe as it is, and why such a universe can even exist. While it answers the first one, at least regarding those aspects of the universe to which it applies, it cannot address the second one on its own.

Interestingly, an equally simple answer can be given for this second question. The question why our Universe even exists suggests that it either couldn't exist at all, or at least exist in some other form. While the first scenario lies, at least currently, outside the boundaries of what physics can even discuss, all that the second scenario requires is a mechanism capable of generating variations in what we currently consider the fundamental laws of nature and, more importantly, their parameters. Probably the most famous theory capable of this is string theory, whose landscape of 10^{200} vacua leaves plenty of room for variations. Taking furthermore seriously the idea of eternal inflation [31–35], it becomes possible that the Universe we can observe is just one out of numerous "islands" within the eternally inflating background, with some or all parameters varying between them. This is the idea of the *multiverse*.

The idea of a multiverse is now, reassuringly, entirely independent of string theory, or any other chosen mechanism assumed to lie the foundation for it. More importantly, it offers a trivial answer to the question why a universe like our even exists - it does, because in the vastness of an infinite multiverse, every possibility is realized at least once, and following the anthropic principle, we must live in one suitable for life. This perspective provides a functioning, although perhaps unsatisfying, explanation for some of the Universe's fine-tuning - maybe most importantly, the cosmological constant problem and the Higgs vev - but it fails when it comes to others [36, 37]. As an example, the metastability of the

[4]Even in these cases, the gauge symmetry could be spontaneously broken in certain generic cases. This is discussed in more detail in section 5.2.3.

[5]In the following, *universe* refers to a part of a multiverse, while the spelling *Universe* is used exclusively for the one we inhabit.

electroweak vacuum, and thus the possibility of rapid extermination of all life, might appear somewhat unattractive from the point of view of the antropic principle. This can now be understood as a hint that, while the idea of a multiverse might have some substance, the anthropic principle requires completion or needs to be replaced.

Abandoning this guiding principle leads now back to the question why we live in the Universe we observe. More fundamentally, it leads to the question how likely our Universe is, and more generally, how likely certain types of universe are. This is the famous *measure problem*, referring to the difficulties that plague any attempt to define a probability measure on the multiverse. One of the most important ideas underlying many attempts to find such a measure is the *principle of mediocrity*, (see, e.g., [38]), which states that we live at asymptotically late times in the evolution of the multiverse, when the relative occupational probabilities of different vacua have reached a near-equilibrium distribution.

A more interesting possibility in the context of the multiverse is based on the idea that we exist at times much earlier than the exponentially-long mixing time for the landscape, while the probability distribution of the multiverse still approaches equilibrium. In this case, a vacuum like ours should not be likely because it is typical according to the approximate, quasi-stationary distribution, but because it has the right properties to be accessed early on in the evolution [39]. From this perspective, a dynamical selection mechanism for vacua based on search optimization has been derived in [27–30]. Their authors find that vacua which reside in optimal regions where the search algorithm defined by local landscape dynamics is efficient are accessed most easily. This idea can be formalized through the definition of an accessibility or early-time measure, which was developed in [28, 30]. Importantly, optimal regions of the landscape give rise to non-equilibrium critical phenomena, in the sense that their vacuum dynamics are tuned to *dynamical criticality*. The central prediction is that optimal regions are characterized by relatively short-lived vacua, with lifetimes of order their de Sitter Page time.[6] For our vacuum, this optimal lifetime is

$$\tau_{\rm Page} \sim \frac{M_{\rm Pl}^2}{H_0^3} \simeq 10^{130} \text{ years}\,. \tag{1.59}$$

Although this lies around 850 orders of magnitude below the central value of the SM, the latter is also highly sensitive to potential beyond-the-SM physics. Indeed, as will be shown throughout chapter 4, well-motivated extensions of the SM, such as even the simplest model for right-handed neutrinos, can easily shorten the vacuum lifetime down to the Page time and even below.

Another such framework is described in [26], whose authors propose that the parameters of the Higgs potential are determined through the dynamics of an additional scalar field, the *apeiron*[7]. This occurs through a dynamical mechanism based on quantum first-order phase transitions in the early Universe, which is shown to naturally produce a near-critical

[6] The de Sitter Page time has also emerged in an entirely different context, as the quantum break time of de Sitter space [40].

[7] A similar approach has been first developed in [41].

Higgs potential. For the quartic coupling λ, this implies the selection of an RG trajectory close to the transition from a stable vacuum to a potential with both a false vacuum at the electroweak scale and a true vacuum at some higher energy, although the existence of the latter requires higher-dimension terms linked to some UV completion to stabilize it. In Sec. 5.1, it will be shown that these are the necessary conditions for metastability, while the favored RG trajectory of λ amounts to the prediction of an ideal lifetime.

This approach will turn out to be particularly interesting in the context of chapter 5, as it allows for a prediction of the Higgs mass parameter and vacuum expectation value. Following the reasoning of [26, 41], the probability distributions for these quantities are localized near the instability scale. This scale appears also naturally as the upper bound on the Higgs mass derived in chapter 5, which is saturated by the predictions made in [26].

Chapter 2

Topological solitons & their moduli spaces

Having the Higgs potential in mind, one might be tempted to assume that - at least on the classical level - the vacuum state of a generic potential is rather simple: Throughout the entirety of space, the field of interest takes a constant value minimizing the potential. And indeed, in many cases, this is exactly what happens.

This does, however, not have to happen. Under very special conditions, such simple configurations can be replaced by ones that are **not** homogeneous in space and yet stable, as they are "wound around the boundary of space". Such configurations are called *topological solitons*.

For any classical field configuration to have finite energy, it is necessary that it converges to some value of vanishing potential energy for $|x| \to \infty$. This implies that the field on the boundary of space $\partial\mathbb{R}^d \tilde{=} S^{d-1} \subset R^d$ defines a map onto the set of all vacuua of the theories potential U, denoted by $\mathcal{V}$:

$$\begin{aligned} \Phi_\infty : S^d &\to \mathcal{V} \\ p &\mapsto \Phi_\infty(p) \coloneqq \lim_{\lambda\to\infty} \Phi(\lambda p) \end{aligned} \tag{2.1}$$

A topological soliton is now a classical configuration of finite energy, whose restriction to the boundary represents a non-trivial winding. Here, *non-trivial* means that there exists no continuous homotopy capable of unraveling the configuration to obtain a constant value on all of $\partial\mathbb{R}^d$. For a much more detailed, precise and complete formulation of this extensive topic, consider, e.g., [42–45].

Topological solitons have a wide range of interesting properties: Due to their winding, they are stable. As their energy is supposed to be finite, they are localized. Being connected to a winding, they appear in discrete numbers. All of these properties motivated the interpretation of solitons as particle-like objects, starting from the early phases of their investigation

[46]. In the Skyrme model, they can indeed be used to obtain several properties of baryons [47, 48]

2.1 Dynamics in the presence of a soliton

The most common picture used to describe the dynamics of a field in the presence of a soliton is to decompose it into the latter and fluctuations around it,

$$\Phi(t,x) = \Phi_s(x) + \delta\Phi(t,x). \tag{2.2}$$

Assuming the fluctuations to be small, their dynamics is to leading order governed by linearized equation of motion

$$(\partial_t^2 - \Omega^2(x))\delta\Phi(t,x) = 0. \tag{2.3}$$

Taking a scalar field in $1+1$ dimensions as example, the operator Ω^2 is given by

$$\Omega^2 = -\partial_x^2 + V''(\Phi_s(x)), \tag{2.4}$$

reducing the effect of the solitonic background to a space-dependent mass term for the fluctuations.

This operator is an example for a one-dimensional Schrödinger operator, for which it is well-known that its eigenfunctions $\{f_n(x)\}_n$ form an orthonormal basis with non-negative eigenvalues,

$$\Omega^2 f_n(x) = \omega_n^2 f_n(x), \tag{2.5}$$

$$\int \mathrm{d}x\ f_m(x) f_n(x) = \delta_{mn}. \tag{2.6}$$

The perturbation $\delta\Phi$ can thus be expanded in terms of this basis:

$$\delta\Phi = \sum_n q_n(t) f_n(x) \tag{2.7}$$

In terms of he expansion parameters $\{q_n\}_n$, the action takes, to quadratic order, the form

$$S[\delta\Phi] = -\int \mathrm{d}t\ M_s + \sum_n \int \mathrm{d}t\ \frac{1}{2}\dot{q}_n^2(t) - \frac{1}{2}\omega_n^2 q_n^2(t) \tag{2.8}$$

This is indeed the action of a set of decoupled oscillators $\{q_n(t)\}_n$ in addition to the action of the background field. An even simpler description of the system is given by its Hamiltonian,

$$H = M_s + \sum_n \left(\frac{1}{2}\dot{q}_n^2(t) + \frac{1}{2}\omega_n^2 q_n^2(t)\right). \tag{2.9}$$

The equation of motion for $\delta\Phi$ can then be solved either directly or via the decomposition (2.7). As can be expected, both approaches lead to the same result, suggesting a solution of the form

$$\delta\Phi = \sum_k a_k^* e^{i\omega_k t} f_k^*(x) + a_k e^{-i\omega_k t} f_k(x). \tag{2.10}$$

2.2 Zero modes & Collective coordinates

This approach is confronted with several problems which can be understood in terms of the system's zero modes. Every symmetry of the theory is related to a zero eigenfunction of Ω^2, satisfying $\Omega^2 f_0 = 0$. These zero modes represent the fluctuations along the symmetries of the system, e.g. $\phi_0 \propto \nabla\Phi_s$ for translations of a translationally invariant system.

Treating this mode as a part of $\delta\Phi$ leads to a breakdown of the usual quantization procedures. One point in the quantization where this can be observed is the free propagator. If one would try to follow the standard procedure for its construction, one would obtain

$$\Delta(t,x;t',x') = \lim_{\epsilon\to 0} \oint\!\!\!\!\!\!\int \frac{1}{2\sqrt{\omega_k^2 - i\epsilon}} e^{-i|t'-t|\sqrt{\omega_k^2-i\epsilon}} f_k(x) f_k^*(x'), \tag{2.11}$$

where the symbol $\oint\!\!\!\!\!\!\int$ is meant as sum over the discrete and integral over the continuous part of the spectrum of Ω^2 [49]. As $\omega_0 = 0$ is part of the discrete spectrum, the propagator constructed in this way has an isolated, discrete singularity and is hence ill-defined.

A second, more technical problem lies in the expansion of the field operator in terms of creation and annihilation operators. The usual perturbative approach is based on the assumption that the linearized theory describes the theory to leading order. However, for $\omega_0 = 0$, the fluctuation caused by ϕ_0 need not be small.

Another problem of this perspective arises from its discrepancy with the interpretation of the soliton as an extended particle. Up to this point, the formalism lacks a way to describe the center-of-mass of motion as well as rotations of the soliton [50].

To find a way around these issues it is useful to observe that the zero mode is given by $f_0(x) \propto \Phi_s'(x)$:

$$\Omega^2\Phi_s'(x) = -\Phi_s'''(x) + V''(\Phi_s)\Phi_s'(x) = \partial_x(-\Phi_s'' + V'(\Phi_s)) = 0 \tag{2.12}$$

In other words, the perturbations arising from the zero mode are of the form $\Phi(x) = \Phi_s(x) - \varepsilon\Phi_s'(x)$. But this is nothing else then the first order expansion of $\Phi(x) = \Phi_s(x-\varepsilon)$, implying that the zero mode arises from the degree of freedom associated to a translation of the soliton. Recalling that the soliton shares many characteristics of a particle it seems natural to interpret ε as this particle's position. The dynamics of this degree of freedom thus corresponds to a motion of the soliton, i.e., its position serves as a dynamical variable, the *collective coordinate* $z(t)$, which manifests through the replacement

$$\Phi_s(x) \to \Phi_s(x - z(t)). \tag{2.13}$$

An important subtlety at this point is that from the mode expansion alone this degree of freedom is **not** uniquely determined, as it contains no information about potential higher order terms. This matter will be revised in section 2.4, where it will be shown that a more thorough analysis leads to

$$\Phi_s(x) \to \Phi_s(\gamma(x - z(t))), \tag{2.14}$$

which of course agrees with (2.13) up to terms of higher order in z.

Settling with (2.13) for now, the action of the collective coordinate can be obtained by introducing it inside the scalar field's action, leading to

$$S[z(t)] = \int dt \ -M_s + \frac{M_s}{2}\dot{z}^2(t). \tag{2.15}$$

The first term, corresponding to the solitonic background, is a constant and has no influence on the the equations of motion whereas the second term is nothing else then the action of a non-relativistic particle of mass M_s with position $z(t)$.

This collective coordinate allows indeed to handle the problems arising from the zero mode and hence to construct a quantum theory of this system. The nonzero modes can be combined into a usual quantum field by promoting it and its conjugate momentum to operators consisting of creation and annihilation operators. This new field ϕ underlies the constraint

$$\int \mathrm{d}x \ \phi(t,x)\Phi'(x) = 0. \tag{2.16}$$

Thus, the canonical commutation relations for $\delta\Phi$ and its conjugate momentum $\delta\Pi$ imply that these new field operators satisfy

$$[\hat{\phi}(t,x), \hat{\pi}(t,x')] = i\delta(x-x') - i\frac{f_0(x)f_0(x')}{M_{\mathrm{sol}}}. \tag{2.17}$$

This is only consistent with the canonical equations for $\delta\Phi$ and $\delta\Pi$ if the collective coordinate and its conjugate momentum p act as quantum mechanical operators,

$$[\hat{z}, \hat{p}] = i, \tag{2.18}$$

in perfect agreeement with their previous interpretation. From here, it follows that the position of the soliton is determined by some wave function $\Psi(t,x) \in L^2(\mathbb{R}, \mathrm{d}x)$ or, in momentum space, $\tilde{\Psi}(t,p) \in L^2(\mathbb{R}, \mathrm{d}p)$. This implies that the full quantum theory of the soliton is formulated on the Fock space $\mathbb{F} = L^2 \otimes \mathbb{F}_p$, where $\mathbb{F}_p$ denotes the Fock space generated by the $\{\hat{a}_k^\dagger\}_k$-operators.

This implies that, for the free theory, the dynamics of the system is split into the soliton's center-of-mass motion and the one of its localized, particle-like excitations. The dynamics along rotational and gauge moduli can be split off in a similar way.

This separation also translates to the theory of a soliton interacting with an external source. Consider the soliton together with some interaction term $\int \mathrm{d}x \ J(t,x)\Phi(t,x)$. Just as $\delta\Phi$, the current J can for any time t be decomposed in terms of the eigenfunctions of Ω^2,

$$J(t,x) = \sum\!\!\!\!\!\!\int_k j^k(t) f_k\big(x - z(t)\big) \equiv F(t) f_0\big(x - z(t)\big) + j\big(t, x - z(t)\big). \tag{2.19}$$

This splitting translates to the equations of motions for ϕ and $z(t)$, yielding

$$M_s \ddot{z}(t) = F(t) = -\frac{d}{dz} V(z) \tag{2.20}$$

$$(\partial_t^2 - \Omega^2)\phi(t,x) = j(t,x), \tag{2.21}$$

with the potential

$$V(z) = \int \mathrm{d}x \; J(t,x)\Phi_s(x - z(t)). \tag{2.22}$$

The consequences of these equations are discussed in great detail in [46].

Higher orders can treated most easily in the path integral formulation, which stands at the center of section 2.4. This approach has been developed in [50–52], while alternative perspectives have been explored in [53, 54].

2.2.1 A first attempt at unification

Amongst all of these perspectives, the one that will turn out most interesting for the discussions of the next chapter was developed in [53]. Similar to the canonical approach, it starts from the mode expansion of the fluctuation,

$$\delta\Phi(t,x) = \sum\!\!\!\!\!\!\int_k q^k(t) f_k(x). \tag{2.23}$$

The free theory can now fully be described in terms of the new parameters $\{q^k(t)\}_k$. Inserting (2.23) into the Hamiltonian of the fluctuation $\delta\Phi$ leads to $\{q^k(t)\}_k$,

$$H_0[q(t)] = M_{\mathrm{sol}} + \frac{1}{2} \sum\!\!\!\!\!\!\int_k (\dot{q}^k)^2(t) + \omega_k^2 (q^k)^2(t). \tag{2.24}$$

From the corresponding action follow the equations of motion,

$$\ddot{q}^k(t) = -\omega_k^2 q^k(t), \tag{2.25}$$

and the commutation relations satisfied by the fluctuation $\delta\Phi$ and its conjugate momentum lead to their pendants for the parameters q:

$$[q^m(t), \dot{q}^n(t)] \propto i\delta_{mn}, \tag{2.26}$$

$$[q^m(t), q^n(t)] = 0 = [\dot{q}^m(t), \dot{q}^n(t)]. \tag{2.27}$$

The main difference of this approach when compared with the usual introduction of a collective coordinate lies now in the intention to treat all the modes, including the zero mode, on an equal footing.

The solutions of the equation of motion (2.25) are given by

$$q^k(t) = \frac{1}{\sqrt{2\omega_k}} \left(a_k^\dagger e^{i\omega t} + a_k e^{-i\omega t} \right) \text{ for } k \neq 0 \tag{2.28}$$

$$q(t) \equiv q^0(t) = q_0 + v_0 t \text{ for } k = 0. \tag{2.29}$$

The $a_k^{(\dagger)}$-operators satisfy the usual commutation relations, so that the dynamics associated with the non-zero modes is equivalent to that obtained via the usual scheme involving a collective coordinate. For equal times, also the commutation relation of the collective coordinate is reproduced, as

$$[q(t), p(t)] = i \quad \text{and} \tag{2.30}$$
$$[q(t), q(t)] = 0 = [p(t), p(t')], \tag{2.31}$$

where $p(t) = M_{\text{sol}} v_0$. However, there are two essential differences. First, it is possible to obtain information about the commutator of the position operator $q(t)$ at different times,

$$[q(t), q(t')] = i M_{\text{sol}}^{-1}(t' - t). \tag{2.32}$$

Second, the relevant operators for the center-of-mass motion are q_0 and v_0, which can be understood as the soliton's initial position and velocity.

In order to analyze the perturbative expansion, one needs to find the propagators of the system's degrees of freedom. As each of the q^k is treated as a mechanical degree of freedom, each of them can be assigned a quantum mechanical propagator. These can be found to be

$$\begin{aligned} \Delta_0(t', t) &= -\frac{1}{2}|t' - t|, \\ \Delta_k(t', t) &= -\frac{i}{2\omega_k} e^{-i\omega_k |t'-t|} \text{ for } k \neq 0. \end{aligned} \tag{2.33}$$

These propagators can then be combined to obtain a propagator for the fluctuation $\delta\Phi$,

$$\Delta(t'x'; t, x) = \sum\!\!\!\!\!\!\int_k f_k(x') \Delta_k(t', t) f_k(x). \tag{2.34}$$

From this, the perturbative treatment of the interactions can be developed in the usual way.

These structures can be rediscovered in higher dimensions. For any symmetry broken due to the existence of the soliton, the spectrum of fluctuations obtains one zero mode, which can be treated by the introduction of a corresponding collective coordinate. This is discussed in the next subsection from the view of Goldstone's theorem.

2.2.2 Connection with Goldstone's theorem

Goldstone's theorem states that every spontaneously broken, continuous symmetry of a given theory manifests as a massless excitation in its spectrum [55]. It does so as a pole of the propagator at $p^2 = 0$, but also in the observation that the energy of this excitation disappears in the case of a vanishing three-momentum, $\lim_{p \to 0} E(p) = 0$, just as all interactions disappear. Such excitations are referred to as *Goldstone modes* or *Goldstone fields*,

the corresponding particles are called *Goldstone bosons*. This can be seen by considering a transformation of the action. Let the field content transform as

$$\Phi^m(x) \to \Phi^m(x) + q^a \Delta_a \Phi^m(x), \tag{2.35}$$

where m labels the different fields of the theory and $\Delta_a \Phi^m(x)$ denotes the action of the transformation's a^{th} generator on the field. The coefficients q^a are, depending on the setting, functions of certain coordinates. The symmetry is spontaneously broken if it leaves the (effective) action invariant, $\delta S[\Phi] = 0$, but not the configuration $\Phi_0^m(x^{n+1}, \dots x^d)$ around which the field is expanded. Here, d denotes the dimension of the underlying spacetime and $x^0 = t$. While this configuration is most frequently chosen to be some constant, it can also be some soliton-like background. For a proper soliton, this background is a function of all spatial coordinates, but there exist also configurations such a branes or strings, which are constant along certain spatial dimensions.

As the above action is a symmetry of the theory, it leaves the effective action invariant,

$$0 = \delta S[\Phi] = \int \mathrm{d}^d x \; \frac{\delta S[\Phi]}{\delta \Phi^m(x)} q^a \Delta_a \Phi^m(x), \tag{2.36}$$

and $\Delta_a \Phi^m(x) \neq 0$ as the symmetry is spontaneously broken. Taking a second functional derivative with respect to the field, one obtains

$$0 = \int \mathrm{d}^d x_1 \; \frac{\delta^2 S[\Phi]}{\delta \Phi^m(x_1) \delta \Phi^n(x_2)} q^a \Delta_a \Phi^m(x_1) + \frac{\delta S[\Phi]}{\delta \Phi^m(x_1)} q^a \frac{\delta \Delta_a \Phi^m(x_1)}{\delta \Phi^n(x_2)}. \tag{2.37}$$

Choosing as a background either a constant vacuum of the theory or a soliton-like configuration $\Phi_0(x^{n+1}, \dots x^d)$, the first functional derivative of the action disappears, and with it the second term in equation (2.37). As Φ_0 is only a function of $(x^{n+1}, \dots x^d)$, the same is true for $\Delta_a \Phi_0^m$. Therefore, for a general symmetry transformation, q^a is in general a function of the remaining $n+1$ spacetime coordinates, $q^a = q^a(x^0, \dots x^n)$, and equation (2.37) can be simplified to

$$0 = \int \mathrm{d}^d x_1^{n+1} \dots \mathrm{d}^d x_1^d \; \left. \frac{\delta^2 S[\Phi]}{\delta \Phi^m(x_1) \delta \Phi^n(x_2)} \right|_{\Phi = \Phi_0(x_1^{n+1}, \dots x_1^d)} \Delta_a \Phi^m(x_1^{n+1}, \dots x_1^d). \tag{2.38}$$

Now, considering the limit of vanishing momenta, the action reduces to the potential term and its functional derivative to

$$\left. \frac{\delta^2 S[\Phi]}{\delta \Phi^m(x_1) \delta \Phi^n(x_2)} \right|_{\Phi = \Phi_0(x_1^{n+1}, \dots x_1^d)} = -\frac{\partial^2 V}{\partial \Phi^m \partial \Phi^n} \big(\Phi_0(x_1^{n+1}, \dots x_1^d) \big) \delta^{(d)}(x_1 - x_2). \tag{2.39}$$

Hence (2.38) leads to

$$0 = -\frac{\partial^2 V}{\partial \Phi^m \partial \Phi^n} \big(\Phi_0(x^{n+1}, \dots x^d) \big) \Delta_a \Phi^m(x^{n+1}, \dots x^d). \tag{2.40}$$

Therefore $\Delta_a \Phi^m$ is a zero eigenvector of the mass matrix, which represents a massless excitation. As a result there exists one such excitation for any independent, broken generator[1]. The general form of such an excitation is then given by

$$\varphi^m(x) = q^a(x^0, \dots x^n)\Delta_a \Phi_0^m(x^{n+1}, \dots x^d), \tag{2.41}$$

where the fields $q^a(x^0, \dots x^n)$ are usually referred to as Goldstone fields or, in the context of soliton-like configurations, moduli fields. The crucial property of these fields is that they are only a function of the coordinates along which the translational symmetry is not broken. Physically speaking, they are functions of the configuration's worldvolume only, leading to the interpretation of them being confined to it.

As an example, consider the Lagrangian

$$\mathcal{L}(\Phi) = \partial_\mu \Phi^* \partial^\mu \Phi - \lambda \left(\frac{\nu^2}{2} - |\Phi|^2 \right)^2. \tag{2.42}$$

Picking the vacuum $\Phi_0 = \frac{\nu}{\sqrt{2}}$ for simplicity, the properly normalized Goldstone mode can be found to be $\varphi(t,x) = q(t,x) \cdot i\nu$, as the $U(1)$-transformation acts on ν via $\nu \to e^{iq(t,x)}\nu \simeq \nu + i\nu q(t,x)$. This Goldstone field can be made manifest in the parametrization

$$\Phi(t,x) = \frac{1}{\sqrt{2}}(\nu + \rho(t,x))e^{iq(t,x)}. \tag{2.43}$$

In terms of the real fields ρ and φ, the Lagrange density takes the form

$$\mathcal{L}(\rho,\varphi) = \frac{\nu^2}{2}\partial_\mu\varphi\partial^\mu\varphi + \frac{1}{2}\partial_\mu\rho\partial^\mu\rho - \frac{m_\rho^2}{2}\rho^2 + \frac{\rho^2}{2}\partial_\mu\varphi\partial^\mu\varphi + \nu\rho\partial_\mu\varphi\partial^\mu\varphi - \frac{\lambda}{4}\rho^4 - \lambda\nu\rho^3, \tag{2.44}$$

where $m_\rho^2 = 2\lambda\nu^2$. Therefore, the field φ enters only via its derivatives, thereby reproducing all the properties that are to be expected from a Goldstone mode.

The field $q(t,x)$ appears as a field on all of spacetime as the chosen vacuum breaks only the internal $U(1)$-symmetry, i.e. is a constant. Taking as another example a soliton in one spatial dimension, one finds a breaking of the full spatial translation symmetry of the system. The soliton transforms under a translation as

$$\Phi_s(x) \to \Phi_s(x - z(t)) \simeq \Phi_s(x) - \Phi_s'(x) \cdot z(t). \tag{2.45}$$

Due to the arguments above, the corresponding Goldstone field z is a function of time, $z(t)$, which is nothing but the collective coordinate.

A straightforward generalization of this example and the focal point of [61] are branes, i.e. configurations which take the form of a soliton along certain spatial dimensions

[1]Note that when considering spacetime translations, it is not guaranteed that all generators are independent. This is not relevant for this work, but discussed in great detail in [56–60].

$(x^1, \ldots, x^{n-1})$, while being constant along the remaining ones, $\Phi_s = \Phi_s(x^1, \ldots, x^{n-1})$. Therefore, they break the translational symmetry in the $(x^1, \ldots, x^{n-1})$-directions, so that the Goldstone fields are of the form $z^k(x^0, \ldots, x^n)$ and act on the brane as

$$\Phi_s \to \Phi_s(x^{n+1} - z^{n+1}(x^0, \ldots, x^n), \ldots x^d - z^d(x^0, \ldots, x^n). \tag{2.46}$$

In the context of soliton-like configurations, these are the well-known moduli fields.

2.3 The moduli space as a unified description of zero modes

As all solitonic zero modes can be treated in a very similar way, their descriptions can be unified into a single concept, the *moduli space*. Consider some arbitrary solitonic configuration involving N fields, $\{\Phi_0^i\}_i$, which can be both gauge and scalar fields. The by now well-established method of dealing with this configuration's zero modes would be to identify their corresponding symmetry parameters $\{z_a\}_a$, with $a \in \{1, ..., M\}$, and promote them to time-dependent parameters. The action describing the dynamics along these parameters can easily be obtained from the theory's underlying action. Further neglecting the dynamics of the non-zero modes, this leads to the action

$$\begin{aligned} S &= \int \mathrm{d}^4x \, \frac{1}{2} \sum_{i \in \text{scalars}} \partial_\mu \Phi_0^i(z(t), x) \partial^\mu \Phi_0^i(z(t), x) + (\text{gauge terms}) - V(\Phi_0(x)) = \\ &= \int \mathrm{d}^4x \, \frac{1}{2} \left(\sum_{i \in \text{scalars}} \partial_{z_a} \Phi_0^i(z(t), x) \partial_{z_b} \Phi_0^i(z(t), x) + (\text{gauge terms}) \right) \dot{z}^a \dot{z}^b + S[\Phi_0] = \\ &= \int \frac{1}{2} g_{ab} \dot{z}^a \dot{z}^b \mathrm{d}t + S[\Phi_0] \end{aligned} \tag{2.47}$$

This again looks the action of a point particle with a trajectory $z(t)$. The space of the *moduli* $\{z^a\}_a$, combining collective coordinates, gauge parameters and all other possible symmetry parameters, is usually referred to as *moduli space*. The object g_{ab} is called *moduli space metric*, and obtained through

$$g_{ab} = \int \mathrm{d}^3x \; \partial_{z_a} \Phi_0^i(z(t), x) \partial_{z_b} \Phi_0^i(z(t), x) + (\text{gauge terms}). \tag{2.48}$$

While the precise expression for the moduli space metric depends on the considered theory and soliton, the overall moduli Lagrangian is universal. In other words, the dynamics of any soliton's moduli is governed by a Lagrangian of the form

$$L(\dot{z}) = \frac{1}{2} g_{ab} \dot{z}^a \dot{z}^b. \tag{2.49}$$

This is not only perfectly reasonable from the point of view of an effective field theory, but could actually be expected. The kinetic term of the moduli, which is a relic of its analogue

in the underlying theory, is simply the lowest order term which can arise from a Lorentz invariant Lagrangian, and the degrees of freedom are simply the symmetry parameters of this theory. Thus, the information about the underlying theory necessary to set up this description is the number of symmetry parameters as well as a finite number of parameters determining g_{ab}.

Before building upon this simple yet powerful picture, it is worthwhile to understand the emergence and relevance of moduli beyond the simplest example of collective coordinates. Thus, the remainder of section investigates two important aspects, the interplay of collective coordinates with gauge invariance and the moduli dynamics of an internal symmetry, using instructive examples.

2.3.1 Collective coordinates in the presence of a gauge field

Going beyond a purely scalar soliton, one of the conceptually most interesting scenarios is the involvement of a gauge field, which is typically necessary to allow for the existence of a soliton in higher dimensions. The interplay between collective coordinates and gauge invariance can be understood most easily using the simple example of scalar field with a suitable potential which transforms under a gauged $U(1)$, which is described by the action [62]

$$S[\Phi] = \int d^4x \ (D_\mu \Phi)^* D^\mu \Phi - \frac{1}{4} F_{\mu\nu} F^{\mu\nu} - V(\Phi). \tag{2.50}$$

The analysis of this model can be notably simplified by performing it in temporal gauge, $A_0 = 0$, and embedding it into a five-dimensional auxiliary spacetime (x^0, x^M) with $M \in 1,2,3,4$ and $A = (A_0, A_1, A_2, A_3, \frac{\Phi}{\sqrt{2}})$ such that $\partial_4 A = 0$. In this spacetime the action of a scalar and a gauge field takes the form $S = \int d^4x \ -\frac{1}{4} F_{\aleph\beth} F^{\aleph\beth}$, where $\aleph, \beth \in 0,1,2,3,4$.

Following the usual procedure, the dynamics of this theory in the presence of a soliton can be described by considering fluctuations around it, $A_M = A^s_M + \delta A_M$. Doing so, a lengthy but straightforward computation leads to the linearized action of the fluctuations δA_M,

$$\begin{aligned} S[\delta A] = &\int d^4x \ \frac{1}{2} F_{OM} F_{OM} + \frac{1}{4} F_{MN} F_{MN} = \dots \\ =&S[A_s] + \int d^4x \ \frac{1}{2} \delta \dot{A}_M{}^2 + \frac{1}{2} \delta A_M (D_M D_N - \delta_{MN} D^2 + 3ig F^s_{MN}) \delta A_N = \\ =&S[A_s] + \int d^4x \ \frac{1}{2} \delta \dot{A}_M{}^2 + \frac{1}{2} \delta A_M L_{MN} \delta A_N. \end{aligned} \tag{2.51}$$

Thus, the collective coordinates are related to the three zero modes of the operator L_{MN},

$$\delta_a A_M = \frac{\partial A^s_M}{\partial x^a} - D_M \varepsilon_a, \tag{2.52}$$

which correspond to an infinitesimal translation up to an infinitesimal gauge transformation characterized by ϵ with $a \in \{1,2,3\}$.

The remaining infinitesimal gauge transformations can be used to set $D_M \delta_a A_M = 0$ by picking ε as $\varepsilon_a = A_a^s$, so that

$$\delta_a A_M = \frac{\partial A_M^s}{\partial x^a} - D_M A_a^s = F_{aM} \tag{2.53}$$

Thus, up to this infinitesimal gauge transformation, a general translation is to leading order described by

$$\delta A_M = -z^a \delta_a A_M. \tag{2.54}$$

The parameters $\{z^a\}_a$ can now again be treated as collective coordinates by promoting them to time-dependent parameters. Doing so and using that the $\delta_a A_M$ are zero modes, the action of these degrees of freedom ultimately becomes

$$\begin{aligned} S[\delta A] =& S[A_s] + \int dt \ \frac{1}{2}\left(\int d^3x \ \delta_a A_M \delta_b A_M \right) \dot{z}^a(t) \dot{z}^b(t) = \\ =& S[A_s] + \int dt \ \frac{1}{2} g_{ab} \dot{z}^a(t) \dot{z}^b(t), \end{aligned} \tag{2.55}$$

with the moduli space metric

$$g_{ab} = \int d^3x \ \delta_a A_M \delta_b A_M. \tag{2.56}$$

2.3.2 Skyrmions and field space rotations

The perhaps most relevant example for zero modes beyond a soliton's position are those related to the $SU(2)$-symmetry of the Skyrme model, which can be linked to the effective description of baryons therein.

The first step towards understanding these modes is of course to construct the underlying soliton, the *Skyrmion*, which can be found through the spherically symmetric hedgehog ansatz

$$U_S(x) = \exp\left(i \frac{x^i}{|x|} \tau_i \cdot F(|x|) \right). \tag{2.57}$$

Through this ansatz, the task of finding the soliton is reduced to determining the function $F(|x|) = F(r)$. On this level, equation (1.19) can be used to translate the condition that the topological charge Q_B take a certain to boundary conditions for $F(r)$. For $Q_B = 1$, it is straightforward to show that $F(0) = \pi$ and $F(r \to \infty) = 0$ must be satisfied. The soliton is then obtained by choosing $F(r)$ such that the energy arising from (1.16) is minimized with these boundary conditions. The energy as a functional of F can be obtained through a straightforward computation which yields [13]

$$E[F] = \frac{2\pi f_\pi}{e} \int_0^\infty dx \ x^2 (F')^2 + \sin^2(F) \left(2 + 2(F')^2 + \frac{\sin^2(F)}{x^2} \right). \tag{2.58}$$

From here, the profile F can be found as the configuration minimizing $E(F)$, which is equivalent to it being a solution to the differential equation

$$-(x^2F' - 2F'\sin^2(F))' + \sin(2F)\left(1 + (F')^2 + \frac{\sin^2(F)}{x^2}\right) = 0 \tag{2.59}$$

This equation can be solved numerically, as is done, e.g., in [13]. Plugging this solution back into (2.58) one finds that $E[F_{min}] = M_S \approx 73\frac{f_\pi}{e}$. As a side result, this provides a relation between the energy - and thus mass - of the Skyrmion to its size, which scales with f_π^{-1}.

The zero modes corresponding to infinitesimal translations can be treated in a similar way as in all previous cases. Besides them, the solution also gives rise to zero modes related to $SU(2)$ transformations of the Skyrmion,

$$U_S \to AU_SA^\dagger, \tag{2.60}$$

which through the standard relation between $SU(2)$ and $SO(3)$ also contain spatial rotations. Following the established procedure, these modes can be treated through the replacement $A \to A(t)$, leading to an action of the form

$$S[A] = \int dt\ \lambda \cdot \mathrm{tr}\big(\dot{A}(t)\dot{A}^\dagger(t)\big) - M_S + O(\dot{A}^4), \tag{2.61}$$

with a numerical prefactor roughly given by $\lambda \approx \frac{53}{e^3 f_\pi}$. To further stress out the similarity with the translational zero modes, A can be parametrized using the so-called *Cayley-Klein parameters* $\{a^i\}_i$ [63], in terms of which it can represented as

$$A(t) = a^0(t)\mathbb{1} + ia^i(t)\tau_i, \tag{2.62}$$

where

$$\sum_{b=0}^{3}(a^b)^2 = 1. \tag{2.63}$$

In terms of the as, the kinetic term of the action can be rewritten as

$$S[a] = \int dt\ 2\lambda \cdot \sum_{b=0}^{3}(\dot{a}^b)^2 + O(\dot{a}^4). \tag{2.64}$$

Together with the constraint (2.63), this action can be identified with that of a point-particle of mass $m = 4\lambda$ moving on a 3-sphere embedded in a four-dimensional space parametrized by the Cayley-Klein parameters.

The physical consequences of this sector of the dynamics is clearest in the quantum theory. As a first step towards its construction, the conjugate momenta of the parameters $\{a^i\}_i$

need to be determined, leading to $\pi_i = \frac{\partial L}{\partial \dot{a}^i} = 4\lambda \dot{a}^i$. In terms of these, the Hamilton operator of the system takes the form

$$H = \pi_i \dot{a}^i - L = 2\lambda(\dot{a}^i)^2 + M_S = M_S + \frac{1}{8\lambda}\sum_{i=0}^{3}\pi_i^2. \tag{2.65}$$

Moving to the analogue of position space in which the $\{\hat{a}^i\}_i$-operators act as multiplication operators, the momentum operators can be represented by $\pi_i \to -i\frac{\partial}{\partial a^i}$. Therefore, the corresponding Hamilton operator is given by

$$\hat{H} = M - \frac{1}{8\lambda}\sum_{i=0}^{3}\left(\frac{\partial}{\partial a^i}\right)^2 = M - \frac{1}{8\lambda}\Delta_{S^3} \tag{2.66}$$

The spectrum of Δ_{S^3}, and thus the eigenfunctions of the Hamiltonian, are the well-known hyperspherical harmonics. Thus, the eigenstates of the Hamiltonian are of the form $|i,j;n\rangle \doteq (a^i + ia^j)^n$, satisfying $-\Delta_{S^3}(a^i + ia^j)^n = n(n+2)(a^i + ia^j)^n$. This implies that the energies of these eigenstates are given by

$$E = \langle i,j;n|\hat{H}|i,j;n\rangle = M_S + \frac{n(n+2)}{8\lambda} \tag{2.67}$$

In other words, these low-energy excitations of the soliton induce an increase of its "angular momentum" in gauge space, which would manifest in a correction to the soliton's mass.

2.4 Path integral analysis & Relativistic collective coordinates

To leading order, the moduli Lagrangian is given by (2.49). However, considering for example the last example discussed in section 2.3.2, it is clear than for a general theory also higher order terms need to be taken into account,

$$L(\dot{z}) \to \frac{1}{2}g_{ab}\dot{z}^a\dot{z}^b + O(\dot{z}^4). \tag{2.68}$$

Returning to the more general perspective of this Lagrangian as a low-energy effective field theory, such higher order terms in $\dot{z}$ are of course not surprising. To be more precise, for the special case of collective coordinates it can actually be expected. Although the Lagrangian (2.49) arises from a Lorentz invariant theory, it appears to violate this symmetry. This tension has been resolved in [64, 65], whose arguments are summarized throughout this section. Considering for simplicity the example of a scalar field in one spatial dimension, Lorentz invariance suggests that the dynamics of the collective coordinate should be described by a Hamiltonian of the form

$$H = \sqrt{M_s^2 + p^2}. \tag{2.69}$$

To obtain such a Hamiltonian, higher order terms in the collective coordinate velocities $\dot{z}$ are necessary. Again falling back to the perspective of effective field theories, the natural origin of such terms would be as remnants of the non-zero modes once they have been integrated out. This would also be consistent with the discussions in sections 2.2 and 2.3, where these modes have simply been set to zero, which is of course not necessarily accurate already at tree-level.

For a single scalar field, the Lagrangian can be related to the Hamiltonian density through

$$\mathcal{L} = \pi\dot{\Phi} - \mathcal{H}, \tag{2.70}$$

where π denotes the canonical momentum of the field Φ and $\mathcal{H}$ is given by

$$\mathcal{H}(\Phi,\pi) = \frac{1}{2}\big(\pi^2 + (\Phi')^2\big) + V(\Phi) \tag{2.71}$$

Describing the quantum theory in terms of wave functionals $\Psi[\Phi]$, the transition amplitude for two states $\Psi_i[\Phi(t\to-\infty,x)]$ and $\Psi_f^*[\Phi(t\to+\infty,x)]$ is given by the path integral

$$A_{fi} \propto \int \mathrm{D}\Phi \int \mathrm{D}\pi\ e^{i\int \mathrm{d}^2x\mathcal{L}}\Psi_f^*[\Phi(t\to+\infty,x)]\Psi_i[\Phi(t\to-\infty,x)]. \tag{2.72}$$

The collective coordinate z and its momentum p can now be introduced as degrees of freedom by inserting a factor of 1 inside the functional integral, similar to the gauge fixing procedure. The momentum p should be identical up to a sign with that initially carried by the field, which can be made manifest through the constraint $p+P=0$, where $P=\int dx\ \pi\Phi'$. The condition for z is given by some function $Q(z)=0$, which can be left arbitrary. Doing this the transition amplitude becomes

$$\begin{aligned} A_{fi} \propto \int \mathrm{D}\Phi\mathrm{D}\pi\bigg(\int \mathrm{D}p\ \delta(p+P)\bigg)\bigg(\int \mathrm{D}z\ \delta(Q(z))\frac{\delta Q}{\delta z}\bigg)\cdot \\ \cdot\exp\bigg(i\int dt\bigg(\int \pi\dot{\Phi}\ dx - H[\Phi,\pi]\bigg)\bigg)\Psi_f^*[\Phi(t\to+\infty,x)]\Psi_i[\Phi(t\to-\infty,x)]. \end{aligned} \tag{2.73}$$

Now z and p can be extracted from the fields in the action. It is easy to see that

$$\dot{\Phi}(t,x) = \partial_t\big(\tilde{\Phi}(t,x-z(t))\big) = -\tilde{\Phi}'(t,\xi)\dot{x} + \dot{\tilde{\Phi}}(t,\xi), \tag{2.74}$$

and hence,

$$\pi(t,x)\dot{\Phi}(t,x) = -\tilde{\pi}(t,\xi)\tilde{\Phi}'(t,\xi)\dot{z} + \tilde{\pi}(t,\xi)\dot{\tilde{\Phi}}(t,\xi). \tag{2.75}$$

As a consequence, the first term of the Lagrange function $\int \pi\dot{\Phi}\ \mathrm{d}x - H[\Phi,\pi]$ becomes

$$\int \mathrm{d}x\ \pi(t,x)\dot{\Phi}(t,x) = -\int \mathrm{d}x\ \tilde{\pi}(t,\xi)\tilde{\Phi}'(t,\xi)\dot{z}(t) + \tilde{\pi}(t,\xi)\dot{\tilde{\Phi}}(t,\xi). \tag{2.76}$$

Recall now that $\int \mathrm{d}t\mathrm{d}x = \int \mathrm{d}t\mathrm{d}\xi$ and that the constraint was given by $p + P = 0$. This implies that

$$\int \mathrm{d}x\ \tilde{\pi}(t,\xi)\tilde{\Phi}'(t,\xi) = \int \mathrm{d}\xi\ \tilde{\pi}(t,\xi)\tilde{\Phi}'(t,\xi) = \int \mathrm{d}x\ \pi(t,x)\Phi'(t,x) = P = -p \tag{2.77}$$

and $H[\Phi,\pi] = H[\tilde{\Phi},\tilde{\pi}]$. This means that the Lagrange function can be rewritten as

$$L = \int \pi\dot{\Phi}\ \mathrm{d}x - H[\Phi,\pi] = p\dot{z} + \int \tilde{\pi}\dot{\tilde{\Phi}}\mathrm{d}\xi - H[\tilde{\Phi},\tilde{\pi}]. \tag{2.78}$$

This recasting also has an effect on the wave functionals. Extracting the degree of freedom z from the field can be understood as decomposing the initial Hilbert-space $\mathbb{H}_\Phi$ into $\mathbb{H}_\Phi = \mathbb{H}_z \otimes \mathbb{H}_{\tilde{\Phi}}$ where $\mathbb{H}_{\tilde{\Phi}}$ denotes the Hilbert space of all wave functionals $\Psi[\Phi]$ together with the equivalence relation $\Phi \sim \Phi'$ if $\Phi(x) = \Phi'(x - z(t))$. Hence, the wave functional $\Psi[\Phi]$ can be rewritten as $\Psi[\Phi] = \Psi[\tilde{\Phi}] \cdot \psi_p(z)$, where $\psi_p(z)$ is the wave function of the degree of freedom $z(t)$. As is known from ordinary quantum mechanics, the wave function of a particle of momentum p is given by $\psi_p(z) = e^{ipz}$. Therefore, the wave functionals of the initial and final state are, assuming them to carry definite momentum, given by

$$\Psi[\Phi(t_i)] = \Psi[\tilde{\Phi}(t_i)] \cdot e^{ip_i z(t_i)} \tag{2.79}$$

$$\Psi[\Phi(t_f)] = \Psi[\tilde{\Phi}(t_f)] \cdot e^{ip_f z(t_f)}. \tag{2.80}$$

Thus, the amplitude for the transition between these states takes the form

$$\begin{aligned} A_{fi} \propto \int \mathrm{D}\tilde{\Phi}\mathrm{D}\tilde{\pi}\mathrm{D}z\mathrm{D}p\ \delta(p+P)\delta(Q(z))\frac{\delta Q}{\delta z}\exp\left(i\int \mathrm{d}t\left(p\dot{z} + \int \tilde{\pi}\dot{\tilde{\Phi}}\ \mathrm{d}\xi - H[\tilde{\Phi},\tilde{\pi}]\right)\right)\cdot \\ \cdot \Psi_f^*[\tilde{\Phi}(t\to+\infty,x)]\Psi_i[\tilde{\Phi}(t\to-\infty,x)]e^{ip_i z(t_i) - ip_f z(t_f)}. \end{aligned} \tag{2.81}$$

The phase factors from the wave functionals can now be combined with the p-dependent term in the first line, leading to

$$\int p\dot{z}\ dt + p_i z(t_i) - p_f z(t_f) = -\int \mathrm{d}t\ \dot{p}z. \tag{2.82}$$

As this is now the only remaining z-dependence, the corresponding path integral can be easily evaluated by decomposing $z(t)$ as $z(t) = \sum_n z^n e_n(t)$, with an arbitrary orthonormal basis $\{e_n\}_n$. The same can be done for $\dot{p}$, $\dot{p} = \sum_n \dot{p}^n e_n$. Thus, the functional integral can be rewritten as an integral over the expansion coefficients $\{z^n\}_n$:

$$\int \mathrm{D}z\ \exp\left(-i\int \dot{p}z\ \mathrm{d}t\right) = \int \prod_i \mathrm{d}z^i\ \exp\left(-i\sum_n \dot{p}^n z^n\right) = \prod_i \delta(\dot{p}^i) = \delta(\dot{p}) \tag{2.83}$$

This is nothing else than the conservation of the center of mass momentum p, i.e., $p_f = p_i = p$. Hence, the p-integral can be evaluated trivially and the transition amplitude becomes

$$\begin{aligned} A_{fi} \propto \int \mathrm{D}\tilde{\Phi}\mathrm{D}\tilde{\pi}\ \delta(p+P)\delta(p_f - p_i)\delta(Q)\frac{\delta Q}{\delta z}\cdot \\ \cdot \exp\left(i\int \mathrm{d}t\left(\int \tilde{\pi}\dot{\tilde{\Phi}}\ \mathrm{d}x - H[\tilde{\Phi},\tilde{\pi}]\right)\right)\Psi_f^*[\tilde{\Phi}(t\to+\infty,x)]\Psi_i[\tilde{\Phi}(t\to-\infty,x)]. \end{aligned} \tag{2.84}$$

The tree level results can be obtained by variation of the action

$$\tilde{S}[\tilde{\Phi},\tilde{\pi}] = \int \mathrm{d}t \left(\int \tilde{\pi}\dot{\tilde{\Phi}}\ \mathrm{d}x - H[\tilde{\Phi},\tilde{\pi}] \right) \tag{2.85}$$

together with the constraint $p + P = 0$, which can be implemented into the action using a Lagrange multiplier $\lambda(t)$. Hence, the full functional that has to be considered is given by

$$S_{\text{eff}} = \int \tilde{\pi}\dot{\tilde{\Phi}} - \frac{1}{2}\tilde{\pi}^2 - \frac{1}{2}(\tilde{\Phi}')^2 - V(\tilde{\Phi})\ \mathrm{d}^2\xi + \int \mathrm{d}t\ \lambda\left(p + \int \tilde{\pi}\tilde{\Phi}'\ \mathrm{d}\xi\right). \tag{2.86}$$

In the case of a single soliton one can always find a static solution, i.e. $\dot{\tilde{\Phi}} = 0 = \dot{\tilde{\pi}}$ as the time-dependence through $z(t)$ has been extracted. Varying (2.86) with respect to λ and the remaining degrees of freedom $\tilde{\Phi}$ and $\tilde{\pi}$ then yields the following equations of motion:

$$0 = p + \int d\xi\ \tilde{\pi}\tilde{\Phi}' \tag{2.87}$$

$$0 = -\tilde{\pi} + \lambda\tilde{\Phi}' \tag{2.88}$$

$$0 = \tilde{\Phi}'' - V'(\tilde{\Phi}) - \lambda\tilde{\pi}' \tag{2.89}$$

The second equation can be used to eliminate $\tilde{\pi}$, leaving only two equations:

$$p = -\lambda \int d\xi\ (\tilde{\Phi}')^2, \tag{2.90}$$

$$0 = (1-\lambda^2)\tilde{\Phi}'' - V'(\tilde{\Phi}). \tag{2.91}$$

Equation (2.91) is solved by function of the form

$$\tilde{\Phi}(\xi) = \Phi_s\left(\frac{1}{\sqrt{1-\lambda^2}}\cdot\xi\right), \tag{2.92}$$

so that it remains to determine λ, and with it the coefficient inside the argument. Using equation (2.90), it is easy to see that it is given by

$$\frac{1}{\sqrt{1-\lambda^2}} = \sqrt{1+\frac{p^2}{M_s^2}} = \gamma. \tag{2.93}$$

Inserting this into the solution (2.92) and restoring the original coordinates, the solution is finally given by

$$\Phi(x) = \Phi_s\left(\sqrt{1+\frac{p^2}{M_s^2}}\xi\right) = \Phi_s\big(\gamma(x-z(t))\big). \tag{2.94}$$

Although the additional factor γ already hints at relativity being restored, this can be seen more clearly by considering the Hamiltonian of the collective coordinate. The field's canonical momentum can be obtained from (2.88), leading to

$$\tilde{\pi}(\xi) = -\frac{p}{\sqrt{p^2+M_s^2}}\tilde{\Phi}'. \tag{2.95}$$

Inserting this relation as well as (2.94) into the total Hamiltonian yields the Hamiltonian of the collective coordinate, which, as expected, reproduces that of a relativistic point particle:

$$H = \int d\xi \, \frac{1}{2}\tilde{\pi}^2(\xi) + \frac{1}{2}(\tilde{\Phi}')^2 + V(\tilde{\Phi}) = \sqrt{M_s^2 + p^2} \tag{2.96}$$

Chapter 3

A new perspective on moduli spaces

The results discussed in this section have been previously published in [1].

Moduli fields play a central role in each study of topological solitons. An interesting perspective on them is as an effective field theory of their underlying theory's low-energy dynamics. Their most appealing property in this context is that their dynamics are independent of most of the underlying theory's specifics, including but not limited to the precise shape of the soliton, the types of fields involved in its formation, the interactions between them, and even the theory's topological characteristics. On this level, the moduli space metric contains all of the information regarding these features.

In other words, knowing the number of moduli and a few parameters is all that is required to acquire a complete description of the system's low-energy dynamics. This theory's simplicity relates to the interpretation of solitons as particle-like entities. On sufficiently large scales, any soliton can be considered as an approximate point particle, or in the case of higher-dimensional objects, a string or domain wall.

When non-zero modes are included, this universality breaks down as the theory of non-zero modes is highly dependent on the type of participating fields as well as their interactions. This chapter describes a method for maintaining the universality of the moduli field description while also covering a sub-sector of the dynamics associated with non-zero modes. As long as the examined configurations are confined sufficiently near to the soliton's center, this technique is viable for all energies allowed by the underlying theory.

3.1 Motivation

Consider the example of a $(1+1)$-dimensional soliton and its collective coordinate, $\Phi_s(x - z(t))$. While the collective coordinate is merely a function of time, the fluctuation

that corresponds to it spans all of spacetime and decays as $\Phi_s'(x)$ for $x \to \infty$. As a result, it is primarily prevalent in the same region as the soliton. Assume that this soliton is interacting with a localized external source that contains both zero and non-zero mode contributions. Such an interaction alters $z(t)$'s equation of motion, hence altering $\dot{z}(t)$. Because $z(t)$ is merely a function of time, yet the fluctuation it causes covers all of space, information about the excitation seems to propagate instantly, in tension with causality. In this case, though, there is no issue. The source necessary for such an interaction is a superposition of the zero as well as the non-zero modes, and would thus excite all the involved modes. As a result, the ensuing excitation can be confined inside the interaction zone. This implies that the soliton only starts to move in the region where the interaction is taking place as soon as the interaction begins.

This excitation then spreads with a velocity smaller than one, causing larger and larger parts of the soliton to move. The soliton is warped during this process as different sections of it move at different speeds. This can be formalized by substituting a local object for the collective coordinate,

$$z(t) \to \mu_m^{-1}\varphi(t,x), \tag{3.1}$$

where an additional factor of μ_m of energy dimension one has been introduced to obtain a dimensionless quantity, the *warp field*.

This field contains the information about the *local velocity*, which in some point x_0 is given by $\mu_m^{-1}\dot{\varphi}(t,x_0)$. Two factors are expected to contribute to this velocity. First, there is a *global velocity* v, which comes from the collective coordinate's dynamics. Second, a local velocity that is governed by the non-zero modes' dynamics.

The width of the soliton provides a another perspective on such a structure. It is generally understood that giving enough energy to any soliton-like configuration causes a (space)-time dependent fluctuation of its thickness [44], which eventually decays into particles. The warp fields might be thought of as an attempt to compactly represent this process.

3.2 Classical warp fields in 1+1 dimensions

3.2.1 Convention and notations

Throughout this section, the potential generating the soliton will be assumed to be symmetric, $V(\Phi) = V(-\Phi)$, with two distinct vacua $\pm\nu$. The considered soliton carries topological charge one, so that a frame exists in which it is static, $\Phi_s = \Phi_s(x)$. This allows to make the scales involved in the soliton manifest through the representation

$$\Phi_s(x) = \nu\sigma(\mu_m x), \tag{3.2}$$

where $\mu_m \propto m_\Phi$ characterizes the localization of the soliton. σ encodes the profile of the soliton, and is in general restricted by $|\sigma(\mu_m x)| < 1$, while σ' denotes its derivative with

respect to the dimensionless argument. A general fluctuation of this background will be denoted by $\delta\Phi$, $\Phi(t,x) = \Phi_s(x) + \delta\Phi(t,x)$, while a fluctuation generated by non-zero modes only will be denoted by ϕ, so that $\Phi(t,x) = \Phi_s(x - z(t)) + \phi(t,x)$.

Two distinct frameworks are discussed in this chapter: one in which the dynamical degrees of freedom are described in terms of ϕ and the collective coordinate, and one in which the warp field φ plays this role. The classical dynamics occur in the first scenario on the phase space of ϕ, denoted by $\mathbb{P}$. The quantum theory unfolds on the Fock space, $\mathbb{F}$, on which the field operators act. The analogous phase and Fock space are labelled $\mathcal{P}$ and $\mathcal{F}$ when φ is used as the degree of freedom.

In general, the linearized equation of motion for ϕ is of the form

$$\big(\partial_t^2 + K^2\big)\phi = 0, \tag{3.3}$$

with an operator K^2 which summarizes derivatives with respect to the position x as well as functions of x. The eigenfunctions of such operators will just as in chapter 2 be labelled $\{f_k\}_k$, allowing to expand ϕ as a linear combination of them through $\phi = \sum\!\!\!\!\!\!\int_k a_k^\dagger e^{i\omega_k t} f_k^* + h.c.$, with some complex coefficients $\{a_k\}_k$. The spectrum of such operators typically consists of both a continuous and a discrete part, and $\sum\!\!\!\!\!\!\int$ refers to the sum over the discrete part and integration over the continuous part, as well as normalization factors where necessary.

The pendant of (3.3) for the warp field will turn out to be of a similar form,

$$\big(\partial_t^2 + \mathcal{K}^2\big)\phi = 0, \tag{3.4}$$

while the eigenfunctions of their operator $\mathcal{K}$ will be labelled $\{g_k\}_k$, the corresponding eigenvalues by ω_k^2.

3.2.2 General dynamics

The action of the warp field can be obtained directly from that of the warped soliton,

$$\Phi(t,x) = \Phi_s(x - \mu_m^{-1}\varphi(t,x)), \tag{3.5}$$

leading to

$$S = \int \mathrm{d}^2x\ \frac{1}{2}\nu^2\big(\sigma'(\mu_m x - \varphi)\big)^2\big(\dot\varphi^2 - (\varphi')^2 - \mu_m^2 + 2\mu_m\varphi'\big) - V\big(\nu\sigma(\mu_m x - \varphi)\big). \tag{3.6}$$

In terms of the dimensionless coordinates $\xi = \mu_m x - \varphi$, Bogomolnyi's equation implies that $\sqrt{2V(\xi)} = \mu_m\nu\sigma'(\xi)$. Thus, it is possible to eliminate the potential from the action (3.6), which thus simplifies to

$$S = \int \mathrm{d}^2x \frac{1}{2}\nu^2\big(\sigma'(\xi)\big)^2\partial_\mu\varphi\partial^\mu\varphi + \nu^2\big(\sigma'(\xi)\big)^2\big(-\mu_m^2 + \mu_m\varphi'\big). \tag{3.7}$$

The second term can now be further simplified by evaluating the spatial integral,

$$\begin{aligned}\int \mathrm{d}x\ \nu^2\big(\sigma'(\xi)\big)^2\big(-\mu_m^2+\mu_m\varphi'\big) &= -\mu_m\int \mathrm{d}x\frac{d\xi}{dx}\ \nu^2\big(\sigma'(\xi)\big)^2 = \\ &= -\int \mathrm{d}\xi\ \mu_m\nu^2\big(\sigma'(\xi)\big)^2 = -M_{\mathrm{sol}} = L[\Phi_s]\end{aligned} \tag{3.8}$$

As a result, the action of the warped soliton, and thus the warp field, takes the compact form

$$S = S[\Phi_s] + \int \mathrm{d}^2x\frac{1}{2}\nu^2\big(\sigma'(\xi)\big)^2\partial_\mu\varphi\partial^\mu\varphi. \tag{3.9}$$

This action resembles that of a typical massless scalar field up to an additional weigth function $\rho(x,\varphi(t,x)) = \nu^2\big(\sigma'(\xi)\big)^2$. Thus, this approach allows to encode all interactions of the underlying theory through a single weight function, which takes the role of the moduli space metric.

In this picture, the perturbative treatment of the theory corresponds to a series expansion of $\rho(x,\varphi)$ in φ, leading to one kinetic as well as infinitely many interaction terms:

$$\mathcal{L}_0 = \frac{1}{2}\nu^2\big(\sigma'(\mu_m x)\big)^2\partial_\mu\varphi\partial^\mu\varphi, \tag{3.10}$$

$$\mathcal{L}_{\mathrm{int}}^{(n)} = \frac{(-1)^n}{2\cdot n!}\nu^2\Big(\big(\sigma'(\mu_m x)\big)^2\Big)^{(n)}\varphi^n\partial_\mu\varphi\partial^\mu\varphi, \tag{3.11}$$

where (n) means the n^{th} derivative with respect to the dimensionless argument $\mu_m x$. An interesting property of this action that it vanishes in the limit $\partial\varphi \to 0$, mimicking the behavior of a Goldstone field.

From this Lagrangian follows the equation of motion,

$$\Box\varphi = \frac{\sigma''(\xi)}{\sigma'(\xi)}\big(\partial_\mu\varphi\partial^\mu\varphi + 2\mu_m\varphi'\big), \tag{3.12}$$

as well as the warp field's canonical momentum ϖ,

$$\varpi(t,x) = \nu^2\big(\sigma'(\xi)\big)^2\dot\varphi(t,x) = \rho(x,\varphi(t,x))\dot\varphi(t,x), \tag{3.13}$$

and its energy-momentum tensor,

$$T^\mu_\nu = \nu^2\big(\sigma'(\xi)\big)^2\left(\partial^\mu\varphi\partial_\nu\varphi - \delta^\mu_\nu\frac{1}{2}\partial^\alpha\varphi\partial_\alpha\varphi\right) = \rho(x,\varphi(t,x))\left(\partial^\mu\varphi\partial_\nu\varphi - \delta^\mu_\nu\frac{1}{2}\partial^\alpha\varphi\partial_\alpha\varphi\right). \tag{3.14}$$

As could be expected based on (3.9), both the conjugate momentum as well as the energy-momentum tensor are identical to that of a free scalar field up to the weight factor ρ.

While not necessary for the discussion of the classical theory, it will prove helpful for the interpretation of the quantum theory to rewrite this action as that of a free scalar field together with a space- and field-dependent integration measure,

$$S[\varphi] = \frac{1}{2}\int \mathrm{d}^2\varsigma_\varphi(x)\partial_\mu\varphi\partial^\mu\varphi, \text{ where } \mathrm{d}^2\varsigma_\varphi(x) = \nu^2\big(\sigma'(\mu_m x-\varphi)\big)^2\mathrm{d}x\mathrm{d}t. \tag{3.15}$$

3.2.3 Essentials of the linearized theory

As a first step, it is advisable to concentrate on the linearized theory to avoid the technical challenges caused by the unlimited number of interaction terms and to prepare for the canonical quantization of this system. This theory provides a reliable description of the system as long as φ is sufficiently small. Using equation (3.10) and (3.11), this can be expected to be true as long as

$$|\varphi(t,x)| \ll \left| n! \frac{\big(\sigma'(\mu_m x)\big)^2}{\big((\sigma'(\mu_m x))^2\big)^{(n)}} \right|^{1/n} \quad \forall n \in \mathbb{N}. \tag{3.16}$$

Taking as an example the usual Φ^4-theory with a Higgs-like potential, it is easy to see that the right-hand side of this equation is bounded from below by $\frac{1}{4}$. Similarly, for the Sine-Gordon model this bound is given by $\frac{1}{2}$. Note that it is, in all theories, always possible to shift φ by a constant, which can be absorbed into the background soliton.

At quadratic order, the action is structurally very similar to its pendant in the full theory,

$$S[\varphi] = \int \mathrm{d}^2x \; \frac{1}{2}\nu^2\big(\sigma'(\mu_m x)\big)^2 \partial_\mu\varphi\partial^\mu\varphi, \tag{3.17}$$

while the equation of motion can be brought to the usual form of a linearized theory,

$$\begin{gathered} \big(\partial_t^2 + \mathcal{K}^2\big)\varphi = 0, \text{ with} \\ \mathcal{K}^2 := -\partial_x^2 - 2\mu_m \frac{\sigma''}{\sigma'}(\mu_m x)\partial_x. \end{gathered} \tag{3.18}$$

The dynamics described by this equation is determined by the properties of the operator $\mathcal{K}^2$. Although it is not hermitian in the usual sense, it is so with respect to the weighted spatial measure $\mathrm{d}\varsigma := \nu^2\big(\sigma'(\mu_m x)\big)^2\mathrm{d}x = \mathrm{d}\varsigma|_{\varphi=0}$. This implies that the eigenfunctions of $\mathcal{K}^2$ form a complete basis and can be orthonormalized with respect to $\mathrm{d}\varsigma$.

Using the relation between ϕ and φ in the linearized theory, it is easy to see that the eigenfunctions of $\mathcal{K}$ are related to those of K in the ϕ-picture through

$$g_k(x) = \frac{f_k(x)}{\nu\sigma'(\mu_m x)} = \rho^{-1/2}(x)\cdot f_k(x). \tag{3.19}$$

These functions can be used to obtain a simple expression for a general solution of (3.18) similar to that of a usual, free scalar field,

$$\varphi(t,x) = \sum\!\!\!\!\!\!\int_{k\neq 0} \alpha_k^* e^{i\omega_k t} g_k^*(x) + \alpha_k e^{-i\omega_k t} g_k(x) + \mu_m v(t-t_0) + \mu_m\zeta. \tag{3.20}$$

The two real parameters v and ζ are of mass dimension 0 and -1 respectively. ζ describes the zero mode, while vt lies in the kernels of both ∂_t^2 and $\mathcal{K}^2$. While ζ describes the soliton's position, the term linear in time leads to a motion of the soliton with constant velocity.

In principle, similar terms would also arise for a usual free scalar field but are usually dropped due to their asymptotic behavior. However, as φ is not canonically normalized, the additional factor of $\rho(x) = \nu^2(\sigma')^2(\mu_m x)$ in the action ensures that their contribution to the action as well as all observables derived from it are finite. Another important property of the expansion (3.20) is the implementation of the solutions' asymptotic behavior. The localization of the soliton implies that $\sigma'(\mu_m x) \to 0$ for $|x| \to \infty$, and thus also $g_k \to \infty$ in this limit. But this does not necessarily apply to φ, as it is possible to choose the coefficients $\{\alpha_k\}_k$ such that $\varphi \to 0$ for $|x| \to \infty$. This observation is crucial for the consistency of the linearized theory, as an asymptotically divergent solution would be in contradiction with the condition (3.16).

The term linear in t is similarly affected by the condition (3.16). It can be proved that this terms implies that the linear approximation is valid only for finite times. Assuming that the right hand side of (3.16) is bounded from below by some constant b, this can be made manifest by demanding that the size of the considered time interval, centered around t_0, satisfies

$$|T| \ll \frac{b}{\mu_m |v|}. \tag{3.21}$$

This inequality can alternatively represented as an upper bound on the velocity for a given time interval of interest,

$$|v| \ll \frac{b}{\mu_m |T|}. \tag{3.22}$$

The effects of larger velocities can then be included perturbatively using v as expansion parameter. Starting from $\varphi^{(1)} = \mu_m v t$, the resulting perturbative series converges to

$$\varphi(t,x) = \mu_m\big(x - \gamma(x - vt)\big), \tag{3.23}$$

thus reproducing the motion of the soliton for relativistic velocities,

$$\Phi_s(x - \varphi(t,x)) = \Phi_s(\gamma(x - vt)). \tag{3.24}$$

3.2.4 Connection to the full linearized theory

A crucial question underlying this discussion is which parts of the full theory's dynamics can actually be recovered through the parametrization in terms of the warp field. As the zero mode can be identified with the collective coordinate, this section is focused on the non-zero modes of φ. Moving to a description in terms of the warp field corresponds, on the linearized level, to a straightforward field redefinition

$$\phi(t,x) \to -\nu\sigma'(\mu_m x)\varphi(t,x). \tag{3.25}$$

This map can be understood as a map r connecting the phase space of the φ-theory $\mathcal{P}$ with its pendant for the ϕ-theory, $\mathbb{P}$. Formally, this corresponds to

$$\begin{aligned} r : \mathcal{P} &\to \mathbb{P} \\ \big(\varphi(x), \varpi(x)\big) &\mapsto \big(r_\phi[\varphi](x), r_\pi[\varpi](x)\big) \equiv \big(-\rho^{1/2}(x)\cdot\varphi(x), -\rho^{-1/2}(x)\cdot\varpi(x)\big), \end{aligned} \tag{3.26}$$

which amounts to an embedding of the φ-phase space into the ϕ-phase space. An important feature of this map is that it converts the mode functions $\{g_k\}_k$ to their pendants $\{f_k\}_k$, leaving the eigenvalue with respect to the kinetic operator unchanged. The image of any solution of the linearized equation of motion for φ is therefore a solution of the linearized equations of motion for ϕ due to its linearity. This means that, under the restrictions imposed by the linearized theories' application, the time evolutions of both theories are identical.

These restrictions on the linearized theory's applicability limit the configurations that may be represented in terms of the warp field. In principle, by inverting (3.25) it is possible to represent each fluctuation ϕ in terms of a corresponding warp field, φ, as

$$\varphi(t,x) = -\nu^{-1}\big(\sigma'(\mu_m x)\big)^{-1}\cdot\phi(t,x). \tag{3.27}$$

An important subtlety of this result is that it requires the applicability of the linearized theory, i.e., the validity of (3.16). In terms of ϕ, this translates to $|\phi| < b\nu\sigma'(\mu_m x)$, which can be understood as the fluctuation being localized near the soliton's center. Thus, on the linear level, the theory of the warp field only captures configurations satisfying this relation.

3.2.5 Connection to the full nonlinear theory & general range of applicability

The last subsection's ideas may also be applied to the entire nonlinear theory. The identification of the zero mode of the warp field with the collective coordinate naturally extends to the nonlinear level, therefore only the map between the non-zero modes must be lifted to the nonlinear theory. This can be achieved through a new map R, defined by

$$\begin{aligned} R : \mathcal{P} &\to \mathbb{P} \\ \big(\varphi(x), \varpi(x)\big) &\mapsto \big(R_\phi(\varphi)(x), R_\pi(\varphi,\varpi)(x)\big), \end{aligned} \tag{3.28}$$

with

$$\begin{aligned} R_\phi(\varphi)(x) &\equiv \nu\sigma(\mu_m x - \varphi(x)) - \nu\sigma(\mu_m x), \\ R_\pi(\varphi,\varpi)(x) &\equiv -\rho^{-1/2}(x,\varphi)\cdot\varpi(x). \end{aligned} \tag{3.29}$$

This map is an embedding of the whole phase space of the warp field, $\mathcal{P}$, into the one of general fluctuations around the soliton, $\mathbb{P}$. Similar to its pendant r, it assigns to every warp

field configuration the corresponding fluctuation. Importantly, it does so in such a way that every solution of the φ-theory is mapped onto one of the ϕ-theory, as it is apparent that the equations of motion of a general fluctuation must also apply to those caused by the warp field.

On the non-linear level, this map also demonstrates that the mode functions of K and $\mathcal{K}$ are no longer equivalent. In the ϕ-picture, a plane wave corresponds to a superposition of φ-waves, and conversely.

The inverse of (3.28) can now be used to establish a condition that configurations must meet so that it is possible to describe them by a warp field. This map is of the general form

$$\begin{aligned} &R^{-1} : \mathbb{P} \supset \mathcal{D}\big(R^{-1}\big) \to \mathcal{P} \\ &\big(\phi(x), \pi(x)\big) \mapsto \big(R_\varphi^{-1}(\phi)(x), R_\varpi^{-1}(\phi,\pi)(x)\big), \end{aligned} \tag{3.30}$$

and acts as

$$\begin{aligned} R_\varphi^{-1}(\phi)(x) &\equiv -\sum_{n=1}^{\infty} \frac{\big(\sigma^{-1}\big)^{(n)}(z)}{\nu^n n!}\bigg|_{z=\sigma(\mu_m x)} \phi^n(t,x), \\ R_\varpi^{-1}(\phi,\pi)(x) &\equiv -\rho^{1/2}\big(x, R_\varphi^{-1}(\phi)\big)\cdot\pi(x). \end{aligned} \tag{3.31}$$

Following the previous reasoning, for any fluctuation $\phi \in \mathcal{D}(R-1)$, this map allows to find the corresponding warp field configuration. The key question now is which kind of fluctuations constitute $D(R^{-1})$. The convergence of the series (3.31) or, equivalently, the invertibility of equation (3.29) constrains this domain. It is simple to deduce a condition for ϕ from the latter one:

$$\left|\frac{\phi(t,x)}{\nu} + \sigma(\mu_m x)\right| < 1, \tag{3.32}$$

with the inequality's saturation corresponding to $\varphi = \pm\infty$. Note that the soliton is centered at $x = 0$ for simplicity's sake, i.e., contributions of the zero modes have been omitted here.

(3.32) is now sufficient to determine $\mathcal{D}(R^{-1})$, for which it implies that

$$\mathcal{D}(R^{-1}) = \{(\phi(x), \pi(x)) \in \mathbb{P} \,||\phi(x)/\nu + \sigma(\mu_m x)| < 1\}. \tag{3.33}$$

Because ϕ is time-dependent in general, it's feasible that a given configuration fulfills (3.32) for some time period T but not for $t \notin T$. A physical explanation of this trait stands at the center of the next subsection.

For a specified time period $T = [t_i, t_f]$, $\mathcal{D}_T(R^{-1})$ can be defined as the set of configurations that stay inside $\mathcal{D}(R^{-1})$ throughout T. In other words, if a configuration is an element

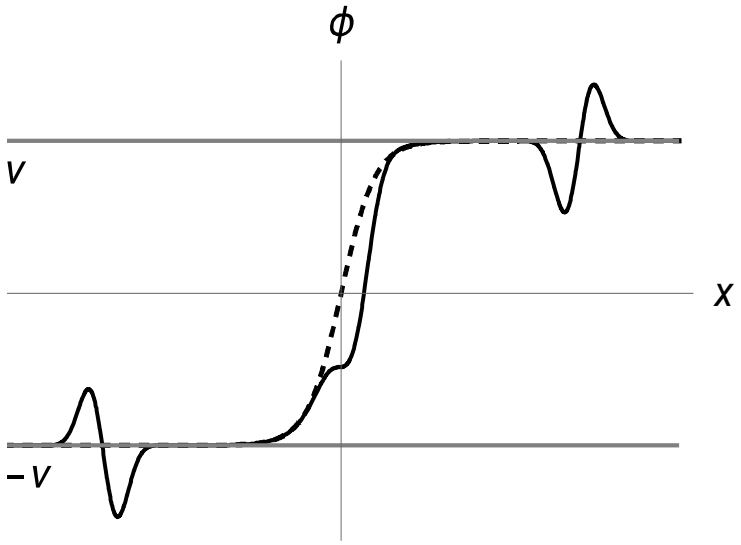

Figure 3.1: The wave package together with the soliton it crosses at three different times (solid line), compared to the unperturbed soliton (dotted line).

of $\mathcal{D}(R^{-1})$ at t_i it can be described in terms of warp fields until $t = t_f$. Formally, this is captured by the following definition:

$$\begin{aligned}\mathcal{D}_T(R^{-1}) = \{(\phi(x),\pi(x)) \in \mathcal{D}(R^{-1}) | (\phi(x),\pi(x)) = (\phi(t_i,x),\pi(t_i,x)) \\ \Rightarrow (\phi(t,x),\pi(t,x)) \in \mathcal{D}(R^{-1}) \forall t \in T\}.\end{aligned} \tag{3.34}$$

The construction of the warp field as an extension of the domain of the Goldstone field is consistent with the conclusion that only configurations localized around the soliton's center can be represented in terms of warp fields. The Goldstone field is a product of the translational symmetry being broken. As the value of the field converges towards a constant value $\pm\nu$, this symmetry is approximately restored in regions sufficiently distant to the soliton's center. As a result, it's logical to assume that the warp field's physical relevance is greatest at the soliton's core and decreases gradually for larger distances.

3.2.6 Incompleteness of the field space

Following the reasoning of the last subsection, the warp fields are only capable of describing a subset of the full theory. Thus it is possible for configurations to propagate out of the sector captured by warp fields - in other words, the warp field space is incomplete. The meaning of this property can be best understood through a simple example. Thus, consider a configuration from $\mathcal{D}_T$ propagating through the soliton as a localized wave package as illustrated in Fig. 3.1.

Taking seriously the picture of the wave package as a particle, this process can be thought of as this particle travelling through the soliton, getting distorted along the way, and perhaps

picking up some phase shift. While the fluctuation is transversing the soliton, the concept of the warp field allows for a different viewpoint suggesting to alternatively understand the wave package as a warping of the latter.

In other words, this process can be understood as a wave packet impacting the soliton and being captured, causing the soliton to warp, as indicated by the warp field. The soliton returns to an unexcited form after the interval T has passed by continually releasing another wave packet. This is consistent with the image painted in the preceding sections. The warp field can be understood as an effective description for the dynamics of such configurations during T, and $\mathcal{D}_T$ is the set of configurations captured by this description within the interval T.

It's hardly surprising that such configurations exist. The warp field can be seen as a fluctuation in the thickness of a domain wall. It is well-known that such disturbances can decay into scalar particles [44], and the concept of the warp field allows for a clear characterization of this decay as the configuration approaching the boundary of the phase space of the warp field theory $\mathcal{P}$, i.e. φ diverging in some point x_0, which corresponds to $\sigma(\mu_m x_0 - \varphi(t, x_0)) = \pm 1$, i.e. $\Phi(x_0) = \pm\nu$.

3.2.7 Scales of the warp field

The region in which the theory's dynamics is dominated by the warp field sector is determined by the spatial extension of the soliton, and thus the parameters of the underlying theory. In the simple setting discussed in this section, these parameters are the asymptotic values the soliton converges towards, the scalar's coupling constant and its mass. For the example of a Higgs-like potential, they are related through $m_\Phi \propto \nu\sqrt{\lambda}$.

The vacua $\pm\nu$ and the mass of the field m_Φ are the most suitable independent parameters since the chosen parametrization does not explicitly depend on the coupling constant λ. It's also worth remembering that the warp field φ is derived from the collective coordinate, i.e. the Goldstone field, not only by expanding its domain, but also by multiplying it by a factor of $\mu_m \propto m_\Phi$, resulting in $\varphi \propto m_\Phi$.

Consider the scenario when $m_\Phi \to 0$, which implies that $\mu_m \to 0$ as well. The soliton is far extended in this limit, while $\varphi \to 0$. This is consistent with the emergence of the warp field as a result of the soliton breaking translational symmetry. The area in which the symmetry is locally broken extends out as the soliton spreads out in this limit. However, the soliton flattens down at the same time, making the symmetry breaking less significant. This limit is equivalent to the one of a weak interaction given a fixed value of ν. Alternatively, this limit can be understood as an ever larger value of φ becoming necessary to describe a given fluctuation ϕ.

The opposite occurs in the limit $m_\Phi \to \infty$, when also $\mu_m \to \infty$. The region impacted by the warp field reduces as the soliton becomes more localized, until the latter is entirely restricted to the soliton, which can be represented as a point particle with increasing

precision. Thus, the warp field becomes synonymous with the collective coordinate in the limit of a heavy field or, equivalently, a strong interaction with fixed ν.

This can also be seen in (3.32), which in the limit of a totally localized soliton can only be solved by $\phi = 0$, implying that the non-zero mode contributions to the warp field must vanish. This also eliminates the problem that taking this limit seems to imply $\varphi \to \infty$. In this limit, the non-zero mode contributions vanish, leaving just the terms representing the collective coordinate. Their prefactor μ_m factorizes out inside the soliton's argument, and can be absorbed into the soliton mass through integration with the weight factor ρ.

The explicit ν-dependence is straightforward: All physical effects generated by the warp field scale as ν^2 since the soliton's energy density scales as ν^2.

3.2.8 A dual picture

The translational Goldstone fields are eaten up by the metric in the presence of gravity, as they may be regarded as the action of some diffeomorphism on the soliton [66]. Because this letter statement also applies to the warp field, it only seems reasonable that it can be absorbed in the same way.

This can be confirmed through a transformation to new coordinates (ξ^0, ξ^1), defined as

$$\big(\xi^0(t,x), \xi^1(t,x)\big) = \big(t, x - \mu_m^{-1}\varphi(t,x)\big). \tag{3.35}$$

Under this transformation, the action of the warped soliton takes the form

$$S[\Phi] = \int \mathrm{d}^2\xi \sqrt{-g_\varphi}\left(\frac{1}{2} g_\varphi^{\mu\nu}(\xi)\partial_\mu\Phi_s(\xi)\partial_\nu\Phi_s(\xi) - V(\Phi_s(\xi(t,x))\right), \tag{3.36}$$

with the effective metric

$$g^\varphi_{\mu\nu}(\xi) = \eta_{\alpha\beta}\frac{\partial x^\alpha}{\partial\xi^\mu}(\xi)\frac{\partial x^\beta}{\partial\xi^\nu}(\xi). \tag{3.37}$$

The warp field can thus be entirely absorbed into this new metric. This suggests that it might be sensitive to take this a step further, and encode the dynamics of the theory entirely in $g^\varphi_{\mu\nu}$. On the formal level this is equivalent to elevating $g^\varphi_{\mu\nu}$ to a field, which will be labeled $g_{\mu\nu}$ to indicate that it is no longer regarded a function of φ. When doing so, a Lagrange multiplicator Λ must be used to implement the information about its structure. This can be achieved by enforcing (3.37). Translated to an equation for $g_{\mu\nu}$, this condition is in $(1+1)$ dimensions equivalent to $R = 0$, where R is the standard Ricci scalar. Imposing this condition thus leads to an action in terms of $g_{\mu\nu}$,

$$S[\Phi_s, g] = \int \mathrm{d}^2\xi\ \sqrt{-g}(\mathcal{L}_S + \Lambda R), \tag{3.38}$$

where $\mathcal{L}_s$ denotes the action of the soliton on the spacetime with metric g. The Lagrange multiplier appears together with the Einstein-Hilbert action, which resembles a kinetic

term for the metric. This action can now be used to derive an equation of motion for $g_{\mu\nu}$, leading to a result structurally similar to Einstein's equation:

$$T^{\mu\nu} = 2(\Lambda G^{\mu\nu} - \nabla^{\nu}\partial^{\mu}\Lambda + g^{\mu\nu}\,\Box_g\,\Lambda). \tag{3.39}$$

Here, $T^{\mu\nu}$ refers to the soliton's energy-momentum tensor evaluated at the new metric $g_{\mu\nu}$, $T^{\mu\nu} = \frac{\delta(\sqrt{-g}\mathcal{L}_s)}{\delta g_{\mu\nu}}$.

Together with the condition $R = 0$, equation (3.39) fully determines the theory's dynamics, which is parametrized by $g_{\mu\nu}$ and Λ. The constraint ensures that $g_{\mu\nu}$ is identical to the Minkowski metric up to a coordinate transformation. This implies in particular that, unlike a the dynamical spacetime of General Relativity, it is not sourced by the remaining matter content.

Instead, equation (3.39) has to be understood as an equation of motion for the Lagrange multiplier Λ. This can be made manifest by contracting both sides with the inverse metric $g_{\mu\nu}$, implying that

$$\Box_g\Lambda = \mathrm{tr}_g(T) = V(\Phi_s(\xi)) = \frac{1}{2}\epsilon_s(\xi). \tag{3.40}$$

This is nothing but the equation of motion for a free scalar field in a flat spacetime coupled to an external source. An interesting, but not surprising, observation is now that just as the warp field, Λ is sensitive to the soliton only through its energy density.

The simplicity of this equation can also be made manifest through a simplified effective action for Λ:

$$S_{\text{eff}} = \int \mathrm{d}^2\xi\sqrt{-g}\left(\frac{1}{2}\partial_\mu\Lambda(\xi)\partial^\mu\Lambda(\xi) + \Lambda(\xi)\epsilon_s(\xi)\right). \tag{3.41}$$

This simple action action fully describes the dynamics of all warp field configurations for which (3.37) is non-degenerate.

3.3 Classical warp fields in higher dimensions

The warp field captures the complete dynamics of the fluctuation ϕ at the soliton's center in the $(1+1)$-dimensional scenario. This is only conceivable because the number of fields coincides with the number of broken translational symmetries. In general, this is not the case since, for a generic theory, the number of fields required to construct a soliton-like configuration is not related to the number of spatial dimensions. The sole exception, of course, are the constraints resulting from Derrick's theorem, which are however irrelevant here.

It is always possible to add warp fields to a given theory by simply converting the collective coordinates corresponding to the soliton's location to fields. The key question is whether

the theory of these warp fields captures a subset of the dynamics of all fields in the underlying theory. If this is the case, their theory will be labelled *sufficient*; otherwise, it will be referred to as *insufficient*.

To make this distinction more accurate, let $\varphi \equiv \{\varphi^a\}_a$ denote the warp fields of a given theory and soliton arising from it. In the conventional picture, this gives rise to fluctuations around the soliton, which can be parametrized by a set of fields $\{\phi_i\}_i$. Then the set of warp fields is *sufficient* if there exists a bijective function $\mathcal{R}$ satisfying

$$\phi_i(t,x) = \mathcal{R}_i[\varphi](t,x) \tag{3.42}$$

while respecting the equations of motion of both pictures. On the level of the linearized theories, this amounts to the existence of an invertible matrix $R_{ia}(x)$ s.t.

$$\phi_i(t,x) = R_{ia}(x)\varphi^a(t,x). \tag{3.43}$$

Section 3.3.1 provides a discussion of the properties of sufficient theories, while section 3.3.2 showcases them for the instructive example of the Skyrme model.

The case of an insufficient theory is more complicated as the warp fields are, as the name suggests, insufficient to describe all degrees of freedom of the underlying theory. Moving to higher dimensions and solitons consisting of more fields does, however, not only increase the number of degrees of freedom and collective coordinate, but typically also leads to the emergence of additional moduli besides the collective coordinates.

These other zero modes reflect, for example, (gauge-)rotations, and because they are massless, they are commonly available in the same regime as the collective coordinates. As a result, they are obvious candidates to serve as the missing degrees of freedom. A theory for which these do indeed close the gap left by the warp fields will be called *extendable*.

This procedure and the properties of the resulting theories are discussed in section 3.3.3 and illustrated for the concrete example of the abelian Higgs model in $2+1$ dimensions in section 3.3.4.

3.3.1 Properties of sufficient theories

A theory is called *sufficient* if its soliton's warp fields capture all degrees of freedom of freedom of the underlying theory, i.e., if there exists a bijective map from the space of warp fields to the field space of the fluctuations in the conventional picture. The central result of this subsection is that the properties of the warp fields are restrictive enough to determine their action up to a few background functions, allowing an efficient effective description for all such theories.

The first such restriction arises from the simple observation that warp fields only enter the theory through the argument of the soliton, where they appear in the combination

$$\xi^i \equiv \mu_m x^i - \varphi^i(t,x). \tag{3.44}$$

In other words, introducing warp fields amounts to transforming all fields involved in the formation of the soliton as well as their partial derivatives as

$$\Phi_s(\mu_m x) \to \Phi_s(\xi), \tag{3.45}$$

$$\partial_\mu \Phi_s(\mu_m x) \to \partial_a \Phi_s(\xi)\big(\mu_m \delta^a_\mu - \varphi^a_{,\mu}\big). \tag{3.46}$$

Note that here and in the following ∂_a refers to the derivative with respect to the dimensionless variable ξ^a.

This has immediate consequences for the structure of the warp field's theory. Assuming that the underlying Lagrangian contains terms up to the N^{th} derivative of its fields, the relations (3.45) and (3.46) imply that the warp field's Lagrangian is of the general form

$$\mathcal{L} = g(\xi) + \sum_{n=1}^{N} C^{\mu_1 \dots \mu_n}_{a_1 \dots a_n}(\xi) \xi^{a_1}_{,\mu_1} \dots \xi^{a_n}_{,\mu_n}. \tag{3.47}$$

The only part of this Lagrangian which is sensitive to the features of the underlying theory are the coefficients $C^{\mu_1 \dots \mu_n}_{a_1 \dots a_n}(\xi)$ and $g(\xi)$. Based on their contraction with the products with the derivatives of the ξ_a it is easy to conclude that these coefficients are symmetric under an exchange of a pair of upper and lower indices,

$$C^{\mu_1 \mu_2 \dots \mu_n}_{a_1 a_2 \dots a_n} = C^{\mu_2 \mu_1 \dots \mu_n}_{a_2 a_1 \dots a_n}. \tag{3.48}$$

To gain further insights into the properties of the Lagrangian (3.47), it is helpful to make use of the warp fields' connection to the collective coordinates to further restrict its parameters. More precisely, in the limit $\nabla\varphi \to 0$ the warp field's theory has to reduce to that of the collective coordinates. This implies immediately that the parameter N is given by the highest order of time derivatives in the theory of the moduli. Furthermore, in the limit $\varphi \to 0$, (3.47) should reduce to the Lagrangian of the unperturbed soliton.

For concreteness, consider the case of a theory with a Lagrangian quadratic in the collective coordinates' time derivatives,

$$L(\dot{z}) = \frac{1}{2} M_{ab} \dot{z}^a \dot{z}^b, \tag{3.49}$$

with some moduli space metric M_{ab}. Following the previous reasoning, the Lagrangian of the corresponding warp fields is of the form

$$\begin{aligned} \mathcal{L}(\varphi, \partial\varphi) =& g(\xi) + C^\mu_a(\xi)\big(\mu_m \delta^a_\mu - \varphi^a_{,\mu}\big) + C^{\mu\nu}_{ab}(\xi)\big(\mu_m \delta^a_\mu - \varphi^a_{,\mu}\big)\big(\mu_m \delta^b_\nu - \varphi^b_{,\nu}\big) = \\ =& \big(g(\xi) + \mu_m C^a_a(\xi) + \mu_m^2 C^{ab}_{ab}(\xi)\big) - \big(2\mu_m C^{\mu b}_{ab}(\xi) + C^\mu_a(\xi)\big)\varphi^a_{,\mu} + C^{\mu\nu}_{ab}(\xi)\varphi^a_{,\mu}\varphi^b_{,\nu}. \end{aligned} \tag{3.50}$$

In the limit $\varphi \to 0$, all terms but those in the first bracket in the second line vanish, so that these need to add up to the Lagrangian, and thus energy density, of the unperturbed soliton evaluated at ξ. This reasoning can be further enhanced by considering the different

terms' scaling with the coefficient μ_m. This allows to identify g with the theory's self-interactions, C_a^a with the contributions arising from kinetic couplings and C_{ab}^{ab} with the soliton's gradient energy:

$$E_{\text{grad}} = -\int \mathrm{d}^3x\ \mu_m^2 C_{ab}^{ab}(\mu_m x), \tag{3.51}$$

$$E_{\text{kc}} = -\int \mathrm{d}^3x\ \mu_m C_a^a(\mu_m x), \tag{3.52}$$

$$E_{\text{int}} = -\int \mathrm{d}^3x\ g(\mu_m x). \tag{3.53}$$

The absence of a term linear in $\dot{z}$ in (3.49) requires that also the term linear in $\dot{\varphi}$ needs to disappear to ensure a correct behavior in the limit $\nabla\varphi \to 0$. In terms of the theory's coefficients, this means

$$2\mu_m C_{ab}^{0b}(\mu_m x) + C_a^0(\mu_m x) = 0. \tag{3.54}$$

Through the same limit, the terms quadratic in $\partial\varphi$ together with the additional spatial integral need to reduce to their pendant for the moduli. This links the coefficients C_{ab}^{00} to the moduli space metric through

$$\int \mathrm{d}^3x\ C_{ab}^{00}(\mu_m x) = \frac{1}{2} M_{ab}. \tag{3.55}$$

An additional simplification can be achieved if it is safe to assume that all indices in the underlying theory are contracted using the (inverse) Minkowski metric $\eta^{\mu\nu}$. If this applies, $C_{ab}^{\mu\nu}$ can be recast as $\eta^{\mu\nu}\rho_{ab}$, with ρ_{ab} serving as a density for the moduli space metric, i.e.,

$$\int \mathrm{d}^3x\ \rho_{ab}(\mu_m x) = \frac{1}{2} M_{ab}. \tag{3.56}$$

Then, the connection between C_{ab}^{ab} and the soliton's gradient energy can be used to relate ρ_{ab} to the latter,

$$\int \mathrm{d}^3x\ \eta^{ab}\rho_{ab}(\mu_m x) = -E_{\text{grad}}. \tag{3.57}$$

The last assumption also requires that $C_{ab}^{0b} = 0$, which, together with (3.54), implies $C_a^0 = 0$.

In summary, the Lagrangian for all such sufficient theories takes the simple form

$$\mathcal{L}(\varphi, \partial\varphi) = -\epsilon_s(\xi) + \rho_{ab}(\xi)\varphi^a_{,\mu}\varphi^{b,\mu} + \kappa_a^b(\xi)\varphi^a_{,b}. \tag{3.58}$$

This simple structure is universal if the theory of a given soliton's moduli is quadratic in their derivatives and the underlying theory's kinetic term is constructed from the metric. It holds to all orders, and the functions ρ_{ab}, κ_a^b and ϵ_s are the only quantities that are sensitive to the intricacies of the underlying theory. These functions can be related to physical features of the underlying soliton by decomposing them in terms of the Cs.

The localization around the soliton's center is one of the major properties of warp fields seen in $1+1$ dimensions and reproduced in higher dimensions. The convergence of the integrals (3.53) means that the weight function, ρ_{ab} (or $C_{ab}^{\mu\nu}$, respectively), must decay at least as $|x|^{-2}$ for $|x| \to \infty$. As a result, all effects that arise from a localized weight function should also manifest in this higher-dimensional situation.

3.3.2 Warp fields of a Skyrmion in $3+1$ dimensions as a sufficient theory

Because of its higher derivative terms, the Skyrme model is a particularly interesting example of a sufficient theory, although it necessitates an extension of the reasoning offered in the previous subsection. This model's Lagrangian consists of terms of second and fourth order of the fields' derivatives, suggesting that terms of up to fourth order in $\xi^a_{,\mu}$ must be considered.

If one further considers it given that the derivative terms in the underlying theory are contracted using the Minkowski metric $\eta^{\mu\nu}$, this information is sufficient to infer the structure of the warp fields' Lagrangian,

$$\begin{aligned}\mathcal{L} =& \frac{1}{2}\rho_{ab}(\xi)\partial_\mu\varphi^a\partial^\mu\varphi^b + (\Lambda^4)_{abcd}(\xi)\partial_\mu\varphi^a\partial^\mu\varphi^b\partial_\nu\varphi^c\partial^\nu\varphi^d - \epsilon_s(\xi) + \\ &+ (\Lambda^1)^i_a(\xi)\partial_i\varphi^a + (\Lambda^2)^{ia}_{jb}(\xi)\partial_i\varphi^j\partial_a\varphi^b + (\Lambda^3)^i_{abc}(\xi)\partial_\mu\varphi^a\partial^\mu\varphi^b\partial_i\varphi^c.\end{aligned} \tag{3.59}$$

As mentioned before, this Lagrangian provides an effective description of all theories with the properties mentioned above, i.e., not only the Skyrme model. For it to describe the latter, all that is necessary is a proper choice of the the coefficients in (3.59).

Following section (2.3.2), the Skyrmion is of the form

$$U_s(r) = \exp\left(iF(r)\hat{x}^a\tau_a\right),$$

with some numerical function $F(r)$ and $\hat{x}^a = \frac{x^a}{r}$. That the theory of fluctuations around this configuration is indeed sufficient can be confirmed on the linear level. To first order, fluctuations around the Skyrmion emerge as elements of the Lie-algebra $\mathrm{su}(2)$. This allows to represent them as a linear combination of its generators, $\{i\tau^a\}_a$, via

$$\delta U(t,x) = \delta U^a(t,x) i\tau_a. \tag{3.60}$$

Meanwhile, introducing the warp fields amounts to leading order to the emergence of a fluctuation of similar structure,

$$U_s(r) \to U_s(r) + i\tau_a\varphi^j(t,x)\mu_m^{-1}\left[\hat{x}^a\hat{x}^j\left(\frac{F(r)}{r} - F'(r)\right) - \delta^a_j\frac{F(r)}{r}\right]. \tag{3.61}$$

Following (3.43), the theory of these warp fields is sufficient if a bijective map can be constructed between the $\{\varphi^a\}_a$ and the fields parametrizing the fluctuations in the conventional picture, i.e., the $\{\delta U^a(t,x)\}_a$. Comparing (3.61) with (3.60), it is easy to see that such a map does indeed exist and can be parametrized through

$$\delta U^a(t,x) = \mu_m^{-1} M^a_j(x)\varphi^j(t,x), \tag{3.62}$$

where

$$M^a_j(x) = \hat{x}^a\hat{x}^j\left(\frac{F(r)}{r} - F'(r)\right) - \frac{F(r)}{r}\delta^a_j. \tag{3.63}$$

This map is indeed bijective, and its inverse can be easily found to be given by

$$(M^{-1})^j_a(x) = \hat{x}^a\hat{x}^j\left(\frac{r}{F(r)} - \frac{1}{F'(r)}\right) - \frac{r}{F(r)}\delta^j_a. \tag{3.64}$$

An interesting observation is now that for $r \to \infty$, M^{-1} diverges as $F(r) \to 0$ in the same limit. Similarly to the $(1+1)$-dimensional case, this, combined with the conditions required for the validity of the linearized theory, limits the applicability of the warp fields to configurations that decay sufficiently fast. More concretely, in agreement with previous reasoning the warp field theory captures only configurations which are localized sufficiently close around the Skyrmion's center.

Once it is confirmed that the warp fields form a sufficient theory, all that remains is to calculate the coefficients in (3.59). This can be done by evaluating the Lagrangian of the underlying theory (1.16) for the warped soliton (3.61). Doing so is straightforward and leads to

$$\begin{aligned}\rho_{ab}(\xi) =& \frac{f_\pi^2}{4}\mathrm{tr}\big(\partial_a U_s(\xi)\partial_b U_s^\dagger(\xi)\big) + \frac{1}{32e^2}\mathrm{tr}\big([\partial_a U_s(\xi), \partial_j U_s^\dagger(\xi)][\partial_b U_s(\xi)\partial^j U_s^\dagger(\xi)] + \\ &+ [\partial_j U_s(\xi), \partial_a U_s^\dagger(\xi)][\partial^j U_s(\xi)\partial_b U_s^\dagger(\xi)]\big) \end{aligned}\tag{3.65}$$

$$(\Lambda^4)_{abcd}(\xi) = \frac{1}{32e^2}\mathrm{tr}\big([\partial_a U_s(\xi), \partial_c U_s^\dagger(\xi)][\partial_b U_s(\xi)\partial_d U_s^\dagger(\xi)]\big) \tag{3.66}$$

$$\begin{aligned}(\Lambda^1)^b_a(\xi) =& \mu_m\frac{f_\pi^2}{4}\mathrm{tr}\big(\partial_{(a} U_s(\xi)\partial_{b)} U_s^\dagger(\xi)\big) + \frac{\mu_m^3}{32e^2}\mathrm{tr}\big([\partial_{(a} U_s(\xi), \partial^j U_s^\dagger(\xi)][\partial_{b)} U_s(\xi)\partial_j U_s^\dagger(\xi)] + \\ &+ [\partial_j U_s(\xi), \partial_{(a} U_s^\dagger(\xi)][\partial^j U_s(\xi)\partial_{b)} U_s^\dagger(\xi)]\big) \end{aligned}\tag{3.67}$$

$$\begin{aligned}(\Lambda^2)^{ia}_{jb}(\xi) =& \frac{\mu_m^2}{16e^2}\mathrm{tr}\big([\partial_j U_s(\xi), \partial_b U_s^\dagger(\xi)][\partial_i U_s(\xi)\partial_a U_s^\dagger(\xi)] + \\ &+ [\partial_j U_s(\xi), \partial_a U_s^\dagger(\xi)][\partial_i U_s(\xi)\partial_b U_s^\dagger(\xi)]\big) \end{aligned}\tag{3.68}$$

$$\begin{aligned}(\Lambda^3)^i_{abc}(\xi) =& \frac{\mu_m}{16e^2}\mathrm{tr}\big([\partial_a U_s(\xi), \partial_c U_s^\dagger(\xi)][\partial_b U_s(\xi)\partial^j U_s^\dagger(\xi)] + \\ &+ [\partial_c U_s(\xi), \partial_a U_s^\dagger(\xi)][\partial^j U_s(\xi)\partial_b U_s^\dagger(\xi)]\big). \end{aligned}\tag{3.69}$$

This result furthermore confirms the line of reasoning underlying (3.59).

3.3.3 Properties of extendable theories

The number of independent fields in most theories that give rise to solitons is typically greater than the number of broken translational symmetries, so that the collective coordinates corresponding to these symmetries fail to produce a sufficient theory. It is now worth noting that the main advantages of developing the theory of warp fields from the collective coordinates, especially their universality and significance for low-energy dynamics, are not unique to this setting. Any massless excitation, i.e. any zero mode, shares them as well.

Because the introduction of warp fields anyway relies on this sector, using potentially existing, extra zero modes to compensate for the missing degrees of freedom seems to be

a logical way to widen the scope of the warp field construction. These extra zero modes will be denoted by $\{\theta^a\}_a$ in what follows, and the fields obtained by promoting them to fields will be labeled $\{\vartheta^a(t,x)\}_a$. These fields will be referred to as *twirl fields* since their corresponding zero modes typically represent (gauge)-rotations, and promoting them to fields may be viewed as a twirling of the configuration.

Similar to the warp fields, these new objects enter the theory's action only through their effect on the soliton. More specifically, they induce a shift in its partial derivatives,

$$\partial_\mu \Phi_s(x) \to \partial_a \Phi_s(\xi,\vartheta)(\mu_m \delta^a_\mu - \varphi^a_{,\mu}) + \partial_{\vartheta^a}\Phi_s(\xi,\vartheta)\vartheta^a_{,\mu}. \tag{3.70}$$

From here, the extended theory including twirl fields can be set up in a similar way as the initial theory. While a theory of the warp fields can be constructed entirely from $\xi^a_{,\mu}$s, the presence of twirl fields manifests through the emergence of terms consisting of combinations of $\vartheta^a_{,\mu}$ with itself and $\xi^a_{,\mu}$. Also the highest order of these new terms is determined by the higher order of derivatives in the theory of moduli and thus also the underlying theory. This determines the Lagrangian of the theory up to the coefficients of these terms, which can again be expected to depend on ξ through the soliton. Because the twirl fields are derived from the parameters of a continuous symmetry, they must vanish from the theory in the limit $\vartheta^a_{,\mu} \to 0$, mimicking the behavior of Goldstone fields in the same way as the warp fields.

Consider now for simplicity once again the scenario of a theory whose moduli are described by a Lagrangian quadratic in their derivatives. Regardless of the field content or the specific shape of the soliton, the most generic Lagrangian, in terms of both warp and twirl fields, is of the form

$$\begin{aligned}\mathcal{L} =& g(\xi) + C^\mu_a(\xi)\big(\mu_m\delta^a_\mu - \varphi^a_{,\mu}\big) + C^{\mu\nu}_{ab}(\xi)\big(\mu_m\delta^a_\mu - \varphi^a_{,\mu}\big)\big(\mu_m\delta^b_\nu - \varphi^b_{,\nu}\big) + \\ &+ D^{\mu\nu}_{ab}(\xi,\vartheta)\partial_\mu\vartheta^a\partial_\nu\vartheta^b + D^\mu_a(\xi,\vartheta)\partial_\mu\vartheta^a + M^{\mu\nu}_{ab}(\xi,\vartheta)\big(\mu_m\delta^a_\mu - \varphi^a_{,\mu}\big)\partial_\nu\vartheta^b.\end{aligned} \tag{3.71}$$

The coefficients $D^{\mu\nu}_{ab}$ are connected to the field space metric of the low-energy theory in the same manner as $C^{\mu\nu}_{ab}$. Furthermore, just as was the case for a theory consisting only of warp fields, the focus on a low-energy theory quadratic in time derivatives means that the terms linear in $\dot\vartheta$ disappear. Assuming that the partial derivatives that comprise the kinetic component are contracted through the metric, the general Lagrangian (3.71) reduces to its final form:

$$\begin{aligned}\mathcal{L}(\varphi,\partial\varphi,\vartheta,\partial\vartheta) =& -\epsilon_s(\xi) + \kappa^b_a(\xi)\varphi^a_{,b} + \rho_{ab}(\xi)\varphi^a_{,\mu}\varphi^{b,\mu} + \\ &+ \omega_{ab}(\xi,\vartheta)\vartheta^a_{,\mu}\vartheta^{b,\mu} + K^j_a(\xi,\vartheta)\vartheta^a_{,j} + L^{\mu\nu}_{ab}(\xi,\vartheta)\varphi^a_{,\mu}\vartheta^b_{,\nu}.\end{aligned} \tag{3.72}$$

Every theory with additional symmetries may be reinforced by twirl fields, much as it is the case for warp fields. The key concern now is whether this approach provides enough degrees of freedom to capture the dynamics of all fields in the underlying theory. Unfortunately, there is no general criteria determining whether this is the case. Nonetheless, this technique significantly broadens the range of applicability of this chapter's approach.

3.3.4 Warp fields of the abelian Higgs model in 2+1 dimensions as an extendable theory

A particularly instructive example for an extendable theory is the abelian Higgs model in $2+1$ dimensions, which gives rise to the Abrikosov-Nielsen-Olesen (ANO) vortex [44], [67]. This is in parts due to its simplicity, but more importantly because it allows for a clear analysis of the interplay between the warp and twirl fields with the underlying theory's gauge invariance.

Once appropriate zero modes have been determined, the derivation of a theory of warp and twirl fields around the vortex is simple using the technique described in the previous paragraph. The vortex has three zero modes, whereas the underlying theory has three physical degrees of freedom, suggesting that it can indeed serve as an extendable theory. However, the primary problem in the context of gauge theories is matching these degrees of freedom. The number of fields comprising the theory of interest is more than the number of physical degrees of freedom due to the theory's gauge invariance. Because the relationship between warp fields and fluctuations is no longer invertible, a straightforward application of the technique used to link the theory of warp fields to the entire theory utilized in the preceding settings is no longer possible. An easy solution to this problem would be to use a sufficient number of gauge transformations to remove the unnecessary fields. Unfortunately, on the Lagrangian level, this is not always achievable. Consider the temporal gauge, which eliminates A_0. Any gauge transformation aiming at removing another field would have to be created by a gauge function involving said field, which is in general a function of time, making it incompatible with the temporal gauge. This is different at the level of the equations of motion, which can be exploited in some circumstances to eliminate the time-dependence of the gauge function. This is precisely the situation in the following example.

The crucial step necessary to achieve this is to realize that a particularly helpful gauge exists. Through this gauge, all redundancies can be removed at the level of the equations of motion. Doing so simplifies the system to three distinct fields, each with its own equation. This allows for the application of the previously outlined techniques, leading to a description of the theory in terms of warp and twirl fields. These fields cause fluctuations that span a three-dimensional subspace of the four-dimensional field space of the (off-shell) fluctuations. This connection between the two theories can then be used to demonstrate that the equations of motion of the fluctuations, when combined with an additional, on-shell gauge condition, imply the equations of the warp fields and vice versa, demonstrating the equivalence of the two approaches up to the usual limitations imposed by the use of warp fields. For the sake of simplicity, all of this is only done for linearized theories.

The first step in this discussion is to review the ANO vortex's primary features. Because of the static character of the soliton underpinning the following discussion, it is convenient to work in the temporal gauge, $A_0 = 0$, which is imposed on the Lagrangian level. The number of real, independent fields is thereby reduced to four, two of which are supplied by

the spatial components of the gauge field Ai. The other two are included in the complex scalar field and can be expressed using the parametrization $\Phi = \frac{1}{\sqrt{2}}\rho \cdot e^{iq\lambda}$, where q is the $U(1)$-charge appearing in the covariant derivative, $D_\mu = \partial_\mu + iqA_\mu$.

When expressed through these fields as well as the gauge-invariant combination $J_i = A_i + \partial_i\lambda$, the Lagrangian takes the form

$$\mathcal{L} = \frac{1}{2}\partial_\mu\rho\partial^\mu\rho + \frac{q^2\rho^2}{2}\dot{\lambda}^2 + \frac{1}{2}\dot{A}_i\dot{A}_i - \frac{1}{4}F_{ij}F_{ij} - \frac{q^2\rho^2}{2}J_iJ_i - V(\rho). \tag{3.73}$$

Crucially for the topology of the vacuum manifold, the potential V depends only on the absolute value of the scalar field, which is thus characterized by $\rho = \nu$ with some real, positive ν. From this, it follows immediately that the vortex solution of winding number one can be parametrized in terms of the spatial radius r and angle α through [44], [67]

$$\rho_s = \nu\sigma(r),\ \lambda_s = \frac{\alpha}{q},\ A_i^s = -\partial_i\alpha_s\big(1 - f(r)\big) = \frac{1}{q}\epsilon_{ij}\frac{x_j}{r}\big(1 - f(r)\big), \tag{3.74}$$

with some functions σ and f, whose precise form is irrelevant for the following discussion. Expanding the Lagrangian (3.73) in terms of the fluctuations around $(\rho_s, \lambda_s, A_i^s)$, which will be referred to as (r, l, a_i), yields, to leading order,

$$\mathcal{L}^{(2)} = \frac{1}{2}\partial_\mu r\partial^\mu r - \frac{q^2}{2}J_i^sJ_i^sr^2 - \frac{1}{2}V''(\rho_s)r^2 + \frac{q^2\rho_s^2}{2}\dot{l}^2 + \frac{1}{2}\dot{a}_i\dot{a}_i - \frac{1}{4}f_{ij}f_{ij} - 2q^2J_i^s\rho_sj_ir - \frac{q^2\rho_s^2}{2}j_ij_i. \tag{3.75}$$

Here, $f_{ij} = \partial_ia_j - \partial_ja_i$ denotes the field strength tensor of the gauge field fluctuation. From this part of the Lagrangian, the linearized eqauations of motions can be deduced:

$$\begin{aligned} \Box r &= -\big(q^2J_i^sJ_i^s + V''(\rho_s)\big)r - 2q^2J_i^s\rho_sj_i, \\ \ddot{l} &= \rho_s^{-2}\partial_i\big(\rho_s^2j_i + 2\rho_sJ_i^sr\big), \\ \ddot{a}_i &= \partial_mf_{mi} - 2q^2J_i^s\rho_sr - q^2\rho_s^2j_i. \end{aligned} \tag{3.76}$$

Although A_0 has been set to zero through gauge-fixing, its equation of motion remains valid as a constraint[1]:

$$\partial_i\dot{A}_i = -q^2\rho^2\dot{\lambda}. \tag{3.77}$$

To match all this to the corresponding extended warp field theory another field needs to be eliminated by fixing the remaining gauge freedom. This can be achieved through the gauge transformation

$$A_i \to A_i + \partial_i\gamma, \quad \lambda \to \lambda - \gamma, \tag{3.78}$$

where γ is given by

$$\gamma = -\frac{1}{\Delta}\big(\partial_iA_i - G[\rho, \alpha]\big), \tag{3.79}$$

[1] Alternativel, this constraint can be obtained through the requirement that not only A_0 vanishes, but also its conjugate momentum [68].

with G being defined through the differential equation $\dot{G} = -q^2\rho^2\dot{\lambda}$. What makes this gauge function relevant in this context is its connection to the constraint (3.77), which implies that $\dot{\gamma} = 0$, so that the gauge transformation characterized by γ is compatible with the previously chosen temporal gauge.

This transformation ultimately imposes a constraint on the vector field,

$$\partial_i A_i = G. \tag{3.80}$$

In terms of the fluctuations around the vortex, (3.80) can be expressed as

$$\partial_i a_i = -q^2\rho_s^2 l. \tag{3.81}$$

At this point, the most important property of this equation is that it can be solved trivially for l, which can thus be eliminated from the remaining equations. As a result, only three fields remain, which correspond to the theory's three dynamical degrees of freedom. This also manifests in the equations of motion, as through (3.81) the equation for l is no longer independent, but is reduced to the divergence of its pendant for a_i.

This theory contains three dynamical degrees of freedom, and the two warp fields arising from the vortex are insufficient to capture their dynamics. Thus, they need to be complemented by a twirl field, which can be constructed from some other zero mode. It is clear from (3.73) such a mode exists in the form of shifting λ by an arbitrary constant. In terms of the underlying theory, this is nothing but a $U(1)$-transformation of the complex scalar, which is also essential in the topological properties of the vortex. This choice is particularly interesting from a technical perspective, as the resulting field can be immediately identified with l. This not only simplifies the translation between the two theories, but furthermore implies that the effective theory actually captures the **full** dynamics of this field, rather than just a subset.

Through the usual reasoning, it is easy to see that this theory is described by a Lagrangian of the form (3.71). For this Lagrangian to actually describe the theory at hand, all that remains is to determine the coefficients within it. This can again be achieved by inserting the warped vortex together with the twistor field into the Lagrangian (3.73) of the full theory:

$$\begin{aligned} C_{ab}^{\mu\nu}(\xi) =& \frac{1}{2}\eta^{\mu\nu}\left(\partial_a\rho_s\partial_b\rho_s + \frac{q^2\rho_s^2}{2}\partial_a\lambda_s\partial_b\lambda_s + \partial_a A_i^s\partial_b A_i^s\right) + \frac{1}{2}\partial_a A_s^\mu\partial_b A_s^\nu, \\ D_a^{\mu\nu}(\xi) =& \frac{q^2\rho_s^2}{2}\eta^{\mu\nu}, \quad C_a^\mu(\xi) = q^2\rho_s^2 A_s^\mu\partial_a\lambda_s, \quad D^\mu(\xi) = q^2\rho_s^2 A_s^\mu, \quad g(\xi) = \frac{q^2\rho_s^2}{2}A_i^s A_i^s. \end{aligned} \tag{3.82}$$

Thus, it remains to connect this description of the theory to that in terms of the usual fluctuations. The fluctuations induced by the warp fields and the twirl field are, to leading order,

$$\begin{aligned} r^\varphi =& -\partial_a\rho_s\varphi^a, \\ l^\varphi =& -\partial_a\lambda_s\varphi^a + \vartheta, \\ a_i^\varphi =& -\partial_a A_i^s\varphi^a. \end{aligned} \tag{3.83}$$

The index φ thereby indicates that the corresponding quantities are to be understood as functions of the fields of the extended warp field theory.

Having constructed both theories as well as the map between them, it is instructive to confirm that they are indeed equivalent, as the proof sheds some light on the non-trivial way in which gauge invariance affects the relation between the two pictures.

The crucial difference between the model at hand and the previous example is that the equivalence can no longer be established at the level of the action, as the three physical degrees of freedom are only manifest on the level of the equations of motion. Thus, the equivalence of the two pictures also needs to be shown on this level.

First, it is easy to show that the equations of motion for the fluctuations in the conventional picture imply those in the picture relying on warp fields. This can be achieved by first expressing the equations of motions for the warp fields in terms of the fluctuations, leading to

$$\rho_s^2 \ddot{l}^\varphi = \partial_i\big(\rho_s^2 j_i^\varphi + 2\rho_s J_i^s r^\varphi\big) \tag{3.84}$$

$$\partial_a\rho_s\big(\,\Box\, r^\varphi + q^2 J_i^s J_i^s r + 2q^2 J_i^s \rho_s j_i^\varphi + V''(\rho_s) r^\varphi\big) = \partial_a A_i^s\big(\partial_m f_{mi} - 2q^2 J_i^s \rho_s r - q^2\rho_s^2 j_i - \ddot{a}_i\big). \tag{3.85}$$

It is now straightforward to show that these equations are, in fact, just linear combinations of the equations of motions for r, l and a_i[2]. Thus, the latter imply those for the warp fields and for the twirl field.

In order to indeed confirm full equivalence of the time evolution in both pictures, it remains to show the inverse direction. The starting point for this argument is again (3.85) and (3.84).

To extract the equations of motions which remain after the second gauge fixing, it is helpful to multiply (3.85) by $\epsilon_{am}\hat{x}_m$. Using the form of the vortex, (3.74), this leads to the relation

$$\hat{x}_i\big(\ddot{a}_i - \partial_m f_{mi} + 2q^2 J_i^s \rho_s r + q^2\rho_s^2 j_i\big) = 0. \tag{3.86}$$

Further taking into account that this equation must hold in two spatial dimensions, it can be concluded that

$$\ddot{a}_i^\varphi - \partial_m f_{mi}^\varphi + 2q^2 J_i^s \rho_s r^\varphi + q^2\rho_s^2 j_i^\varphi = \Gamma\epsilon_{im}\hat{x}_m. \tag{3.87}$$

The yet unknown function Γ will ultimately reveal itself as a manifestation of the gauge choice on the fluctuation's field space. Before exploring this connection, it is convenient to first derive a similar equation for the fluctuation r. This can be achieved in a similar way as for (3.87), namely by multiplying equation (3.85) with $\hat{x}^a$, which combines with the coefficient $\partial_a\rho_s$ on the left hand side to a scalar function.

[2]Note that this line of reasoning is massively simplified through usage of all four equations of motion before the last gauge redundancy has been fixed.

The terms containing a_i can then be eliminated using (3.87), ultimately leading to the following equation:

$$\Box r^{\varphi} + q^2 J_i^s J_i^s r + 2q^2 J_i^s \rho_s j_i^{\varphi} + V''(\rho_s) r^{\varphi} = \Gamma \cdot \frac{1 - f + r f'}{q r^2 \nu \sigma'(r)}. \tag{3.88}$$

And indeed, (3.87) and (3.88) coincide with the equations for a_i and r obtained in the conventional picture up to the terms on their right-hand sides. These terms can now be eliminated by recalling that the desired relation should not connect the new fields with the full space of fluctuations, but only map onto a subset determined by the gauge condition (3.81). This implies in particular that taking the divergence of the equation for a_i yields the equation of motion for l, which is thus no longer independent. This behavior is reproduced in the extended warp field theory, as the left hand side of equation (3.87) can be identified with its pendant in equation (3.84). Comparing the remainders of these equations, it is straightforward to obtain an equation for Γ,

$$\partial_i \Gamma \epsilon_{im} \hat{x}_m = 0. \tag{3.89}$$

Again making use of the dimensionality of the underlying space, this implies that Γ can depend only on the radius, $\Gamma = \Gamma(r)$. But as the dynamical fields in both pictures are in general not radially symmetric, it follows that Γ cannot depend on them - in other words, it is of 0^{th} order in the fluctuations, and would therefore have to arise from a linear source term in the Lagrangian. But as the fluctuations are, by definition, fluctuations around a classical solution, such a term cannot exist. In other words, consistency demands that $\Gamma = 0$, so that the equations of motion of the full theory are reproduced.

This means that if the theory of warp fields is supplemented by a twirl field, it can capture the dynamics of all degrees of freedom of the underlying theory. The theory's construction is simple, and its outcomes are in perfect agreement with the reasoning in section 3.3.4. This description also has the intriguing quality of allowing for a redundancy-free discussion of the system's dynamics. The only fundamental difficulty with this technique arises only when attempting to connect the theory with the description in terms of the common fluctuations. Its origin, however, is not in the features of the warp or twirl fields, but in the underlying theory and its residual gauge redundancy.

3.4 Quantization of the warp field

The foundations of the warp field's quantum theory can be constructed from the operators $\hat{\varphi}$, $\hat{\varpi}$ and the Fock space $\mathcal{F}$ they are acting on. To investigate the general features of this theory, it is helpful to consider only the simple case of the free theory in one dimension - it can be expected that interactions can be treated perturbatively, although to this date no rigorous analysis exists.

3.4.1 Linearized theory

Just as for a regular scalar field, the solutions (3.20) of the linearized equations of motion can be used to represent the operators φ and ϖ as

$$\begin{aligned}\hat{\varphi}(t,x) =&\mu_m \hat{v}(t-t_0) + \mu_m \hat{\zeta} + \sum\!\!\!\!\!\!\int_k \hat{\alpha}_k^* e^{i\omega_k t} g_k^*(x) + \hat{\alpha}_k e^{-i\omega_k t} g_k(x),\\ \hat{\varpi}(t,x) =&i\nu^2(\sigma')^2(\mu_m x)\cdot\left(\mu_m \hat{v} + \sum\!\!\!\!\!\!\int_k \hat{\alpha}_k^\dagger \omega_k e^{i\omega_k t} g_k^*(x) - \hat{\alpha}_k \omega_k e^{-i\omega_k t} g_k(x)\right).\end{aligned} \tag{3.90}$$

The usual equal time commutation relations can be imposed on these operators, leading to

$$\begin{aligned}[\hat{\varphi}(t,x), \hat{\varpi}(t,x')] =&i\delta(x-x') \text{ and}\\ [\hat{\varphi}(t,x), \hat{\varphi}(t,x')] =&0 = [\hat{\varpi}(t,x), \hat{\varpi}(t,x')].\end{aligned} \tag{3.91}$$

These relations can be translated to equations for the operators emerging through the mode expansion (3.90), i.e., $\{\alpha_k^{(\dagger)}\}_k$ and $\hat{v}$, $\hat{\zeta}$. Denoting by $\mathcal{I}_c$ and $\mathcal{I}_d$ the continuous and discrete parts of the spectrum, these operators satisfy

$$[\hat{\alpha}_k, \hat{\alpha}_p^\dagger] \propto \begin{cases}\delta(k-p), & \text{for } k,p \in \mathcal{I}_c\\ \delta_{kp}, & \text{for } k,p \in \mathcal{I}_d\end{cases}, \tag{3.92}$$

$$[\hat{\zeta}, \hat{v}] = iM_{\text{sol}}^{-1}. \tag{3.93}$$

In (3.92), two normalization constants sensitive to the chosen normalization of the mode functions and eigenstates have been dropped for the sake of generality.

Given the interpretation of the soliton as a particle-like object and ζ and v as its position and velocity, it makes sense to define a new operator, $\hat{p} = M_{\text{sol}}\hat{v}$, which allows for the recovery of the commutation relation of a particle. Note that this treatment is not unique to warp fields, as it has initially been proposed in the context of the conventional picture in [53]. The commutation relations (3.93) also determine the structure of the theory's Fock space, which combines a sector of particle-like excitations, $\mathcal{F}_p$, with that of the collective coordinate, $L^2(\mathbb{R}, \mathrm{d}x)$,

$$\begin{aligned}\mathcal{F} =&L^2(\mathbb{R}, \mathrm{d}x) \otimes \mathcal{F}_p, \text{ where}\\ \mathcal{F}_p =&\bigoplus_{n=0}^{\infty} S_n\left(L^2(\mathbb{R}, \mathrm{d}\varsigma)\right)^{\otimes n}.\end{aligned} \tag{3.94}$$

In accordance with the usual convention, the excitations represented by $\mathcal{F}_p$ and created by $\hat{\alpha}_p^\dagger$ have been named *warpions* [1].

Compared to the Fock space of a usual scalar field, $\mathcal{F}_p$ stands out due to its spatial measure $\mathrm{d}\varsigma$. This property can be derived from the full Fock space creation/annihilation operators $\mathcal{A}^{(\dagger)}$, which can be expressed through the $\alpha^{(\dagger)}$-operators via

$$\mathcal{A}^{(\dagger)}[f] = \sum\!\!\!\!\!\!\int_k f^k \alpha_k^{(\dagger)}, \tag{3.95}$$

where f^k denotes the coefficients of f with respect to the $\{g_k\}_k$-basis. As an immediate consequence, the usual creation and annihilation operators can be understood as their Fock space counterparts for a single mode function,

$$\alpha_k^{(\dagger)} = A^{(\dagger)}[g_k]. \tag{3.96}$$

It is well known that the commutator of these operators is determined by the scalar product on the one-particle sector $\mathcal{H}$ of the Fock space, $(f,g)_{\mathcal{H}}$, through [69]

$$[\mathcal{A}[f], \mathcal{A}^\dagger[g]] = (f,g)_{\mathcal{H}}. \tag{3.97}$$

The crucial observation is now that equations (3.96), (3.93) and (3.97) are inconsistent with one another on the usual $(L^2, \mathrm{d}x)$ as the mode functions $\{g_k\}_k$ are not orthonogonal, or even normalizable, with respect to the measure $\mathrm{d}x$. They are, however, with respect to the measure $\mathrm{d}\varsigma$, so that the above relations can be consistently realized on $\mathcal{H} = (L^2, \mathrm{d}\varsigma)$.

Before commenting on this feature's physical interpretation in the next subsection, it is important to note that these commutation relations can be used to derive the warp field's propagator, which consists of contributions from both non-zero and zero modes.

The terms linked to the non-zero modes can, in the usual manner, be determined by taking the vacuum expectation value of the time-ordered product of the non-zero mode parts of $\hat{\varphi}$ with itself. The result can be expressed most compactly through the propagator of the fluctuation ϕ in the conventional picture, to which it is related via

$$\Delta_\varphi^{nz}\big((t,x),(t',x')\big) = \frac{\Delta_\phi\big((t,x),(t',x')\big)}{\big(\nu\sigma'(\mu_m x)\big)\big(\nu\sigma'(\mu_m x')\big)}. \tag{3.98}$$

The contribution of the zero modes can be obtained through a slightly modified procedure outlined in [53], which ultimately yields

$$\Delta_\varphi^0(t,t') \propto |t-t'|. \tag{3.99}$$

3.4.2 Interpretation of the probability measure

The quantum theory of the warp field, like the classical theory, has a strong similarity to the theory of a typical scalar field, with the key variation being the presence of the weight function $\rho(x) = \nu^2(\sigma')^2(\mu_m x)$ and the odd asymptotic behavior of the mode functions. The quantum theory, on the other hand, exposes the full significance of these functions, namely that they impose a probability measure proportional to the weight function ρ. This is simply a particle physics equivalent of the classical theory's localization condition. While

warpion-wave functions spread over all of spacetime, the corresponding probability density, when weighted with ρ, is concentrated in the same area as the soliton.

The emergence of ρ in the measure on $\mathcal{H}$ also carries the localization to the expectation values of Fock space observables. Consider some observable $\hat{O}$ acting on the one-particle sector of the Fock space. Its lift to the full Fock space $\mathcal{F}$, $\mathcal{O}$, can then be defined through its action on the state $|\Psi\rangle = |\Psi_1(x), \Psi_2(x_1, x_2), \ldots\rangle$:

$$\begin{aligned} \mathcal{O}\,|\Psi\rangle &= |(\mathcal{O}\Psi)_1(x), (\mathcal{O}\Psi)_2(x_1, x_2), \ldots\rangle\,, \text{ where} \\ \big(\mathcal{O}\Psi\big)_n(x_1, \ldots x_n) &= \sum_{i=1}^{n} \hat{O}(x_i)\Psi_n(x_1, \ldots x_n). \end{aligned} \tag{3.100}$$

Note that, to highlight the effect of the probability measure, $\mathcal{O}$ has been assumed not to act on the L^2-subspace describing the collective coordinate, which has thus been suppressed in the notation. The symbol $\hat{O}(x_i)$ refers to the action of the one-particle operator $\hat{O}$ on the i^{th} argument of the wave function $\Psi_n(x_1, \ldots x_n)$.

Having at hand equation (3.100), it is straightforward to derive the expectation value of $\mathcal{O}$ with respect to some Fock space state $|\Psi\rangle$,

$$\begin{aligned} \langle\Psi|\,\mathcal{O}\,|\Psi\rangle &= \langle\Psi_1|(\mathcal{O}\Psi)_1\rangle + \langle\Psi_2|(\mathcal{O}\Psi)_2\rangle + \cdots = \\ &= \int \mathrm{d}\varsigma(x)\ \Psi_1^*(x)\hat{O}\Psi_1(x) + \\ &\quad + \int \mathrm{d}\varsigma(x_1) \int \mathrm{d}\varsigma(x_2)\ \sum_{i=1}^{2} \Psi_2^*(x_1, x_2)\hat{O}(x_i)\Psi_2(x_1, x_2) + \ldots. \end{aligned} \tag{3.101}$$

The contribution of each n-excitation state thus enters with n integrals, each corresponding to one of the excitations, which is the essential feature of this equation. The contribution of each warpion to any physical observable is again weighted by the density of the soliton, because the measure of integration is $\mathrm{d}\varsigma$ and hence weighed by the function ρ.

3.4.3 Embedding into the theory of the conventional picture

The zero mode of the warp field may be readily recognized using the collective coordinate as described in [53], just as it can in the classical case. Consider the following map between the one particle Hilbert spaces of the φ and the ϕ theories to extend this finding to non-zero modes:

$$\begin{aligned} \iota &: \mathcal{H} \to \mathbb{H} \\ \Psi(x) &\mapsto \rho^{1/2}(x)\Psi(x) \end{aligned} \tag{3.102}$$

This map respects the structure underlying the mode expansion, $\iota(g_k) = f_k$ and $a_k = \iota\alpha_k\iota^{-1}$, and can thus be understood as an isometry. Due to the additional limitations imposed by the linearized theory's applicability, only a subset of $\mathcal{H}$ may be studied, hence this map must be interpreted as an embedding in this context.

This map can be extended to the full Fock space through the usual procedure [69]. This implies that through this map, the action of $\{\alpha_k^\dagger\}$ on $\mathcal{F}_p$ can be identified with that of $\{a_k^\dagger\}$ on $\mathbb{F}$.

This relation also extends to the propagator, and thus, the time evolution of the warpion and scalar particle wave functions. Let $\psi(t',y) = \not{f}_{k\neq 0}\psi_k(t')g_k(y)$ denote some wave function of a single warpion. The propagator then allows to express the wave function at some later time t through this initial configuration:

$$\begin{aligned}\psi(t,x) =& \int \Delta_\varphi\big((t,x),(t',y)\big)\psi(t',y')\mathrm{d}^2\varsigma(y) = \\ =&\frac{1}{\nu\sigma'(\mu_m x)}\int \Delta_\phi\big((t,x),(t',y)\big)\big(\nu\sigma'(\mu_m y)\psi(t',y)\big)\mathrm{d}^2 y = \\ =&\iota^{-1}\bigg(\int \Delta_\phi\big((t,x),(t',y)\big)\iota(\psi)(t',y)\mathrm{d}y\bigg) = \\ =&\iota^{-1}\big(\iota(\psi)(t,x)\big),\end{aligned} \tag{3.103}$$

where the measure is defined as $\mathrm{d}^2\varsigma(y) = \mathrm{d}t'\mathrm{d}\varsigma(y)$.

This confirms that, as could be expected, the time evolutions calculated in both pictures are equivalent. It furthermore demonstrates that the asymptotic behavior of the warp field propagator Δ_φ, which grows exponentially for large x, poses no problem, but is in fact consistent with the result obtained in the conventional picture.

The embedding also allows for an interpretation of the particle-like warpions. When moving beyond the leading order analysis, it is evident that the one-to-one connection of a warpion of momentum k to a scalar particle with the same momentum breaks down. Instead, it can be expected that a single warpion must be considered as a localized superposition of multi-particle states that can be prepared for some finite duration T before dispersing.

3.4.4 Quantum representation of the local velocity via the warp field

In the theory of the warp field, the notion of a local velocity arises naturally both in the classical as well as in the quantum theory as $v_{\mathrm{loc}} = \mu_m^{-1}\dot{\varphi}$. However, as this theory captures only a subset of the larger theory described by the usual fluctuation ϕ, the embedding can be used to recover the local velocity as an observable of the ϕ-theory.

As a first crucial step towards this goal, the non-zero mode part of φ needs to be represented as an observable on the ϕ-Fock space $\mathbb{F}$. Such a representation can be easily obtained from its pendant on the one-particle Hilbert space $\mathbb{H}$, where it takes the form of a series in $\hat{\phi}$. This can be achieved easily through the expansion (3.31):

$$\hat{\varphi}_\phi(t,x) = -\sum_{n=1}^{\infty}\frac{\big(\sigma^{-1}\big)^{(n)}(z)}{\nu^n n!}\bigg|_{z=\sigma(\mu_m x)}\hat{\phi}^n(t,x). \tag{3.104}$$

Similarly, the local velocity v_{loc} can be represented as a series in ϕ and π, and thus as an observable on $\mathbb{H}$. Setting out from (3.104), this is straightforward and leads to

$$\hat{v}_{\text{loc}} = -\sum_{n=1}^{\infty} \frac{\left(\sigma^{-1}\right)^{(n)}(z)}{\mu_m \nu^n n!}\bigg|_{z=\sigma(\mu_m x)} (\hat{\phi}^{n-1}\hat{\pi} + \cdots + \hat{\pi}\hat{\phi}^{n-1}), \tag{3.105}$$

where

$$\mathcal{D}(\hat{v}_{\text{loc}}(t,x)) = \{|\Psi\rangle \in \mathcal{F}_\phi : \hat{\varphi}(t,x)\,|\Psi\rangle \in \mathcal{F}_\phi\}. \tag{3.106}$$

Because the $\{\hat{a}k^{(\dagger)}\}_k$ operators form ϕ and π, they only act on $\mathcal{F}_p$ and are unaffected by the L^2-piece of the systems dynamics. This demonstrates that the velocity of the soliton can be separated into a global component, which corresponds to the dynamics associated with the zero mode, and a local component, which can be completely characterized in terms of $\mathbb{F}$.

3.4.5 Comparison with the classical theory

The existence of the warp field is linked to the breaking of the underlying theory's translational symmetry in both the classical as well as the quantum picture. This relationship is represented in the classical theory by the weight function ρ in the action, whereas in the quantum theory it is reflected by the probability measure of the Fock space of warp particles. This extra factor causes the effects of warp field configurations to be localized to the same region as the soliton in the classical theory. In the quantum theory, this causes the wave function in that region to dominate the expectation value of any observable. Much like in classical theory, the weight factor is proportional to the soliton's energy density.

The warp field, as well as the local velocity, can be represented as observables of the full dynamical theory of fluctuations around the warp field in both quantum and classical theory. The local velocity is thus determined by the dynamics of the non-zero modes, whilst the global velocity is determined by the collective coordinate.

This is possible because the quantum theory of φ can be shown to be a subset of the general dynamical theory of fluctuations around the soliton, just like in the classical theory. The collective coordinate, in particular, is entirely contained within the warp field, allowing its dynamics and operator structure to be replicated.

Chapter 4

The lifetime of the electroweak vacuum

This chapter contains some results of [2].

The RG evolution of the Higgs' quartic coupling supports a somewhat disturbing scenario: The very vacuum we live in, and thus many of the laws of nature we observe, might not be stable. While the potential barrier protecting us from the abyss is many orders of magnitudes larger than the electroweak scale, it is not impervious to tunneling. Thus, it can be expected that at some point the Higgs field will indeed tunnel through it, ending the universe as we know it. Fortunately, however, the typical timescale for the probability of this process to become of order 1 is reassuringly large, with the best current estimate hinting at a time of order 10^{983} years.

4.1 Vacuum decay in Quantum Field Theory

The decay rate from the basin of the false vacuum FV into some region R can be defined in terms of two probabilities:

- The probability that the field remains in the basin, $P_{FV}(t)$.
- The probability that the field tunneled into R, $P_R(t)$.

Assuming that these two cover all of field space, they satisfy $\frac{d}{dt}P_{FV} = -\frac{d}{dt}P_R$. The decay rate from FV into R is then defined by

$$\Gamma_R = -\frac{1}{P_{FV}}\frac{d}{dt}P_{FV} = \frac{1}{P_{FV}}\frac{d}{dt}P_R, \tag{4.1}$$

so that $P_{FV}(t) \sim e^{-\Gamma t}$. A rigorous calculation of the decay rate has recently been developed for the simpler case of a quantum mechanical particle, which can be easily generalized to a quantum field [70, 71]. It is nevertheless still interesting to derive the resulting expression

directly. This can be done most efficiently in the Schrödinger picture of quantum field theory. Denoting by ϕ_{FV} the false vacuum and labeling the configurations in the region R by φ_f, it is given by

$$P_R = \int_R D\varphi_f |\langle \varphi_f, t|\phi_{FV}, 0\rangle|^2 \sim \int_R D\varphi_f |D_F(\phi_{FV}, 0|\varphi_f, t)|^2, \tag{4.2}$$

where a normalization factor, which will cancel out in the end, has been dropped and D_F denotes the path integral

$$D_F(\phi_{FV}, 0|\varphi_f, t) = \int_{\varphi(0)=\phi_{FV}}^{\varphi(t)=\varphi_f} D\varphi\ e^{iS[\varphi]} \sim \langle \varphi_f, t|\phi_{FV}, 0\rangle\,. \tag{4.3}$$

A good way to quantify the transition from FV to R is to consider the boundary Σ separating the two regions. The tunneling connecting FV to R can be made manifest by splitting the propagator into two pieces, the propagation from FV until Σ and its evolution beyond. This decomposition can be quantified through the following identity:

$$\begin{aligned} &D_F(\phi_{FV}, 0|\varphi_f, t) = \\ &\quad = \int_0^t dt_0 \int_\Sigma D\sigma \int_{\varphi_1(0)=\phi_{FV}}^{\varphi_1(t_0)=\sigma} D\varphi_1 \delta(T_\Sigma[\varphi_1] - t_0) e^{iS[\varphi_1]} \int_{\varphi_2(t_0)=\sigma}^{\varphi_2(t)=\varphi_f} D\varphi_2 e^{iS[\varphi_2]} \end{aligned} \tag{4.4}$$

The functional T_Σ maps each field configuration to the time when it first passes through Σ, so that $\delta(T_\Sigma[\varphi_1] - t_0)$ filters out field space paths which first leave FV at the time t_0.

This expression, and all following calculations, can be simplified by defining a propagator describing the dynamics until Σ is crossed for the first time,

$$\bar{D}_F(\phi_{FV}, 0|\sigma, t_0) = \int_{\varphi_1(0)=\phi_{FV}}^{\varphi_1(t_0)=\sigma} D\varphi_1 \delta(T_\Sigma[\varphi_1] - t_0) e^{iS[\varphi_1]}. \tag{4.5}$$

Using this new quantity, recognizing the last integral in (4.4) as $D_F(\sigma, t_0|\varphi_f, t)$ and assuming time translation invariance, equation (4.4) can be rewritten as

$$D_F(\phi_{FV}, 0|\varphi_f, t) = \int_0^t dt_0 \int_\Sigma D\sigma \bar{D}_F(\phi_{FV}, 0|\sigma, t_0) D_F(\sigma, 0|\varphi_f, t - t_0). \tag{4.6}$$

This expression can then be used to calculate P_R:

$$\begin{aligned} P_R &\sim \int_R D\varphi_f |D_F(\phi_{FV}, 0|\varphi_f, t)|^2 = \\ &= \int_R D\varphi_f \int_\Sigma D\sigma \int_\Sigma D\sigma' \int_0^t dt_0 \int_0^t dt_0' \\ &\quad \bar{D}_F^*(\phi_{FV}, 0|\sigma, t_0) D_F^*(\sigma, 0|\varphi_f, t - t_0) \bar{D}_F(\phi_{FV}, 0|\sigma', t_0') D_F(\sigma', 0|\varphi_f, t - t_0') = \\ &= \int_\Sigma D\sigma \int_\Sigma D\sigma' \int_0^t dt_0 \int_0^t dt_0' \bar{D}_F^*(\phi_{FV}, 0|\sigma, t_0) \bar{D}_F(\phi_{FV}, 0|\sigma', t_0') \cdot \\ &\quad \cdot \int_R D\varphi_f D_F^*(\sigma, 0|\varphi_f, t - t_0) D_F(\sigma', 0|\varphi_f, t - t_0') \end{aligned} \tag{4.7}$$

Now, assuming that the probability of back-tunneling from R into FV is negligible, one can use that

$$\int_R D\varphi_f \, |\varphi_f\rangle \langle\varphi_f| \approx \mathbb{1}. \tag{4.8}$$

This implies that the last line of (4.7) can be simplified to

$$\int_R D\varphi_f D_F^*(\sigma, 0|\varphi_f, t - t_0) D_F(\sigma', 0|\varphi_f, t - t_0') = D_F\sigma', 0|\sigma, t_0 - t_0'). \tag{4.9}$$

Furthermore, the time integrals can be rearranged by splitting them into two regions with $t_0 > t_0'$ and $t_0 < t_0'$. It can then be seen easily that this amounts to

$$\int_0^t dt_0 \int_0^t dt_0' = \int_0^t dt_0 \int_0^{t_0} dt_0' + \int_0^t dt_0' \int_0^{t_0'} dt_0. \tag{4.10}$$

Combining (4.9) and (4.10), P_R becomes

$$\begin{aligned}
P_R \sim & \int_0^t dt_0 \int_0^{t_0} dt_0' \int_\Sigma D\sigma \int_\Sigma D\sigma' \\
& \bar{D}_F^*(\phi_{FV}, 0|\sigma, t_0) \bar{D}_F(\phi_{FV}, 0|\sigma', t_0') D_F(\sigma', 0|\sigma, t_0 - t_0') + \\
& + \int_0^t dt_0' \int_0^{t_0'} dt_0 \int_\Sigma D\sigma \int_\Sigma D\sigma' \\
& \bar{D}_F^*(\phi_{FV}, 0|\sigma, t_0) \bar{D}_F(\phi_{FV}, 0|\sigma', t_0') D_F(\sigma', 0|\sigma, t_0 - t_0') \\
= & \int_0^t dt_0 \int_\Sigma D\sigma \; \bar{D}_F^*(\phi_{FV}, 0|\sigma, t_0) \cdot \\
& \cdot \int_0^{t_0} dt_0' \int_\Sigma D\sigma' \bar{D}_F(\phi_{FV}, 0|\sigma', t_0') D_F(\sigma', 0|\sigma, t_0 - t_0') + \\
& + \int_0^t dt_0' \int_\Sigma D\sigma' \; \bar{D}_F(\phi_{FV}, 0|\sigma', t_0') \cdot \\
& \cdot \int_0^{t_0'} dt_0 \int_\Sigma D\sigma \bar{D}_F^*(\phi_{FV}, 0|\sigma, t_0) D_F^*(\sigma', 0|\sigma, t_0' - t_0)
\end{aligned} \tag{4.11}$$

The terms collected in the end of each line are now nothing but the left hand side of (4.4), so that they can be simplified even further:

$$\begin{aligned}
P_R \sim & \int_0^t dt_0 \int_\Sigma D\sigma \; \bar{D}_F^*(\phi_{FV}, 0|\sigma, t_0) D_F(\phi_{FV}, 0|\sigma, t_0) + \\
& + \int_0^t dt_0' \int_\Sigma D\sigma' \; \bar{D}_F(\phi_{FV}, 0|\sigma', t_0') D_F^*(\phi_{FV}, 0|\sigma, t_0) = \\
= & \int_0^t dt_0 \int_\Sigma D\sigma \Big(\bar{D}_F^*(\phi_{FV}, 0|\sigma, t_0) D_F(\phi_{FV}, 0|\sigma, t_0) + \\
& + \bar{D}_F(\phi_{FV}, 0|\sigma', t_0') D_F^*(\phi_{FV}, 0|\sigma, t_0) \Big)
\end{aligned} \tag{4.12}$$

The two remaining terms are trivially related through complex conjugation, ensuring that P_R is indeed real. As a next step, the remaining path integrals need to be evaluated in

euclidean time. To do so, it is helpful to write them out:

$$P_R \sim \int_0^t dt_0 \int_\Sigma D\sigma \int_{\varphi_1(0)=\phi_{FV}}^{\varphi_1(t_0)=\sigma} D\varphi_1 \delta(T_\Sigma[\varphi_1]-t_0) e^{-iS[\varphi_1]} \int_{\varphi_2(0)=\phi_{FV}}^{\varphi_2(t_0)=\sigma} D\varphi_2 e^{-iS[\varphi_2]} + c.c. \tag{4.13}$$

To ensure convergence, the sign of the euclidean time depends on the prefactor of the euclidean action in the exponent:

- If the exponent is $-S$, the euclidean time needs to be defined as $\tau = -it$. This transformation also flips the boundaries of the path integral.
- If the exponent is S, the euclidean time needs to be defined as $\tau = it$.

While the transformation of the action is straightforward, that of the δs requires some more care, but is ultimately not particularly insightful [71]. In summary, depending on which of the above definitions is used, the delta picks up a phase factor of $\pm i$, where the overall prefactor can be chosen such that P_R is positive. Besides moving to euclidean time, one can now also eliminate the time integral by right away considering $\frac{d}{dt}P_R$ instead of P_R:

$$\begin{aligned}
\frac{d}{dt}P_R \sim \int_\Sigma D\sigma \Bigg(& i \int_{\varphi_1(-\tau)=\sigma}^{\varphi_1(0)=\phi_{FV}} D\varphi_1 \delta(\mathcal{T}_\Sigma[\varphi_1]-\tau) e^{-S_E[\varphi_1]} \int_{\varphi_2(0)=\phi_{FV}}^{\varphi_2(\tau)=\sigma} D\varphi_2 e^{-S_E[\varphi_2]} - \\
& - i \int_{\varphi_1(0)=\phi_{FV}}^{\varphi_1(\tau)=\sigma} D\varphi_1 \delta(\mathcal{T}_\Sigma[\varphi_1]-\tau) e^{-S_E[\varphi_1]} \int_{\varphi_2(-\tau)=\sigma}^{\varphi_2(0)=\phi_{FV}} D\varphi_2 e^{-S_E[\varphi_2]} \Bigg) = \\
= \int_\Sigma D\sigma \Bigg(& - i \int_{\varphi_1(-\tau)=\phi_{FV}}^{\varphi_1(0)=\sigma} D\varphi_1 \delta(\mathcal{T}_\Sigma[\varphi_1]) e^{-S_E[\varphi_1]} \int_{\varphi_2(0)=\sigma}^{\varphi_2(\tau)=\phi_{FV}} D\varphi_2 e^{-S_E[\varphi_2]} + \\
& + i \int_{\varphi_2(-\tau)=\phi_{FV}}^{\varphi_2(0)=\sigma} D\varphi_2 e^{-S_E[\varphi_2]} \int_{\varphi_1(0)=\sigma}^{\varphi_1(\tau)=\phi_{FV}} D\varphi_1 \delta(\mathcal{T}_\Sigma[\varphi_1]-\tau) e^{-S_E[\varphi_1]} \Bigg)
\end{aligned} \tag{4.14}$$

The important observation is now that after the change to euclidean time, performing the σ-integral allows to combine these integrals into two expressions which are identical up to the sign in front of them. Thus, (4.7) ultimately takes the form

$$\frac{d}{dt}P_R \sim 2 \left| \mathrm{Im} \int_{\varphi(-\tau)=\phi_{FV}}^{\varphi(\tau)=\phi_{FV}} D\varphi \; \delta(\mathcal{T}_\Sigma[\varphi]) e^{-S_E[\varphi]} \right|. \tag{4.15}$$

A similar procedure, just without the necessity to enforce the crossing of Σ, can be applied to calculate P_{FV}, leading to

$$P_{FV} \sim \int_{\varphi(-\tau)=\phi_{FV}}^{\varphi(\tau)=\phi_{FV}} D\varphi \; e^{-S_E[\varphi]} \tag{4.16}$$

The dropped coefficients here agree with those in (4.7), so that they cancel out in the decay rate:

$$\frac{\Gamma(t)}{2} = \frac{\left| \mathrm{Im} \int_{\varphi(-\tau)=\phi_{FV}}^{\varphi(\tau)=\phi_{FV}} D\varphi \; \delta(\mathcal{T}_\Sigma[\varphi]) e^{-S_E[\varphi]} \right|_{\tau=it}}{\int_{\varphi(-\tau)=\phi_{FV}}^{\varphi(\tau)=\phi_{FV}} D\varphi \; e^{-S_E[\varphi]}} \tag{4.17}$$

A crucial subtlety one might want to keep in mind is that the decay rate is **not** defined for all times t - for small enough times and a generic initial state, it is possible that some non-trivial dynamics can spoil the exponential fall-off of the probability P_{FV}. Similarly, for sufficiently large times and a potential with an actual true vacuum, reflection effects might lead to some back-tunneling from R to FV.

In cases in which the lifetime can be expected to be larger than the typical scale of the system (and thus the size of the instanton), the relation (4.17) can be further simplified by taking the limit $t \to \infty$ on the right hand side. This step can also be justified by considering that t should anyways be sufficiently large for the exponential fall-off to settle in.

Lastly, the δ can be dropped by restricting the domain of the path integral in the numerator, leading to

$$\frac{\Gamma}{V} = \lim_{T\to\infty} \frac{1}{TV} \frac{\mathrm{Im} \int_{\mathcal{C}_b} D\varphi \; e^{-S_E[\varphi]}}{\int_{\mathcal{C}_{FV}} D\varphi \; e^{-S_E[\varphi]}}, \tag{4.18}$$

where $\mathcal{C}_b$ and $\mathcal{C}_{FV}$ denote properly chosen paths in field space.

Through a saddle point approximation, the expression for the decay rate can be reduced to a Gaussian integral,

$$\begin{aligned} \frac{\Gamma}{V} &= \lim_{T\to\infty} \frac{1}{TV} \frac{\mathrm{Im} \int D\phi \; \exp(-S_E[\Phi_b] - \int d^4x \; \phi S_E''[\Phi_b]\phi)}{\int D\phi \; \exp(-S_E[\Phi_{fv}] - \int d^4x \; \phi S_E''[\Phi_{fv}])\phi} \simeq \\ &\simeq \lim_{T\to\infty} \frac{1}{TV} e^{-(S_E[\Phi_b]-S_E[\Phi_{fv}])} \cdot \frac{\mathrm{Im} \int D\phi \; \exp(-\int d^4x \; \phi S_E''[\Phi_b]\phi)}{\int D\phi \; \exp(-\int d^4x \; \phi S_E''[\Phi_{fv}]\phi)}. \end{aligned} \tag{4.19}$$

By properly shifting the potential, it is now possible to set $S_E[\Phi_{fv}] = 0$. The *instanton* Φ_b minimizes the euclidean action under the appropriate boundary conditions and will be discussed in the next section, whereas the remaining path integrals can be related to functional determinants of the fluctuation operator and are discussed in section 4.3.

So far, this discussion was restricted to the case of a single scalar field. Although this is sufficient for the SM, the existence of more involved composite Higgs models, the (ν)MSSM and other models with additional scalars motivates a generalization of equation (4.19). Doing so is straightforward and can be done efficiently by combining all involved scalars into a single tuple $\Phi^i = \Phi_b^i + \delta\Phi^i$, in terms of which the decay rate becomes

$$\frac{\Gamma}{V} \simeq \lim_{T\to\infty} \frac{1}{TV} e^{-S_E[\Phi_b]} \cdot \frac{\mathrm{Im} \int D\delta\Phi \; \exp(-\int d^4x \; \delta\Phi^m \frac{\delta^2 S_E}{\delta\Phi^m \delta\Phi^n}[\Phi_b]\delta\Phi^n)}{\int D\delta\Phi \; \exp(-\int d^4x \; \delta\Phi^m \frac{\delta^2 S_E}{\delta\Phi^m \delta\Phi^n}[\Phi_{fv}]\delta\Phi^n)}. \tag{4.20}$$

Assuming no change in the vacuum of the gauge fields, their influence on the decay rate is only through loop corrections, which will be discussed in section 4.3.

4.2 Instantons & Euclidean Action

The path-integral in (4.19) is dominated by the configuration that minimizes the euclidean action, the so-called instanton, which is a solution of the equation $-\Delta_4\Phi_b + \nabla_\Phi V(\Phi_b) = 0$. Imposing rotational symmetry of the solution, this implies that

$$\left(-\partial_r^2 - \frac{3}{r}\partial_r\right)\Phi_b(r) + \nabla_\Phi V(\Phi_b) = 0, \tag{4.21}$$

where r denotes the radius in the four-dimensional, euclidean spacetime.

For such a solution to indeed describe a transition from the false vacuum, it has to satisfy the boundary conditions $\lim_{r\to\infty}\Phi_b(r) = \Phi_{fv}$ as well as $\Phi_b'(0) = 0$ and $\Phi_b(0) \in R$. Together with equation (4.21), these conditions imply that the configuration at zero euclidean time τ, $\Phi_b(\tau = 0)$ has zero energy. This configuration represents the bubble created through the tunneling process, which at its center takes values beyond the potential barrier separating false and true vacuum.

A simple and efficient way to understand the solutions to (4.21) is by considering an analogous mechanical problem. By replacing $r \to t$, equation (4.21) can be understood as the equation of motion of a point particle with position Φ_b moving in the inverse potential with time-dependent friction $\propto \frac{3}{r}$. In this setup, the boundary conditions of the bounce correspond to a setup in which the point particle starts at rest from some initial position $\Phi_b(0)$, then rolls down the potential and converges towards the top of the inverted potential's local maximum corresponding to the false vacuum for $t \to \infty$.

When no analytical solution of (4.21) is available, this picture offers a simple understanding of the most commonly used algorithm for the search of numerical solutions, the so-called *shooting method*. For most generic potentials, it is clear that there exists precisely one initial value $\Phi_b(0)$ for which the above behavior occurs. If the particle starts from a point where the potential is too small, typically characterized by a small $\Phi_b(0)$, it won't have enough energy to roll up the hill separating it from the true vacuum and instead oscillate within the well representing the potential barrier without ever reaching the true minimum. Inversely, if this behavior occurs for a particular $\Phi_b(0)$, it is clear that it is smaller than the desired value. If $\Phi_b(0)$ instead corresponds to a too large potential energy, typically linked to a large $\Phi_b(0)$, the particle will reach the true minimum within finite time, pass through it and roll down the inverted potential at the other side.

The value of $\Phi_B(0)$ corresponding to the instanton can thus be determined through a simple algorithm:

1. Pick an arbitrary value for $\Phi_b(0)$.
2. Numerically integrate equation (4.21) with this value.
3. If the corresponding solution reaches the maximum representing the true vacuum within finite time, pick a smaller $\Phi_b(0)$.

4. If it does not reach the maximum representing the true vacuum, but has a turning point at some larger $r \equiv t$, pick a larger $\Phi_b(0)$.

Through iterative application of this simple procedure it is possible to determine the correct value of $\Phi_b(0)$ to arbitrary precision.

4.3 Functional determinants

From equation (4.19) it is evident that the leading order term e^{-S} is insufficient to obtain a reasonable result for the decay rate due to the prefactor $\frac{1}{TV}$, which vanishes both through the limit $T \to \infty$ and for infinitely large spaces. Thus, the only way to obtain a finite but non-vanishing decay rate is if the leading order corrections are of the form

$$(\text{gaussian terms}) = TV \cdot \mu_\gamma^4 \ldots, \tag{4.22}$$

where μ_γ^4 is some constant of energy dimension four. Furthermore, equation (4.19) lacks the information at which renormalization scale the parameters of the potential need to be evaluated.

The natural place to search for the solution to these issues are the fluctuations of the scalar fields, which enter the path integral to leading order through the Gaussian

$$\int D\phi \ \exp\left(-\int d^4x \ \delta\Phi^i(-\delta_{ij}\Delta_4 + W_{ij}[\Phi_b])\delta\Phi^j\right), \tag{4.23}$$

where $W_{ij}[\Phi_b] \coloneqq \frac{\partial^2 V}{\partial\Phi^i\partial\Phi^j}(\Phi_b)$. It is well-known that this expression can be related to the functional determinant of the operator $(O_\Phi)_{ij} = -\delta_{ij}\Delta_4 + W_{ij}[\Phi_b]$. In the context of the SM, and in particular in the limit of an approximately scale invariant potential, this perspective is plagued by several problems of technical nature. This motivated the authors of [7] to express the integrand of equation (4.23) through a rescaled operator $(\hat{O}_\Phi)_{ij} = \gamma_\Phi^{-1} \cdot (O_\Phi)_{ij}$ as

$$\int D\phi \ \exp\left(-\int \mathrm{d}^4x \ \gamma_\Phi(x)\delta\Phi^i(\hat{O}_\Phi)_{ij}\delta\Phi^j\right). \tag{4.24}$$

While in the pure SM, the choice $\gamma_\Phi = V''(\Phi_b)$ has been shown to avoid all problems arising when using the form (4.23), γ_Φ is in principle arbitrary, and can be chosen to maximally simplify the potential of interest. To emphasize this universality, the only assumption regarding γ_Φ throughout the remainder of this discussion will be that $[\gamma_\Phi] = E^2$, so that $\hat{O}_\Phi$ is dimensionless.

To perform a Gaussian path integral like (4.23), it is helpful to decompose the fluctuations

with respect to the eigenfunctions χ_i^j of $\hat{O}$, which satisfy

$$\hat{O}^k_{\Phi,j}\chi^j_i = \lambda_i \chi^k_i, \tag{4.25}$$

$$\sum_i \int d^4x\ \gamma(x)\chi^i_n\chi^i_m = 2\pi\delta_{nm}, \tag{4.26}$$

$$\delta\Phi^i = \sum_n \phi^n \chi^i_n. \tag{4.27}$$

Note that, as $\hat{O}$ is only hermitian with respect to the measure $d\gamma := d^4x \cdot \gamma_\Phi$, it is also this measure with respect to which the eigenfunctions are orthogonal. Through this decomposition, the path integral can be written as

$$\int D\delta\Phi ... \propto \prod_i \int d\phi^i, \tag{4.28}$$

where a normalization factor has been dropped. This factor will cancel with its pendant in the numerator of (4.20), which can be evaluated similarly.

Combining equation (4.25) and (4.26), the path integral over the fluctuations can finally be evaluated as a Gaussian:

$$\begin{aligned}\int D\delta\Phi \exp\left(-\frac{1}{2}\int d^4x\ \delta\Phi^i(O)_{ij}\delta\Phi^j\right) &\propto \\ \propto \prod_i \int d\phi^i \exp\left(-\frac{1}{2}\int d^4x\ \gamma(x)\sum_n \phi^n\chi^i_n(\hat{O}_\phi)_{ij}\sum_n \phi^n\chi^j_n\right) &= \\ = \prod_i \int d\phi^i \exp\left(-\sum_n\sum_m \phi^n\phi^m\frac{1}{2}\int d^4x\ \gamma_i(x)\chi^i_n(\hat{O})_{ij}\chi^j_m\right) &= \\ = \prod_i \int d\phi^i \exp\left(-\sum_n\sum_m \phi^n\phi^m\frac{1}{2}\lambda_m\int d^4x\ \gamma_i(x)\chi^i_n\chi^i_m\right).\end{aligned} \tag{4.29}$$

Using the orthogonality of the mode functions (4.27), this expression can be reduced to a product of Gaussian integrals:

$$\begin{aligned}\int D\delta\Phi \exp\left(-\frac{1}{2}\int d^4x\delta\phi^i(O)_{ij}\delta\phi^j\right) = \prod_i \int d\phi^i \exp\left(-\pi\sum_n(\phi^n)^2\lambda_n\right) = \\ = \prod_i \int d\phi^i \prod_n \exp\left(-\pi(\phi^n)^2\lambda_n\right) = \prod_n \frac{1}{\sqrt{\lambda_n}}\end{aligned} \tag{4.30}$$

In general, this expression can now be related to the determinant of the fluctuation operator $\hat{O}_\phi$,

$$\prod_i \sqrt{\lambda_i} = \sqrt{\det(\hat{O})} = \prod_{i\in\text{fields}} \sqrt{\det(\hat{O}_i)}. \tag{4.31}$$

However, the situation is more complicated when dealing with the scalar determinants, as the spectrum of $\hat{O}_\phi$ contains four translational zero modes. Just like in the context of solitons, these need to be treated non-perturbatively through the introduction of collective coordinates. On the level of the scalar field, this amounts to splitting the fluctuation as

$$\delta\Phi^i = \bar{\phi}^i + z^\mu \partial_\mu \Phi_b^i. \tag{4.32}$$

where $\bar{\phi}$ is the fluctuation of the scalar field with zero modes removed.

As always for collective coordinates, the mode functions with zero eigenvalue are related to the derivatives of the instanton via $\chi_{0,\alpha} = N\partial_\alpha \Phi_b$, with some normalization factor N. This normalization will turn out to be crucial, as it also connects the expansion parameter $\phi^{0,\alpha}$ with the collective coordinates z_μ via

$$N\phi^{0,\alpha}\partial_\alpha \Phi_b^i = z^\mu \partial_\mu \Phi_b^i. \tag{4.33}$$

From this expression it is easy to see that, when moving to collective coordinates, the differential of the fluctuation $\phi^{0,\alpha}$ transforms as

$$d\phi^{0,\alpha} = \frac{1}{N} dz^\alpha \tag{4.34}$$

Thus, the integral over the zero mode fluctuations can be brought to the form

$$\int \prod_\alpha d\phi^{0,\alpha} = \frac{1}{N^4} \int d^4 z = \frac{1}{N^4} TV. \tag{4.35}$$

While this expression is still divergent, it is now evident that this divergence cancels with the factor of $(TV)^{-1}$ in the definition of the decay rate, leaving only the normalization factor N^{-4}. This term can be computed by recalling the normalization condition for the mode functions,

$$\begin{aligned} \sum_i \int d^4x\ \gamma(x) N^2 (\partial_\alpha \Phi_b^i)^2 &= 2\pi \\ \Rightarrow N = \sqrt{\frac{2\pi}{\int d^4x\ \gamma(x) \sum_i (\partial_\alpha \Phi_b^i)^2}} &\sim \frac{1}{[\gamma]^{\frac{1}{2}}} \sim \frac{1}{E}, \end{aligned} \tag{4.36}$$

which holds for all α because of the instanton's spherical symmetry. Thus, moving to collective coordinates not only solves the potential issues of the zero modes, but also allows to make explicit the dimensionful prefactor of the decay rate in equation (4.22), $\mu_\gamma \sim \frac{1}{N}$. After extracting the zero modes, the path integral over the scalar fluctuations reduces to

$$\begin{aligned} \int D\delta\Phi \exp\left(-\frac{1}{2} \int d^4x \delta\phi^i (O_\Phi)_{ij} \delta\phi^j \right) &= \prod_i \int d\phi^i \exp\left(-\frac{1}{2} \sum_n (\phi^n)^2 2\pi\lambda_n \right) = \\ &= TV \frac{1}{N^4} \prod_{n\neq 0} \frac{1}{\sqrt{\lambda_n}}. \end{aligned} \tag{4.37}$$

Besides the zero modes, the spectrum around the instanton contains another mode of particular interest. It was shown in [72] that the fluctuations around all reasonable instantons contain precisely one mode with a negative eigenvalue. The corresponding Gaussian integral can be performed through analytic continuation and choosing a path s.t. that the decay rate is positive, effectively leading to the replacement $\lambda^{-\frac{1}{2}} \to i|\lambda|^{-\frac{1}{2}}$ in equation (4.37). The conceptual significance of this result can be understood from formula (4.19). The decay rate is sensitive only to the imaginary part of the functional determinants, and it is this mode which renders the determinant imaginary - in other words, without it, the decay rate would vanish.

It remains to calculate the product of the positive non-zero eigenvalues. They can be understood as the determinant of $\hat{O}_\phi$ with zero modes removed, denoted by $\hat{O}'_\phi$. While this expression on its own will turn out to be divergent, the exact same divergence can be found in the normalization factor $\frac{1}{Z}$, which can also be understood as a functional determinant:

$$\frac{1}{Z_\Phi} = \left[\int D\phi \ \exp(-S[\Phi_{fv}] - \delta\Phi_i \frac{\delta^2 S}{\delta\Phi_i \delta\Phi_j}[\Phi_{fv}]\delta\Phi_j \right]^{-1} = \det\left(\frac{\delta^2 S}{\delta\Phi_i \delta\Phi_j}[\Phi_{fv}] \right). \tag{4.38}$$

Recall now that in equation (4.24), when rescaling the fluctuation operator, a prefactor was dropped. Also this can now be justified, as the exact same term can be achieved by rescaling the fluctuation operator around the false vacuum:

$$F_\Phi = \frac{\delta^2 S}{\delta\Phi_i \delta\Phi_j}[\Phi_{fv}] \cdot \frac{1}{\gamma(x)} = \frac{-\delta_{ij}\Delta_4 + \partial_{\Phi_i}\partial_{\Phi_j} V[\Phi_{fv}]}{\gamma(x)}, \quad \frac{1}{Z_\Phi} \propto \det(F_\Phi)^{\frac{1}{2}}, \tag{4.39}$$

where the $\propto$ indicates the canceled prefactor, which cancels with its pendant from the bounce.

Altogether, the path integral over the scalar fluctuations becomes

$$\frac{1}{Z_\Phi} \int D\Phi(\dots) = \frac{1}{N^4} \sqrt{\frac{\det(F_\Phi)}{\det(\hat{O}'_\Phi)}}. \tag{4.40}$$

Thus, it remains to calculate the ratio of these functional determinants. As a first step, it can be reduced to a one-dimensional problem by decomposing the fluctuations in terms of hyperspherical harmonics, which formally corresponds to representing the four-dimensional operator Laplace as a direct sum, $\Delta = \bigoplus_{s,l,m} \left(\partial_r^2 + \frac{3}{r}\partial_r - \frac{s(s+2)}{r^2} \right)$. Doing so leads to a decomposition of the operators F_Φ and $\hat{O}'_\Phi$ as direct sums over their reduction on subspaces of constant s, $F_\Phi = \oplus_s F_{\Phi,s}$, and similarly for $\hat{O}'_\Phi$.

Taking into account the degeneracy arising from the operators' dependence on s alone, this implies that

$$\frac{\det(F_\Phi)}{\det(\hat{O}'_\Phi)} = \prod_s \left(\frac{\det(F_{\Phi,s})}{\det(\hat{O}'_{\Phi,s})} \right)^{(s+1)^2}. \tag{4.41}$$

In the best case scenario, the eigenvalues of the operators F_s and $\hat{O}'_{h,s}$ can be calculated analytically for all s. This is now unfortunately not the case for most potentials, in particular if the instanton itself is only known numerically. However, for each s and for all potentials and instantons, the ratio $\det(F_s)/\det(\hat{O}'_{h,s})$ can be calculated through the famous *Gelfand-Yaglom method*.

Consider two arbitrary one-dimensional differential operators $\hat{O}_1$ and $\hat{O}_2$ acting on a set of N fields, $\{\Phi^i\}_i$. Assume further that for each of these operators, a set of independent zero mode ensembles regular at the origin is known, i.e. two sets of functions $\zeta^j_{1,i}$ and $\zeta^j_{2,i}$ where the upper index j labels the different fields involved and the lower index i different ensembles, i.e.,

$$(\hat{O}_a)^k_j \zeta^j_{a,i} = 0 \text{ for } a \in \{1,2\} \text{ and } i \in \{1,...,N\}. \tag{4.42}$$

The Gelfand-Yaglom method then states that the ratio of the functional determinants of the two differential operators can be obtained directly from these zero modes through the relation

$$\frac{\det(\hat{O}_1)}{\det(\hat{O}_2)} = \lim_{x\to\infty} \frac{\det\big(\zeta_2(0)\big)}{\det\big(\zeta_1(0)\big)} \cdot \frac{\det\big(\zeta_1(x)\big)}{\det\big(\zeta_2(x)\big)}.$$

In the case of a single scalar field, this reduces to

$$\frac{\det(\hat{O}_1)}{\det(\hat{O}_2)} = \lim_{x\to\infty} \frac{\zeta^0_2(0)}{\zeta^0_1(0)} \cdot \frac{\zeta^0_1(x)}{\zeta^0_2(x)}, \tag{4.43}$$

where ζ^0_a denotes a zero mode of $\hat{O}_a$. While this equation would in principle allow for the numerical evaluation of the functional determinant, it is plagued by a numerical instability arising from the exponential growth of ζ^0_a for large x. For a single field, a well-established way around this issue is to instead right away derive a differential equation for the ratio $\rho(r) = \frac{\zeta^0_1(r)}{\zeta^0_2(r)}$, so that equation (4.43) becomes

$$\frac{\det(\hat{O}_1)}{\det(\hat{O}_2)} = \lim_{x\to\infty} \rho(x) = \rho_\infty, \tag{4.44}$$

where furthermore the boundary condition $\zeta^0_2(0) = \zeta^0_1(0)$ has been imposed to simplify the relation.

This procedure can easily be generalized for the case of multiple fields. As the functional determinant only depends on the determinant of ζ_a, it is possible to choose ζ_2 to be diagonal in field space,

$$\zeta^1_2 = (z^1, 0, 0, 0, ...),\ \zeta^2_1 = (0, z^2, 0, 0, ...), ... \ . \tag{4.45}$$

Thus, in parallel to the quantity ρ, a set of rescaled zero modes can be defined as

$$\rho^1 = \frac{1}{z^1} \cdot \zeta^1_1,\ \rho^2 = \frac{1}{z^2} \cdot \zeta^2_1, ... \ . \tag{4.46}$$

Again choosing proper boundary conditions at $x = 0$, this leads to a simple expression for the functional determinants,

$$\frac{\det(\hat{O}_1)}{\det(\hat{O}_2)} = \lim_{x\to\infty} \det\big(\rho^1(x), \rho^2(x), ...\big). \tag{4.47}$$

To apply this method to vacuum decay, it needs to be modified to remove the zero mode contributions. To do so, consider $\hat{O}_\epsilon = \hat{O} + \epsilon$. Through this replacement, each of the zero modes picks up an eigenvalue ϵ. Thus, for sufficiently small ϵ, the functional determinant satisfies $\det(\hat{O}_\epsilon) = \epsilon^n \cdot \det(\hat{O}')$, where n is the number of zero modes. Defining $\rho_\epsilon(x)$ in analogy with ρ in (4.47), the determinant with zero modes removed can therefore be obtained through

$$\frac{\det(\hat{O}_1')}{\det(\hat{O}_2)} = \lim_{\epsilon\to 0} \lim_{x\to\infty} \det(\rho_\epsilon(x)) \cdot \epsilon^{-n}. \tag{4.48}$$

When no analytical calculation is possible, the right hand side can be calculated numerically for any given ϵ, and yields the exact determinant once the limit $\epsilon \to 0$ is taken.

Thus, the ratio of functional determinants of the false vacuum and bounce fluctuation operators can be characterized through

$$\ln\left(\frac{\det(\hat{O}_\Phi)}{\det(F_\Phi)}\right) = \sum_{s=0}^{\infty} \ln \rho_\infty^s, \tag{4.49}$$

where ρ_∞^s is the defined through (4.44) for the angular momentum s, and s does not refer to the n^{th} power of ρ_∞. This sum is, of course, ill-defined and divergent. The first issue are the zero modes, which can however easily be removed following the procedure leading to equation (4.48). For the special case of the translational zero modes, this is simplified by the observation that these lie entirely in the $s = 1$ subspace, so that only ρ_∞^1 needs to be regularized.

Besides zero modes, the spectrum of the scalar operator also contains a negative eigenmode for which $s = 0$. As previously explained, its imaginary part can be factored out and cancels out in (4.20). In equation (4.49), this amounts to another replacement, namely $\rho_\infty^0 \to |\rho_\infty^0|$.

Lastly, the sum is divergent for $s \to \infty$. The origin of this divergence can be located by expanding the functional determinant as a series of Feynman diagrams. This procedure is described in great detail in [7], revealing the origin of the divergence in the terms corresponding to diagrams with up to two insertions of the fluctuation potential. This corresponds to expanding ρ_∞ as a perturbative series in the latter,

$$\rho_\infty = \rho_\infty^{(0)} + \rho_\infty^{(1)} + \rho_\infty^{(2)} + \rho_\infty^{(3)} + \dots \ . \tag{4.50}$$

As the divergence arises from diagrams with up to two insertions of the potential, it can be removed by subtracting all corresponding terms within the expansion of ρ,

$$\ln \rho_\infty \to \ln \rho_\infty - (\ln \rho_\infty)^{(1)} - (\ln \rho_\infty)^{(2)} = \ln \rho_\infty - \rho_\infty^1 + \frac{1}{2}(\rho_\infty^1)^2 - \rho_\infty^1. \tag{4.51}$$

This suggests to renormalize (4.49) by splitting it into finite and divergent parts. As the divergent parts can be identified with usual Feynman diagrams, they can also be cancelled by the usual counter terms. Schematically, this amounts to

$$\ln \rho_\infty = \left(\ln \rho_\infty - \rho_\infty^{(1)} + \frac{1}{2}\big(\rho_\infty^{(1)}\big)^2 - \rho_\infty^{(1)} \right) + \left(\rho_\infty^{(1)} - \frac{1}{2}\big(\rho_\infty^{(1)}\big)^2 + \rho_\infty^{(1)} - \delta S_{\mathrm{ct}} \right). \tag{4.52}$$

The terms in the first bracket are finite and can, if necessary, be calculated numerically. As the terms in the second line correspond to well-known loop diagrams, they can be calculated perturbatively, allowing to isolate and absorb the divergence. Taking as an example the scalar field determinants with $O_\phi = -\Delta_4 + V''(\Phi_b)$ and $W(r) = V''(\Phi_b(r)))$, this procedure yields

$$\begin{gathered} \sum_{s=0}^{\infty} (s+1)^2 \left(\rho_\infty^{s,(1)} - \frac{1}{2}\big(\rho_\infty^{s,(1)}\big)^2 + \rho_\infty^{s,(1)} \right)_{fin} = -\frac{1}{2} \int \frac{\mathrm{d}^4 q}{(2\pi)^4} |\tilde{W}(q)|^2 B_{0,\mathrm{fin}}(q^2, \mu^2), \\ \text{where } B_{0,\mathrm{fin}}(q^2, \mu^2) = (4\pi)^{-2} \left(2 + \ln \frac{\mu^2}{q^2} \right). \end{gathered} \tag{4.53}$$

The path integral over the remaining fields can be evaluated in a very similar way. Given that they do not participate in the tunneling on the level of the instanton, they only contribute via the instanton's effect on their fluctuation operators. These can be calculated using the same methods as the scalar determinants, up to one critical difference. While for scalar and gauge fields, the Gaussian integrals over the fluctuation operators yield $\frac{1}{\sqrt{\det(O_b)}}$, their Grassmannian counterparts for fermions lead to $\sqrt{\det(O_f)}$. Thus, the pendant of (4.40) for fermions is given by

$$\frac{1}{Z_\Psi} \int D\Psi(\dots) = \sqrt{\frac{\det(\hat{O}_\Psi)}{\det(F_\Psi)}}. \tag{4.54}$$

4.4 Examples

4.4.1 The Standard Model

At energies above the instability scale, the SM Higgs potential is approximately given by the classically scale invariant quartic potential

$$V(h) \simeq -\frac{1}{4}|\lambda| h^4 . \tag{4.55}$$

The instanton of this potential can be found analytically, leading to a one-parameter family of solutions representing the scale invariance of the potential,

$$H_b^R = \sqrt{\frac{8}{|\lambda|}} \frac{1}{1 + \frac{r^2}{R^2}} \cdot \frac{1}{R}. \tag{4.56}$$

For each of these solutions, the euclidean action is given by

$$S_E[H_b^R] = \frac{8\pi^2}{3|\lambda|}. \tag{4.57}$$

These solutions gives rise to four translational zero modes, which can be dealt with through the introduction of collective coordinates:

$$\chi_{0,i} \propto \partial_i H_b^R = \hat{x}_i \partial_r H_b^R = -2\sqrt{\frac{8}{|\lambda|}} \frac{1}{(1+r^2/R^2)^2} \cdot \frac{\hat{x}_i}{R}. \tag{4.58}$$

Using the weight function $\gamma = V''(\Phi_b)$, this leads to a Jacobian factor

$$\frac{1}{N^4} = \frac{36}{25\pi^2} S_E[\Phi_b]^2 \frac{1}{R^4}. \tag{4.59}$$

The theory's scale invariance also manifests in a zero mode corresponding to a rescaling of the bounce, the *dilation mode*,

$$\chi_{0,d} \propto \partial_R H_b^R = \sqrt{\frac{8}{|\lambda|}} \frac{r^2/R^2 - 1}{(1+r^2/R^2)^2} \cdot \frac{1}{R^2}. \tag{4.60}$$

This mode can be treated in parallel to the translational zero modes by replacing $\phi_{0,d}$ with the parameter R underlying the scale invariance. As the relation between the unnormalized dilation mode (4.60) with the normalized zero mode is identical to that of a single translational mode under the replacement $R \leftrightarrow z_\alpha$, the Jacobian of the transformation from fluctuation to scale R is given by

$$d\phi^{0,d} = \frac{1}{N} dR = \sqrt{\frac{\sum_i \int d^4x \gamma(x) (\partial_R \Phi_b)^2}{2\pi}} dR. \tag{4.61}$$

The normalization factor N happens to also agree with that of the translational zero modes. Thus, after extracting the zero modes the decay rate becomes

$$\frac{\Gamma}{V} = \left(\frac{6 S_E[\Phi_b]}{5\pi}\right)^{\frac{5}{2}} \int \frac{dR}{R^5} e^{-\frac{8\pi^2}{3|\lambda|}} \prod_{\text{fields}} (...). \tag{4.62}$$

As this integral appears to be highly divergent at $R \to 0$, one might conclude that the vacuum is highly unstable. This would also appear reasonable from a semi-classical point of view, understanding the configuration at $\tau = 0$ as a bubble of true vacuum: As there are infinitely many bubbles of different size and each of them tunnels into existence with a finite probability, the overall decay probability is infinite.

This conclusion is now, fortunately for us who inhabit this vacuum, spoiled by two observations. First of all, as the divergence is linked to arbitrarily small values of R, it is possible that gravitational effects might save the vacuum. This is indeed partially true, as will be

discussed in subsection 4.4.2. Furthermore, due to the RG dependence of the coupling - and thus, the euclidean action - not all instantons contribute equally. In particular, for small and large enough R, the vacuum is stabilized, as λ becomes positive.

This suggests that the solution to the apparent divergence lies the renormalization scale dependence of (4.62). A first, rigorous treatment of the latter has been given in [7], where it is used to explicitly perform the R-integral. The underlying technique is however specific to the Standard Model, and might not be applicable to theories without the classical scale invariance. Thus, in preparation of later sections, it is worthwhile to modify their approach in the following way.

Clearly, in equation (4.62), the quartic coupling needs to be evaluated at some RG scale μ. However, at the same time, the decay rate as an observable quantity should be independent of the RG scale. The only way this inconsistency can be resolved is through quantum corrections to the euclidean action. Reversely, this allows for an efficient calculation of the corrections necessary to achieve scale independence. To see how, consider the condition that the euclidean action, together with its quantum corrections, is independent of the RG scale around some reference scale μ_R:

$$0 = \frac{d}{d\ln\mu}\frac{\Gamma}{V} \sim (...)\frac{d}{d\ln\mu}\left(-\frac{8\pi^2}{3\,|\lambda(\mu)|} + \delta S_E\right)_{\mu=\mu_R}. \tag{4.63}$$

Thus, to ensure independence of the RG scale at two-loop order, one needs that

$$\frac{8\pi^2}{3\lambda^2}\beta_\lambda(\mu_R) = \frac{d}{d\ln\mu}\delta S_E(\mu_R), \tag{4.64}$$

which is solved trivially by

$$\delta S_E(\mu_*) = \frac{8\pi^2}{3\lambda^2}\beta_\lambda(\mu_R)\ln\left(\frac{\mu}{\mu_R}\right) + O(\ln(\mu)^2), \tag{4.65}$$

with some yet to be determined reference scale μ_R.

Clearly, this procedure can be continued for arbitrary orders in $\ln\frac{\mu}{\mu_R}$, leading to a series in this logarithm. The crucial observation is now that the necessary reference scale μ_R is **not** determined by scale independence alone.

To understand the significance of the reference scale μ_R, all one needs to do is to recognize the relevant quantum corrections as the series expansion of the euclidean action around the scale μ_R, so that resumming them leads to

$$\frac{\Gamma}{V} \sim \int \frac{dR}{R^5} e^{-\frac{8\pi^2}{3|\lambda(\mu_R)|}}(...). \tag{4.66}$$

Thus, the reference scale μ_R is nothing but the RG scale to which the instanton characterized by R is sensitive. Intuitively, one would clearly expect that $\mu_R \sim \frac{1}{R}$, as R is the

only scale within the instanton, and both characterizes the typical field values as well as its spatial size. And indeed, an explicit calculation performed in [7] shows that $\mu_R = \frac{1}{2R}$, as the leading order corrections of all determinants can be combined into

$$\delta S_E^{log} = -\frac{\partial S_E}{\partial \lambda} \cdot \beta_\lambda(\mu) \cdot \ln\left(\frac{R\mu}{2}\right). \tag{4.67}$$

While the factor 2 in the logarithm can be easily extracted and kept within the corrections, the scale dependent parts enter the resummation, leading to the replacement $\lambda(\mu) \to \lambda(R^{-1})$ in the euclidean action.

If one is interested in actually performing the R-integral, this step makes things significantly more difficult. However, it does allow to evaluate the R-integral through a saddle point approximation, picking the scale $\mu_* \sim 10^{17}$ GeV, where $\beta_\lambda(\mu_*) = 0$. This is the first example for the *instanton scale*.

Note that as long as one does not aim for maximal accuracy, one can in fact forego the explicit calculation of μ_R through the evaluation of loops and simply use the estimate $\mu_R \sim \frac{1}{R}$. Most reasonable choices of μ_R will differ by at best one order of magnitude from this estimate, which can be quantified through replacing μ_R as $\mu_R \to \alpha\mu_R$, where α is an $O(1)$ parameter. Now, as the decay rate is obtained through integrating over all bounces this uncertainty can simply be absorbed into the R-integral,

$$\frac{\Gamma}{V} \sim \int \frac{dR}{R^5} \exp\left(\frac{8\pi^2}{3|\lambda(\alpha\mu_R)|}\right) = \alpha^{-4} \int \frac{dR}{R^5} \exp\left(\frac{8\pi^2}{3|\lambda(\mu_R)|}\right), \tag{4.68}$$

thus inducing a change in the decay rate of at best four orders of magnitude, which is indeed tiny compared to the overall uncertainty of several hundred orders of magnitude. Unfortunately, for a general potential without scale invariance, such a behavior can in general not be expected, making a more careful analysis necessary.

Returning to the SM and taking into account all loop corrections, the decay rate per unit volume is thus given by

$$\frac{\Gamma}{V} = \int \frac{\mathrm{d}R}{R^5}\, \mathrm{e}^{-S_\mathrm{E}(\lambda(R^{-1}),R)} D\big(R^{-1}\big), \tag{4.69}$$

where the factor $D\big(R^{-1}\big)$ collects the functional determinants. In the special case of the SM, they can be calculated analytically, leading to

$$\begin{aligned} D\big(R^{-1}\big) \equiv & \frac{72}{\sqrt{6}\pi^2} S_\mathrm{E}^4\left(\lambda(R^{-1}), R\right) \exp\Bigg[12\zeta'(-1) - \frac{25}{3} + \pi^2 - \gamma_\mathrm{E} - \frac{3}{2}\ln 2 - \frac{3}{2} S_\mathrm{fin}^+(X) - 3S_\mathrm{fin}^+(Y) + \\ & + \frac{3}{2} S_\mathrm{fin}^{\bar\psi\psi}\left(\sqrt{Z_t}\right) + \frac{3}{2} S_\mathrm{fin}^{\bar\psi\psi}\left(\sqrt{Z_b}\right) - 3S_\mathrm{loops}^{\bar\psi\psi}(Z_t) - 3S_\mathrm{loops}^{\bar\psi\psi}(Z_b) - \qquad (4.70) \\ & - \frac{1}{2} S_\mathrm{diff}^\mathrm{AG}(X) - S_\mathrm{diff}^\mathrm{AG}(Y) - S_\mathrm{loops}^\mathrm{AG}(X) - 2S_\mathrm{loops}^\mathrm{AG}(Y)\Bigg], \qquad (4.71) \end{aligned}$$

with $X \equiv -\frac{g^2+g'^2}{12\lambda}$, $Y \equiv -\frac{g^2}{12\lambda}$, and $Z_i \equiv \frac{y_i^2}{\lambda}$. The correction $S^+_{\text{fin}}(x)$ appearing in the exponent is given by

$$\begin{aligned} S_{\text{fin}}(x) =& x^2\left(6\gamma_{\text{E}} + 51 - 6\pi^2\right) + 6x + \frac{11}{36} + \ln 2\pi + \frac{3}{4\pi^2}\zeta(3) - 4\zeta'(-1) - \ln\left(\frac{\cos\left(\frac{\pi}{2}\kappa_x\right)}{6\pi x}\right) \\ & - x\kappa_x\left[\psi^{(-1)}\left(\frac{3+\kappa_x}{2}\right) - \psi^{(-1)}\left(\frac{3-\kappa_x}{2}\right)\right] + \\ & + \left(6x - \frac{1}{6}\right)\left[\psi^{(-2)}\left(\frac{3+\kappa_x}{2}\right) + \psi^{(-2)}\left(\frac{3-\kappa_x}{2}\right)\right] \\ & + \kappa_x\left[\psi^{(-3)}\left(\frac{3+\kappa_x}{2}\right) - \psi^{(-3)}\left(\frac{3-\kappa_x}{2}\right)\right] - 2\left[\psi^{(-4)}\left(\frac{3+\kappa_x}{2}\right) + \psi^{(-4)}\left(\frac{3-\kappa_x}{2}\right)\right], \end{aligned} \tag{4.72}$$

where $\kappa_x \equiv \sqrt{1-24x}$ and ψ^n is the polygamma function. The other corrections to the action are

$$S^{\text{AG}}_{\text{diff}}(x) = x^2\left(121 - 12\pi^2\right) - \frac{45}{2}x^2\,; \tag{4.73}$$

$$S^{\text{AG}}_{\text{loops}}(x) = -\frac{5}{18} - \frac{1}{3}\left(\gamma_{\text{E}} - \ln 2\right) - x\Big(7 + 6(\gamma_{\text{E}} - \ln 2)\Big) - 9x^2\left(\frac{1}{2} + \gamma_{\text{E}} - \ln 2\right); \tag{4.74}$$

$$S^{\bar{\psi}\psi}_{\text{loops}}(x) = -x\left(\frac{13}{8} + \frac{2}{3}(\gamma_{\text{E}} - \ln 2)\right) + x^2\left(\frac{5}{18} + \frac{1}{3}(\gamma_{\text{E}} - \ln 2)\right), \tag{4.75}$$

as well as

$$\begin{aligned} S^{\bar{\psi}\psi}_{\text{fin}}(x) =& 16\psi^{(-1)}(2) - \frac{8}{3}\psi^{(-2)}(2) + \frac{4}{3}x^2(1-\gamma_{\text{E}}) - \frac{x^4}{3}(1-2\gamma_{\text{E}}) \\ & - \frac{4}{3}x(1-x^2)\Big[\psi^{(-1)}(2+x) - \psi^{(-1)}(2-x)\Big] + \frac{4}{3}x(1-3x^2)\Big[\psi^{(-2)}(2+x) + \psi^{(-2)}(2-x)\Big] \\ & + 8x\Big[\psi^{(-3)}(2+x) - \psi^{(-3)}(2-x)\Big] - 8\Big[\psi^{(-4)}(2+x) + \psi^{(-4)}(2-x)\Big]. \end{aligned} \tag{4.76}$$

4.4.2 The Standard Model with Gravity

Before performing the integral over the dilatation mode, the decay rate at NLO takes the form

$$\frac{\Gamma}{V} = \int \frac{\mathrm{d}R}{R^5}\, \exp\left(-\frac{8\pi^2}{3\,|\lambda\,(R^{-1})|}\right) D\big(R^{-1}\big)\,. \tag{4.77}$$

Because the scale $\mu_\star$ is so close to the Planck mass, a reliable calculation of the decay rate needs to take into account gravitational corrections, which have been explored to leading order, e.g., in [73–75]. When moving to NLO, these corrections complicate the preceding prescription by including terms in the Euclidean action that explicitly violate scale invariance. The impact of such terms on the decay rate has first been investigated with a particular emphasis on the interaction of gravitational corrections with the RG

running in [73]. In general, breaking scale invariance explicitly alters the Euclidean action not just directly through the new term, but also indirectly through changing the scale of the dominant bounce.

One approach to understand this is to examine (4.77), complemented with the gravitational term. Assuming that the latter is subdominant, the saddle point of the path integral can be approximated to leading order by the family of bounces (4.56). Adding the leading-order gravitational correction to the Euclidean action given in, e.g., [75] results in a modified version

$$\frac{\Gamma}{V} = \int \frac{\mathrm{d}R}{R^5}\ \exp\left(-\frac{8\pi^2}{3\left|\lambda\left(R^{-1}\right)\right|} - \frac{256\pi^3}{45\lambda^2\left(R^{-1}\right)}\frac{1}{\left(RM_{\mathrm{Pl}}\right)^2}\right) D\left(R^{-1}\right). \tag{4.78}$$

Although the technique developed in [7] for evaluating the R-integral is impeded by the gravitational factor, a good approximation can be obtained through a saddle-point approximation:

$$\frac{\Gamma}{V} \simeq \mathrm{e}^{-S_{\mathrm{E}}(\lambda(\mu_S),\mu_S)}\sqrt{\frac{2\pi}{\frac{\mathrm{d}^2}{\mathrm{d}\ln\mu^2}S_{\mathrm{E}}\left(\lambda(\mu_S),\mu_S\right)}}\,\mu_S^4\cdot D(\mu_S)\,, \tag{4.79}$$

with the Euclidean action

$$S_{\mathrm{E}}\left(\lambda(\mu_S),\mu_S\right) = \frac{8\pi^2}{3|\lambda(\mu_S)|} + \frac{256\pi^3}{45\lambda^2(\mu_S)}\frac{\mu_S^2}{M_{\mathrm{Pl}}^2}\,. \tag{4.80}$$

All couplings, as well as the corrections summarized in Λ, are evaluated at the saddle point $R^{-1} = \mu_S$ minimizing the Euclidean action, which is the solution of

$$\beta_\lambda(\mu_S)\left(\frac{64\pi}{15}\frac{\mu_S^2}{M_{\mathrm{Pl}}^2} - \lambda(\mu_S)\right) = \lambda(\mu_S)\frac{64\pi}{15}\frac{\mu_S^2}{M_{\mathrm{Pl}}^2}\,. \tag{4.81}$$

This result is identical to the rate given in [75] up to a factor of $\mathcal{O}(1)$. The left-hand side of (4.81) is suppressed by β_λ. This implies that the effect of the gravitational term, which is to lower μ_S relative to μ_*, becomes significant for values of μ_S already one order of magnitude below M_{Pl}, giving rise to sub-Planckian values of μ_S even if μ_* is larger than M_{Pl} by several orders of magnitude. Thus $\mu_S < \mu_*$ in general, with approximate equality $\mu_S \simeq \mu_\star$ whenever $\mu_\star \ll M_{\mathrm{Pl}}$.

From here, obtaining the lifetime of the vacuum is straightforward as long as one is interested only in leading order corrections. The functional determinants depend only on the bounce, which in this approximation agrees with that of the pure SM except for the change in the instanton scale. Thus, the results of the previous subsection can be re-used.

4.4.3 Standard Model with a general dimension-six term

This effect can be observed in a similar way in SM extensions with an extended Higgs potential, like models with a (partially) composite Higgs models or a second, heavy Higgs

doublet like the (ν)MSSM. After integrating out the heavier degrees of freedom, the most general Higgs potential takes the form

$$V_{\text{full}}(H) = -\frac{m_h^2}{4}H^2 + \frac{\lambda}{4}H^4 + \frac{C_6}{\Lambda^2}H^6 + \dots \,. \tag{4.82}$$

The values of the Wilson coefficients at the matching scale Λ can be obtained through standard techniques. By simple power counting and anticipating that μ_S will ultimately be smaller than Λ, as motivated by the analysis of the last subsection, it can be expected that for most generic potentials only the dimension-six term will be truely important.

At lower energies, the running of the coefficients $\{C_{2n}\}_{n>2}$ is determined by their beta functions. They do, however, also affect the running of the remaining parameters through additional terms in their beta functions. For the relevant example of the dimension-six operator, these are suppressed by a factor of $\frac{m_h^2}{\Lambda^2}$ [76], which will turn out to be necessarily much smaller than 1 for metastable vacua. These corrections in the beta functions can therefore be neglected with good accuracy. The main effect that the dimension-six operator has on the decay rate is thus through its influence on the instanton scale μ_S.

The correction of the potential through the dimension-six term can be treated perturbatively at good accuracy as long as

$$\left|\frac{\Delta V_{\text{eff}}}{V_{\text{eff}}}\right| = \left|\frac{4C_6}{\lambda}\right| \cdot \frac{H^2}{\Lambda^2} \ll 1\,. \tag{4.83}$$

Using the bounce solution, which is to leading order determined by (4.56), $H_R(r)$ is obviously largest at its center. There,

$$H_R(r) \leq H_R(0) \simeq 2\sqrt{2}\mu_S/\sqrt{|\lambda(\mu_S)|}, \tag{4.84}$$

which applies for the dominant bounce with $R = \mu_S^{-1}$. Together with (4.83), this motivates the definition of the expansion parameter

$$\epsilon \equiv \left|\frac{32C_6}{\lambda^2}\right| \cdot \frac{\mu_S^2}{\Lambda^2}. \tag{4.85}$$

When performing numerical calculations, the regime of validity of the perturbative treatment can be restricted to $\epsilon \leq 1$. Considering the dependence of the lifetime on λ and Λ, both of these terms are smallest for short-lived vacua, for which the approximation can thus be expected to be most accurate.

Moving to the potential complemented by the dimension-six operator, (4.82), induces a correction to the bounce Euclidean action (4.80), which is given by

$$\Delta S_{\text{E}} = \frac{128\pi^2 C_6}{5|\lambda|^3}\frac{1}{R^2\Lambda^2}\,. \tag{4.86}$$

The decay rate (4.78) becomes therefore to leading order

$$\frac{\Gamma}{V} = \int \frac{\mathrm{d}R}{R^5} \exp\left(- \frac{8\pi^2}{3\,|\lambda\,(R^{-1})|} - \frac{128\pi^2 C_6(R^{-1})}{5|\lambda(R^{-1})|^3} \frac{1}{(R\Lambda)^2} - \frac{256\pi^3}{45\lambda^2\,(R^{-1})} \frac{1}{\left(RM_{\mathrm{Pl}}\right)^2} \right) \cdot \Lambda\big(R^{-1}\big)\,. \tag{4.87}$$

Just as it was the case for the gravitational correction, the new term can be expected to have two effects. On the one hand it should stabilize the vacuum as it increases the value of the Euclidean action. The strength of this effect should scale with $\frac{C_6}{\Lambda_f^2}$, implying that it is most prominent either for large C_6 or small Λ. On the other hand, it should change the instanton scale μ_S, moving it further away from $\mu_\star$. Especially for $\Lambda \lesssim \mu_\star$, μ_S should be shifted to scales smaller than or close to Λ.

This can be my explicit through an analysis similar to that of the gravitational term. Once again the R-integral can be evaluated through a saddle point approximation, which is dominated by the bounce corresponding to the scale μ_S determined by the equation

$$\beta_\lambda(\mu_S)\left(\frac{64\pi}{15}\frac{\mu_S^2}{M_{\mathrm{Pl}}^2} - \lambda(\mu_S) - \frac{144}{5}\frac{C_6}{\lambda(\mu_S)}\frac{\mu_S^2}{\Lambda^2}\right) + \beta_{C_6}(\mu_S)\frac{48}{5}\frac{\mu_S^2}{\Lambda^2} = \frac{64\pi}{15}\lambda(\mu_S)\frac{\mu_S^2}{M_{\mathrm{Pl}}^2} - \frac{96}{5}C_6(\mu_S)\frac{\mu_S^2}{\Lambda^2}\,. \tag{4.88}$$

The decay rate in this approximation can then again be read off from (4.79) by using the new Euclidean action

$$S_{\mathrm{E}} = \frac{8\pi^2}{3|\lambda(\mu_S)|} + \frac{128\pi^2 C_6(\mu_S)}{5|\lambda(\mu_S)|^3}\frac{\mu_S^2}{\Lambda^2} + \frac{256\pi^3}{45\lambda^2(\mu_S)}\frac{\mu_S^2}{M_{\mathrm{Pl}}^2}\,. \tag{4.89}$$

Also the functional determinants remain structurally the same, with the only difference being μ_S.

4.5 Lifetime of the vacuum

One of the features of vacuum decay via the creation of a bubble is that it does not occur simultaneously throughout the entirety of space. Rather, the field tunnels beyond the potential barrier only within a small region - the bubble - which then starts spreading with finite velocity. Thus, the simplistic definition of the vacuum's lifetime one might think of coming from quantum mechanics - the time until tunneling occurs - is not necessarily appropriate in the context of field theory. Since the region of true vacuum spreads only with a finite velocity, even after a nucleation event a large, potentially infinitely large, part of space remains in the false vacuum. Furthermore, in an expanding spacetime cosmological horizons prevent the bubble from ever reaching most of space. Thus, a sensitive definition of the vacuum's lifetime in the context of field theory should - at the most fundamental level - depend not only on time until a single bubble is formed, but also take into account the spacetime's causal structure.

A simple definition capable of doing so is the following: *The lifetime of the false vacuum is the time when the probability that a bubble was formed within the past lightcone of any*

given point in space becomes of order one. Formally, this corresponds to the equation

$$1 \simeq \int^{t=\tau} \mathrm{d}t \int_{\text{past lightcone}} \mathrm{d}V(t) \frac{\Gamma}{V}, \tag{4.90}$$

which depends on the scale factor $a(t)$ through the spatial volume measure $dV(t)$ as well as through the boundaries of the past light-cone. By moving to conformal time, defined through $a \cdot \mathrm{d}\eta = \mathrm{d}t$, the latter is given by a sphere of radius $\overline{r}(\eta) = \eta_0 - \eta$, where η_0 denotes the conformal time at the light-cone's center and $\eta = 0$ corresponds to the initial singularity. Thus, equation (4.90) becomes

$$\begin{aligned} 1 \simeq & \frac{\Gamma}{V} \int^{t=\tau} \mathrm{d}t \int_{\text{past lightcone}} \mathrm{d}V(\eta) = \frac{\Gamma}{V} \int^{t=\tau} \mathrm{d}t \left(\frac{4\pi}{3} \big(a(\eta) \cdot (\eta_0 - \eta)\big)^3 \right) = \\ = & \frac{4\pi}{3} \frac{\Gamma}{V} \int_0^{\eta(\tau)} \mathrm{d}\eta \; a(\eta)^4 \cdot (\eta_0 - \eta)^3. \end{aligned} \tag{4.91}$$

Assuming a sufficiently large lifetime for our universe the contribution of the radiation and matter dominated eras to the spacetime volume of the light-cone become negligible, so that the scale factor can be approximated as $a(\eta) = (1 - H\eta)^{-1}$, and thus $\eta(t) = e^{Ht}$, where the dS Hubble constant H is related to the current Hubble constant through $H = \sqrt{\Omega_\Lambda} H_0$. Inserting this into (4.91), the lifetime of our vacuum can be determined:

$$\begin{aligned} 1 \simeq & \frac{4\pi}{3} \frac{\Gamma}{V} \int_0^{\eta(\tau)} \mathrm{d}\eta \frac{(\eta_0 - \eta)^3}{(1 - H\eta)^4} = \\ = & -\frac{4\pi}{3} \frac{\Gamma}{V} \cdot \frac{1}{H^4} \left(\ln(1 - H\eta_0) + \frac{1}{6} \big(6(H\eta_0) + 3(H\eta_0)^2 + 2(H\eta_0)^3 \big) \right) = \\ = & \frac{4\pi}{3H^4} \frac{\Gamma}{V} \left(H\tau - \frac{11}{6} + O(e^{-Ht_0}) \right) \simeq \tau \cdot \frac{4\pi}{3H^3} \cdot \frac{\Gamma}{V}, \end{aligned} \tag{4.92}$$

where the last approximation corresponds to the limit $\tau \gg \frac{1}{H}$, which is linked to the initial assumption of approximate vacuum energy dominance. Now, solving (4.92) for τ is trivial, leading to

$$\tau \simeq \frac{3H^3}{4\pi} \cdot \left(\frac{\Gamma}{V} \right)^{-1} \sim \mu_\gamma^{-1} \frac{1}{(H \cdot \mu_\gamma)^3} e^{S_{\text{eucl}}}. \tag{4.93}$$

4.6 Numerical results

Having established everything necessary to calculate the lifetime of the electroweak vacuum in the SM and typical extensions, this section presents its currently most accurate numerical values for some particularly interesting models.

4.6.1 The Standard Model with gravity

Given the existence of an analytical expression for the lifetime in the Standard Model, all that is required to obtain a numerical value are the couplings' RG trajectories. These can

be obtained by integrating the beta functions given in section A.2 with the initial values of the relevant couplings at the top mass given in [4],

$$\lambda(M_t) = 0.12607\,; \quad y_t(M_t) = 0.9312\,; \quad y_b(M_t) = 0.0155334\,; \quad y_\tau(M_t) = 0.0102566$$
$$g_s(M_t) = 1.1618\,; \quad g'(M_t) = 0.358545\,; \quad g(M_t) = 0.64765\,. \tag{4.94}$$

Using the couplings obtained in this way, relation (4.79) leads to the - currently most accurate - result for the lifetime,

$$\tau_{\text{EW}} \sim 10^{983^{+1410}_{-430}} \text{ years.} \tag{4.95}$$

4.6.2 The νMSM with gravity

In the context of vacuum decay, right-handed neutrinos manifest primarily through their Yukawa couplings. Assuming them to be approximately of the form (1.23) allows for the following replacements in the νMSM's beta functions given in Appendix A.2:

$$Y_\nu Y_\nu^\dagger Y_\nu \to Y_\nu \cdot \left(Y_1^2 + Y_2^2 + Y_3^2\right), \tag{4.96}$$
$$\text{Tr}\left(Y_\nu^\dagger Y_\nu\right) \to Y_1^2 + Y_2^2 + Y_3^2\,. \tag{4.97}$$

Another consequence of the approximate $B - \tilde{L}$ symmetry is a restoration of the heavy neutrinos mass degeneracy, so that the νMSM can be matched with the pure SM at the scale $\mu \simeq M$. This reduces the number of parameters to four: the heavy neutrino mass M, and the three couplings $Y_1(M)$, $Y_2(M)$ and $Y_3(M)$.

More importantly, when combined with this symmetry, the decay rate's general insensitivity to all properties of the neutrinos except their Yukawa couplings gives rise to an additional, effective $SO(3)$ symmetry among Y_1, Y_2 and Y_3[1]. In the context of electroweak vacuum decay, the Yukawa matrix can therefore be simplified by rotating its components as

$$Y \to \begin{pmatrix} 0 & 0 & 0 \\ 0 & |Y| & 0 \\ 0 & 0 & 0 \end{pmatrix}, \text{ where } |Y|^2 = Y_1^2 + Y_2^2 + Y_3^2\,. \tag{4.98}$$

Thus, only the two parameters M and $|Y(M)|$ remain[2].

The beta functions of the extended SM can be found in the literature to two-loop accuracy [82]. Thus, the only missing element to enhance the NLO formula (4.79) is the functional determinant of the neutrinos' kinetic terms. Noting that the regime is determined by $M \lesssim \mu_I$, the masses of all neutrino states are negligible at scales relevant to the instanton. It is therefore straightforward to conclude that the neutrino fluctuations' determinant agrees with that of the top quark if one replaces y_t by $|Y|$.

[1] This symmetry would be broken, e.g., through the neutrino contribution to the running of the tau Yukawa coupling. However, considering the smallness of the latter as well as of the interval over which the neutrino contribution is relevant, the corresponding terms can be safely neglected for the sake of simplicity.

[2] This is equivalent to the assumption of a hierarchy between the neutrinos' Yukawa couplings, which is often used in the literature to simplify results [77–81].

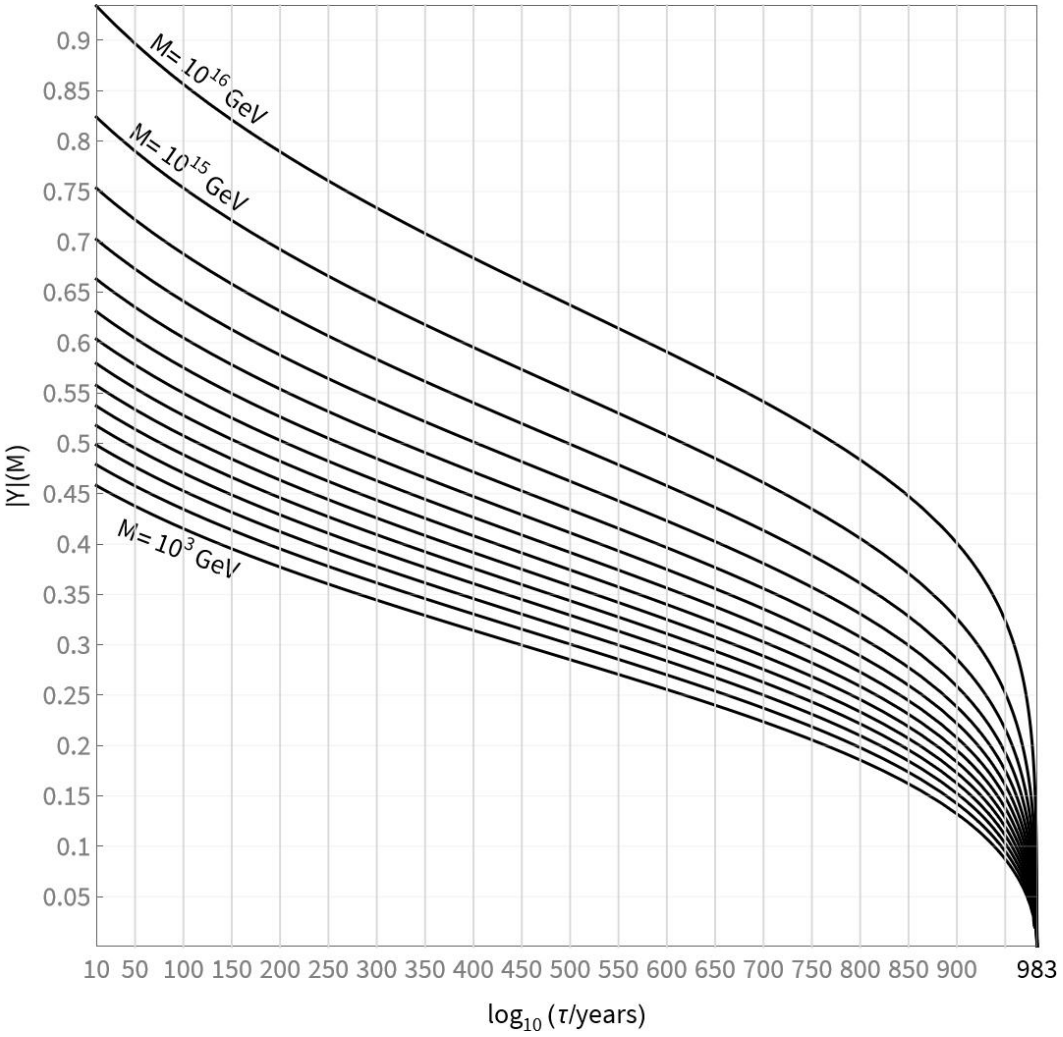

Figure 4.1: The value of $|Y(M)|$ necessary to realize a given lifetime, shorter than the central value of 10^{983} years for the pure SM. Each curve corresponds to a different value of M, in increasing order of magnitude.

Having at hand all terms in (4.79) supplemented with the neutrino determinant, the lifetime can be calculated numerically. The first step towards this goal is to match the SM couplings with those of the $B-\tilde{L}$ symmetric νMSM at the scale M, which can be achieved through the procedures outlined in [83, 84] and combining them with the threshold corrections for λ and y_t found in [77][3]. Then, given a value of $|Y(M)|$, the couplings can be run up to the Planck scale at two-loop accuracy using the full νMSM beta functions found in [82]. Their pendants in the conventions used throughout this work are given in the appendix.

From the running of the couplings, the instanton scale μ_S can again be derived by solving (4.81). An important observation is here that μ_S is smaller than $\mu_\star$ by many orders of magnitude, as the right-handed neutrino Yukawa couplings suitable to have a notable effect on the lifetime generally push $\mu_\star$ to values even above the Planck scale. Nevertheless, as explained in Sec. 4.4.2, the gravitational corrections ensure that μ_S remains below the Planck scale due to their relatively enhanced dependence on the scale.

Figure 4.1 presents the value of $|Y(M)|$ necessary to achieve a certain lifetime for all relevant values of M. It does so for lifetimes ranging from 10^{10} years to the SM central value of 10^{983} years. This plot allows furthermore for the conversion of any prediction of the vacuum's lifetime to a constraint on the relevant properties of the right-handed neutrinos, given either a large hierarchy between the Yukawa couplings or the $B-\tilde{L}$ symmetry. It thus also contains the so far most accurate stability bounds for the Yukawa couplings, which correspond to the values on left boundary of Fig. 4.1. For $M = 10^{12} - 10^{15}$ GeV, these results are practically identical to the ones derived in [77], with a small difference due to a more rigorous treatment of the gravitational corrections and more recent experimental data used for the matching of the SM couplings.

4.6.3 The SU(4)/Sp(4) composite Higgs model

To leading order, this realization of compositeness manifests through the dimension-six term with a Wilson coefficient C_6 given by

$$C_6(\Lambda_f) = -\frac{\pi^2}{12}\lambda(\Lambda_f). \tag{4.99}$$

From here, the decay rate can be calculated using the procedure developed in section 4.4.3. This approximative scheme is justified provided that

$$\frac{1}{6}\frac{\mu_S^2}{|\lambda(\mu_S)|f^2} < 1\,. \tag{4.100}$$

In the pure composite Higgs model, the conditions for the validity of this approximation - a short lifetime or a large Λ_f - are equivalent, as different lifetimes are achieved by considering different values for f. This ceases to be true once right-handed neutrinos are taken into account in Sec. 5.1.4.

[3]The authors of [77] pointed out to me a small typo in their Eq. G(20), where a factor of $\frac{1}{4}$ in the first term has to be replaced by $\frac{1}{2}$. This has been taken into account in what follows.

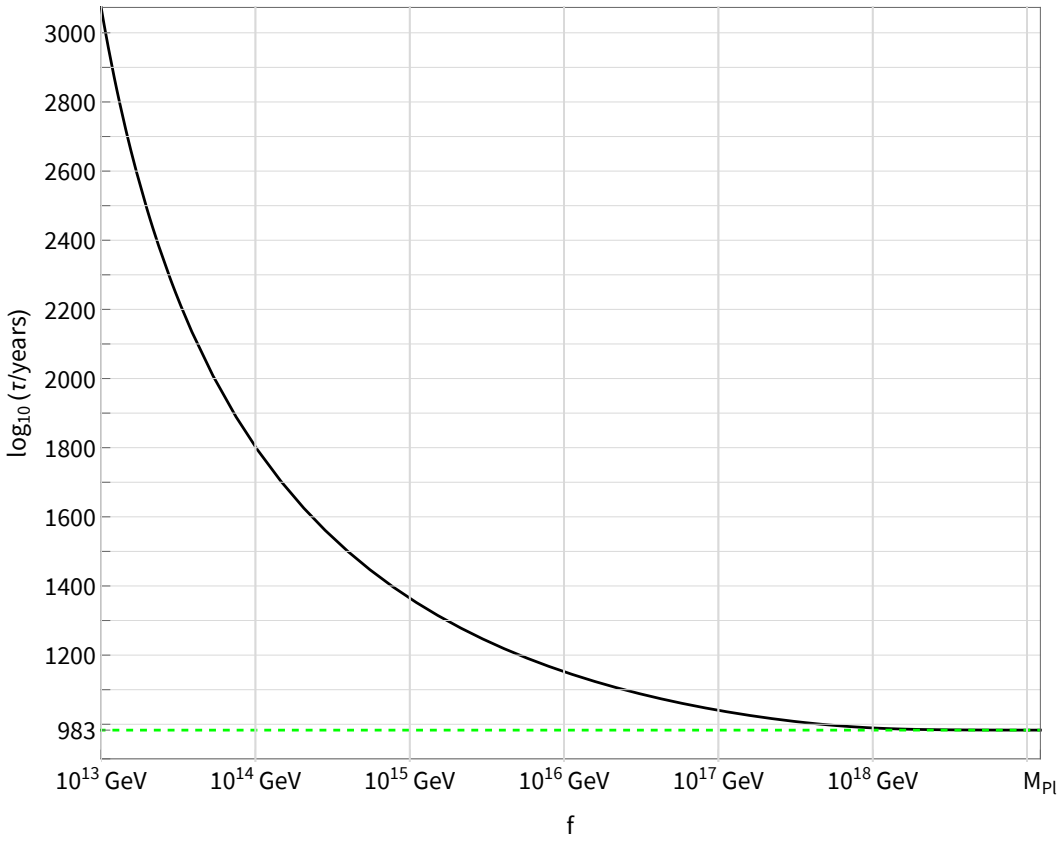

Figure 4.2: The lifetime of the electroweak vacuum in the minimal composite Higgs model, for different values of the technipion decay constant f. The central value of the lifetime in the pure SM, denoted by the green dashed line, is recovered in the limit $f \to M_{\rm Pl}$.

The first step in a numerical analysis is once again the RG evolution of the SM couplings from their observed low energy values, now up to Λ_f. There, C_6 needs be matched using (4.99), and run then down to lower energies through integration of its one-loop beta function [76], which is also given in the appendix in proper conventions. Because the effect of compositeness has the largest impact if μ_S is roughly comparable to f, this yields a sufficient level of accuracy. Knowing the running of the couplings, equations (4.88) and (4.89) can be solved simultaneously, thus allowing to determine μ_S, from which the numerical value of $S_{\mathrm{E}}(\mu_S)$ can be obtained, and with it the lifetime (4.79) of the electroweak vacuum as a function of f.

Figure 4.2 depicts the vacuum's lifetime as a function of the technipion decay constant f. This demonstrates that the dimension-six operator has indeed a stabilizing effect on the vacuum, as the lifetime decreases monotonically with growing f. Importantly, the central value for the electroweak lifetime in the pure SM (represented by the green dashed line) is recovered in the limit $f \to M_{\mathrm{Pl}}$.

4.6.4 The SU(4)/Sp(4) composite Higgs model with right-handed neutrinos

Anticipating the results of chapter 5, a particularly interesting scenario is a simultaneous realization of massive neutrinos and a composite Higgs. The most relevant cases have a small value of M, so that the following analysis is, for concreteness, restricted to $M \sim 1-5$ TeV, corresponding to the tightest bounds on the Higgs mass (see Fig. 5.3) without violating any experimental constraints for $M \gtrsim 2$ TeV. With these values fixed, the parameters that need to be scanned are f and $|Y(M)|$.

The SM couplings can be matched at the scale M through the same strategy as before, especially implementing the threshold corrections for λ and y_{t}. From the matching scale, they can be run through their three-loop beta functions, while neglecting the contributions $\sim m_h^2/\Lambda_f^2$. The coefficient C_6 needs to be matched at the scale Λ_f, while its values at lower energies can again be found by integrating its one-loop beta function. This is once again justified as the most interesting scenarios are those in which μ_S is not too far away from Λ_f.

Doing so ultimately yields the lifetime of the vacuum for each pair of values $|Y(M)|$ and f. Equivalently, the resulting relation can be understood as the value of $|Y(M)|$ necessary to achieve every possible lifetime for any given f. It is this relation which is depicted in Fig. 4.3, letting f range from 10^6 GeV up to the Planck scale. In principle, smaller values of f would be equally possible and even more interesting for the purposes of chapter 5, but are not accessible by the underlying perturbative analysis. The red shading signalizes zones of different values of the expansion parameter ϵ for $M = 1$ TeV, as defined in (4.85) and varying from 0.1 to 1. Just as could be expected from the arguments presented below (4.85), the perturbative expansion is indeed most reliable for shorter lifetimes and larger f.

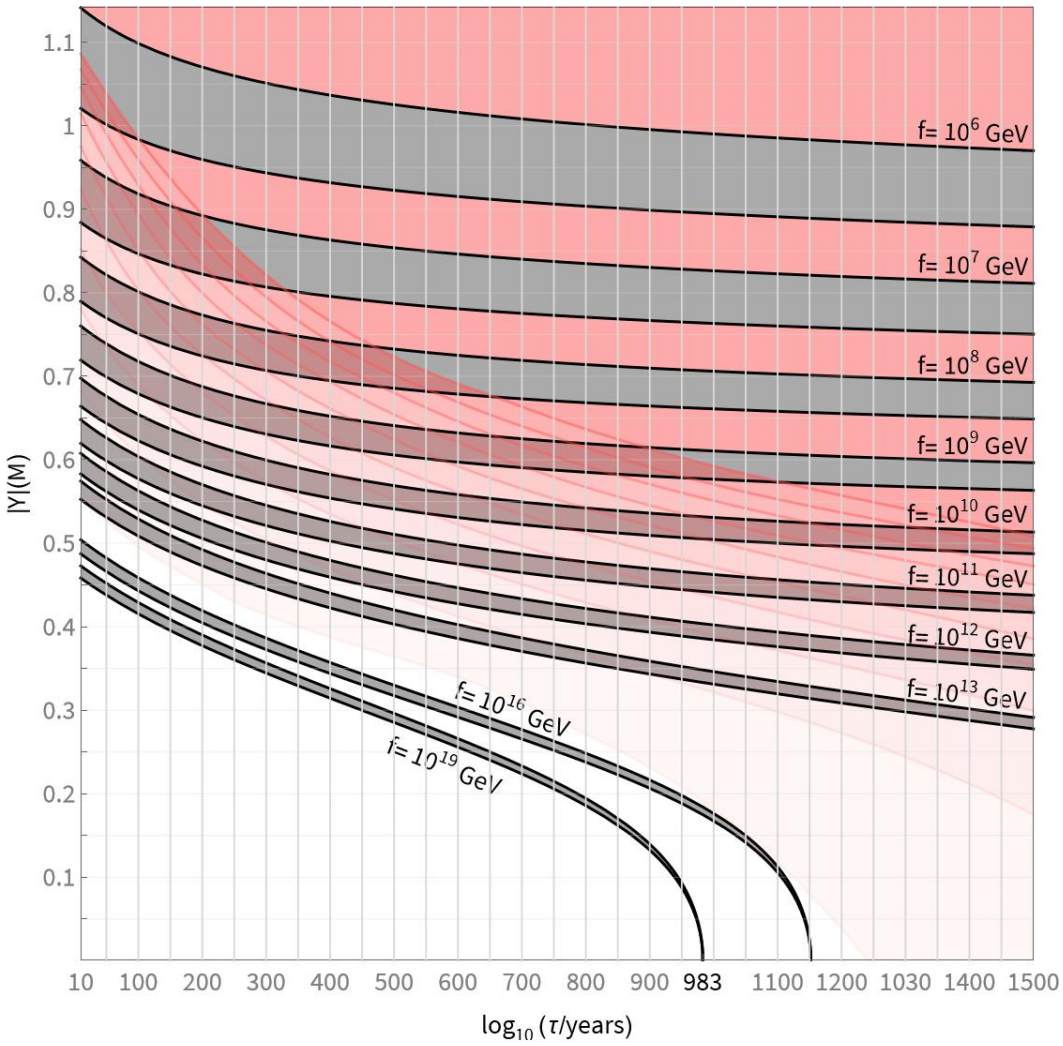

Figure 4.3: The value of $|Y(M)|$ necessary to realize a given lifetime for different values of f. The gray bars cover the range $M = 1 - 5$ TeV. In the white region, the expansion parameter defined in (4.85) is smaller than 0.1 for $M = 1$ TeV, in the dark red region larger than 1. The shaded regions indicate the transition in steps of $\Delta\epsilon = 0.1$.

Chapter 5

Connecting the fine-tunings of the Higgs sector

This chapter outlines the central results of [2] and some yet unpublished insights.

The hierarchy problem as well as the origin of the electroweak vacuum's metastability are, each on its own, amongst the biggest mysteries of particle physics. Assuming that there is no connection between them, it appears as if **both** parameters of the Higgs potential need to be independently fine-tuned - if the Higgs hadn't been found, it would probably be considered very unattractive at this point.

There is, however, also an optimistic perspective on this issue arising from its relation with another issue of the SM: There is no explanation for the form of the Higgs potential, and in particular the sign of the quadratic term, which is responsible for spontaneous symmetry breaking. Thus, it remains a possibility that the Higgs potential is generated through some yet unknown UV mechanism - and thus, that the fine-tunings of both m^2 and λ share **one** single origin. This idea is supported by the main result of this chapter, which implies that a small Higgs mass is a necessary condition for metastability.

5.1 Upper bound on the running Higgs mass from metastability

On first look, it may appear as if converting the vacuum lifetime to a constraint on the Higgs mass is a challenging task. Although the lifetime is highly sensitive to the quartic coupling, it has no explicit dependence on the vacuum expectation value and consequently the Higgs mass. The observation underlying the following reasoning is that, when the quartic coupling becomes negative, the existence of a non-trivial electroweak vacuum requires the effective

potential to develop a minimum at field values below the instability scale μ_I.

This connection has first been explored in [6]. In the SM, the full RG-improved effective potential is of the form

$$V_{\text{eff}}(H) = -\frac{m_h^2}{4} e^{2\Gamma[H]} H^2 + \frac{1}{4}\Big(\lambda(H) + \lambda_1(H) + \dots\Big) e^{4\Gamma[H]} H^4 \,. \tag{5.1}$$

Here, λ_n specifies non-logarithmic corrections to λ at n-loop order.

As a minimum of this potential, the electroweak vacuum satisfies $\frac{\mathrm{d}}{\mathrm{d}H} V_{\text{eff}}(H)\big|_{H=v} = 0$, which amounts to

$$\frac{m_h^2}{v^2} = \frac{e^{2\Gamma(v)}}{1+\gamma(v)}\left(2\Big(\lambda(v) + \lambda_1(v) + \dots\Big) + \frac{1}{2}\Big(\beta_\lambda(v) + \beta_{\lambda_1}(v) + \dots\Big)\right), \tag{5.2}$$

where γ denotes the Higgs field's anomalous dimension.

Because the metastable vacuum satisfies this equation, it only exists if (5.2) can be solved in the first place. A first limitation on its solutions follows immediately from (5.1): At scales somewhat greater than the instability scale,, $\lambda(\mu)$ becomes sufficiently negative to compensate for the positive loop corrections $\{\lambda_n(\mu)\}_n$. As a result, at those scales, both the quadratic and quartic terms have a negative sign, and no extremum can arise. This indicates that the upper bound arises for v of the same order as the instability scale, motivating the approximation $\lambda(v) \simeq \beta_\lambda(\mu_I) \ln \frac{v}{\mu_I}$. Therefore, λ becomes effectively one-loop [85], and a consistent leading-order perturbative expansion of (5.2) must account for all one-loop terms. This includes, in particular, λ_1, which was omitted in [6].

At one-loop accuracy, the condition (5.2) can thus be brought to the form

$$m_h^2 = v^2\left(2\ln\frac{v}{\mu_I} + 2\frac{\lambda_1(\mu_I)}{\beta_\lambda(\mu_I)} + \frac{1}{2}\right)\beta_\lambda(\mu_I) \,. \tag{5.3}$$

Understood as a function of v, the right-hand side is bounded from above since $\beta_\lambda(\mu_I) < 0$. Maximizing over v, this implies the inequality

$$m_h^2 \lesssim |\beta_\lambda(\mu_I)| \exp\left(-\frac{3}{2} - 2\frac{\lambda_1(\mu_I)}{\beta_\lambda(\mu_I)}\right)\mu_I^2 \,. \tag{5.4}$$

Another interesting perspective on equation (5.3) has recently been developed in [26]. For values of m_h^2 larger than the bound (5.4), the Higgs potential has no extremum at all. Meanwile, if m_h^2 is strictly smaller than the bound but larger than 0, the right hand side of equation (5.3) has two solutions, corresponding to the top of the potential barrier and the vev, which – neglecting the non-logarithmic term λ_1 for now – ranges from 0 to $e^{-1/4}\mu_I$. For $v = e^{-3/4}\mu_I$ the inequality (5.4) is saturated. In this case the effective potential has only one extremum, which turns out to be a saddle point at $H = v$, where corrections from

to the running of λ cancel the tree-level mass parameter m_h^2 in $\frac{\mathrm{d}^2}{\mathrm{d}H^2}V_{\mathrm{eff}}(H)$. Thus, based on the relation between mass and instability scale, the potential can be classified into one of two categories and the bound (5.4) represents the transition between these two. It is in this sense that it serves as critical point at the center of the probability distribution derived in [26], whose result is therefore consistent with the bound (5.4) on the running Higgs mass, which is saturates.

In a similar way, the potential can be classified based on the sign of m_h^2, with $m_h^2 > 0$ describing the above scenario. If, in contrast, $m_h^2 < 0$, the potential would no longer permit spontaneous symmetry breaking without the influence of further quantum corrections and there exists only one solution to (5.3). This solution is of course the sphaleron, i.e. the point on top of the potential wall, which can be found beyond the instability scale. Because in this scenario the potential's only minimum lies at $H = 0$, the bound (5.4) is still satisfied.

Equation (5.3) can furthermore be used to obtain an upper bound on the Higgs' vev. It is straightforward to see that the largest value for v allowing for a solution is given by

$$v \leq \exp\left(-\frac{1}{4} - \frac{\lambda_1(\mu_I)}{\beta_\lambda(\mu_I)}\right)\mu_I. \tag{5.5}$$

Sec. 5.1.3, discusses an extension of the Higgs potential by a dimension-six operator of the form $\Delta V = \frac{C_6}{\Lambda_f^2}H^6$, where to leading order $C_6 \sim \lambda$. This term leads to a correction in (5.4) of order $\lambda\frac{v^2}{\Lambda_f^2}$. As argued in Sec. 5.1.3, this correction is suppressed compared to the terms originating from the pure SM as $v^2 \lesssim \mu_I^2 \ll \Lambda_f^2$, so that it can justifiably be neglected in the context of a perturbative discussion, i.e., in Secs. 5.1.3 and 5.1.4.

Unfortunately, (5.4) on its own fails to explain the observed Higgs mass, and in particular its smallness compared to its natural value, for two reasons. First, it merely shifts the question to why the instability scale lies so far below the Planck scale, or the scale of new physics setting the natural value for the Higgs mass, respectively, and why it exists in the first place. Furthermore, it could be satisfied by a Higgs mass just slightly below the instability scale, which, assuming ongoing validity of the Standard Model, is roughly 10^{11} GeV, leaving unexplained an additional eight orders of magnitude to reach the electroweak scale.

These two points are addressed in the following. The first issue is resolved immediately through the assumption of metastability, which requires the existence of the instability scale. Thus, the quartic coupling must become negative at the instability scale μ_I, and then continue to drop off enough to reach some negative value $\lambda(\mu_S)$ which corresponds to the desired lifetime. Taking into account that λ depends only logarithmically on the scale, this running connects scales several orders of magnitude apart. Together with relation (5.4), this hierarchy provides an upper bound for the Higgs mass parameter and therefore also the electroweak scale, as sketched in Fig. 5.1. This bound, however, only restricts the value of the Higgs mass relative to the instanton scale at which the quartic coupling needs to be evaluated in the calculation of the lifetime. However, as was shown in section 4.4.3, this scale lies below the natural value of the Higgs mass.

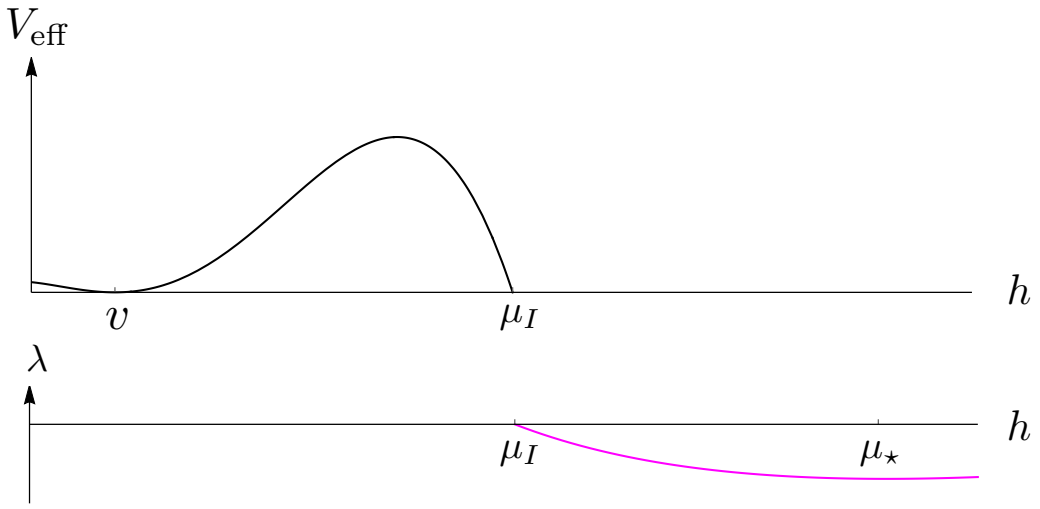

Figure 5.1: The effective potential as well as the running of the quartic coupling, not to scale. If the scale $\mu_\star$ where the quartic coupling reaches a minimum lies significantly below the Planck scale, then $\mu_S \simeq \mu_\star$.

To circumvent the second issue, Secs. 5.1.2 and 5.1.3 discuss the possibility that beyond-the-SM physics lowers the instability scale, and thus strengthens the bound on the Higgs mass.

For the purpose of an approximate analytical treatment, it suffices to use the leading-order expression for the decay rate:

$$\frac{\Gamma}{V} \propto \mu_S^4 \exp\left(-\frac{8\pi^2}{3|\lambda(\mu_S)|}\right), \tag{5.6}$$

where μ_S satisfies (4.81). It is important to keep in mind that, although the correction through either gravity or a dimension-six term can in principle have a significant impact on S_{E} and thus the decay rate, the validity of the description applied here of course requires $\mu_S \ll M_{\text{Pl}}$, or $\mu_S \ll \Lambda$ respectively. In other words, the assumptions underlying this discussion also imply that the direct correction to the numerical value of S_{E} is small and can be safely neglected for the purpose of this estimate.

As a result, the decay rate is to leading order fully determined by the two parameters $\lambda(\mu_S)$ and μ_S. For a given μ_S, equation (5.6) implies that a larger $\lambda(\mu_S)$ (i.e., smaller $|\lambda(\mu_S)|$) gives rise to a smaller decay rate, and thus corresponds to a longer lifetime. More precisely, (4.92) and (5.6) can be combined into

$$\begin{aligned}\lambda(\mu_S) &\simeq -\frac{8\pi^2}{223.14 + 3\ln\left(\frac{\mu_S^4}{H_0^3\text{GeV}}\right) + 3\ln\left(\frac{\tau_{\text{EW}}}{\text{yrs}}\right)} \\ &\simeq -\frac{8\pi^2}{1551.15 + 12\ln\left(\frac{\mu_S}{4\times10^{16}\text{GeV}}\right) + 3\ln\left(\frac{\tau_{\text{EW}}}{\text{yrs}}\right)},\end{aligned} \tag{5.7}$$

where in the last step $H_0 \simeq 10^{-42}$ GeV was substituted and μ_S has been normalized to its SM value. An important subtlety can be observed in the first line of (5.7), where a large contribution arises from the ratio of the large ratio of H_0 and μ_S. As a result, the hierarchy between Hubble constant and instanton scale can, in principle, play a significant role in determining the lifetime. This means that the metastability of our vacuum does not only require a conspiracy of SM couplings, but also an independent tuning of the Hubble and instanton scales.

Going forward, the decisive observation is that, once a lifetime τ_{EW} and an instanton scale μ_S have been specified, equation (5.7) fully determines the quartic coupling at the instability scale $\lambda(\mu_S)$. The pair μ_S and $\lambda(\mu_S)$ furthermore determines $\beta_\lambda(\mu_s)$ through (4.81). This provides all the necessary data to perform a RG evolution and determine the instability scale μ_I at which λ crosses zero.

For the purpose of deriving a rough estimate, the quartic coupling can be expanded around μ_S and evaluated at μ_I:

$$0 = \lambda(\mu_I) = \lambda(\mu_S) + \beta_\lambda(\mu_S)\big(\ln\mu_I - \ln\mu_S\big) + \frac{1}{2}\beta'_\lambda(\mu_S)\big(\ln\mu_I - \ln\mu_S\big)^2 + \dots \tag{5.8}$$

This implies that, to leading order,

$$\mu_I \simeq \mu_S \cdot \exp\left(-\frac{|\lambda(\mu_S)|}{|\beta_\lambda(\mu_S)|}\right). \tag{5.9}$$

In the regime where $\mu_S \simeq \mu_\star$, which occurs whenever $\mu_\star \ll M_{\text{Pl}}$ or $\mu_\star \ll \Lambda$ respectively, this estimate becomes unreliable since $\beta_\lambda(\mu_\star) = 0$. Instead, the dominant contribution arises from the otherwise subleading order. The result for such cases is an even larger hierarchy,

$$\mu_I \simeq \mu_\star \cdot \exp\left(-\sqrt{2\frac{|\lambda(\mu_\star)|}{\beta'_\lambda(\mu_\star)}}\right). \tag{5.10}$$

For most generic parameters, the right-hand sides of (5.9) and (5.10) cause a significant hierarchy between the instability scale μ_I and the instanton scale μ_S. This estimate furthermore provides insights into the dependence of the bound on the Higgs mass on the lifetime. Keeping μ_S constant, a shorter lifetime implies a smaller value of μ_I, which then requires a smaller value of m_h, and thus corresponds to a stronger bound on the Higgs mass.

5.1.1 Metastability bounds in the Standard Model with Gravity

A natural first example for the consequences of the inequality (5.4) is the SM under the assumption that it remains valid up to the Planck scale, taking into account the Yukawa couplings of the top and bottom quark's and that of the tau. Following [6], it is commonplace to characterize the vacuum through the parameters $y_{\text{t}}(M_{\text{Pl}})$ and $\lambda(M_{\text{Pl}})$, while,

for simplicity, fixing all other couplings at the Planck scale to their SM-extrapolated values. In the context of vacuum selection, this convention can be understood as the parameters $y_t(M_{Pl})$ and $\lambda(M_{Pl})$ being subject to the mechanism responsible for picking the vacuum.

To apply the inequality (5.4), the relevant couplings need to be determined at the instability scale, which itself can be obtained from the RG running of the quartic coupling λ. This can be done by combining the beta functions given in the appendix, enhanced by tau and bottom Yukawa couplings, with the matching condition (4.94).

Once the RG evolution of these couplings has been determined through integration of their beta functions, μ_S follows from equation (4.81), which can then be used to calculate the decay rate, and thus, through (4.79), the lifetime of the vacuum. Repeating this for a sufficiently tight mash of vacua leads to a set of data points $(y_t(M_{Pl}), \lambda(M_{Pl}), \mu_S, \tau_{EW}, \overline{m}_h)$, where $\overline{m}_h$ denotes the upper bound on the running Higgs mass for the considered vacuum. When scanning the landscape of potential vacua, it is inevitable to run into those whose dominant instanton reaches into a Planckian regime at its center, $H_{R=\mu_S^{-1}}(r=0) \sim M_{Pl}$. Due to the possibility of quantum gravity effects it is impossible to make reliable statements about the decay rate at such scales, so that the corresponding sets of parameters will in the following be ignored.

This last point also ensures that gravitational corrections are small, as it guarantees that the natural expansion parameter, $\epsilon_{grav} = \frac{1}{\sqrt{\lambda(\mu_S)}} \frac{\mu_S^2}{M_{Pl}^2}$ is smaller than $\frac{1}{8}$. Furthermore, as is argued, e.g., in [86], the effect on the decay rate arising from higher-order gravitational corrections due to back-reactions should be negligible.

The relation between the lifetime and $\overline{m}_h$ can be extracted from the data points through replacing $\lambda(M_{Pl})$ by the lifetime while keeping $y_t(M_{Pl})$ as a second parameter. The result is presented in Figure (5.2), which clearly shows that once a lifetime has been imposed, a hierarchy of several orders of magnitude arises naturally, without the need for further fine-tuning of the couplings.

Although insufficient to explain the full hierarchy, this result establishes a strong connection between metastability and the smallness of the Higgs mass. In summary, any framework which offers a fundamental reason for vacuum metastability, such as the early-time approach to eternal inflation, requires the running Higgs mass to be sufficiently small for the electroweak vacuum to exist, with shorter lifetimes leading to stronger bounds.

This remains true even for the Standard Model extensions considered in the following sections and is at least qualitatively independent of the choice of independent parameter(s) determining the properties of different vacua. This universality could of course be expected from the simplicity of (5.9) and (5.4) and might be nothing but a mathematical peculiarity. It is, however of course equally reasonable to consider the possibility that it does play a role in setting the value of the Higgs mass.

What makes this possible is the enormous sensitivity of these results to physics at high

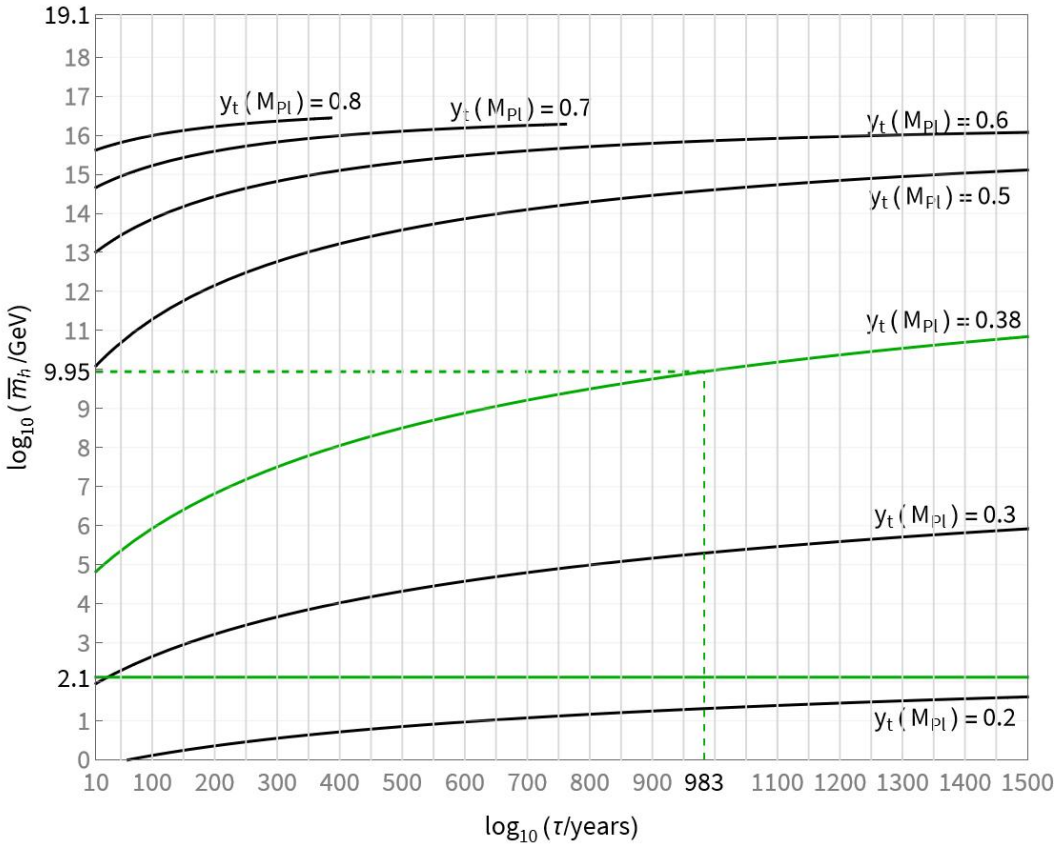

Figure 5.2: The upper bound $\overline{m}_h$ on the running mass as a function of the vacuum's lifetime for different values of $y_t(M_{\mathrm{Pl}})$. The dashed green line represents the central values of parameters inferred from experiments, and the solid green line marks the measured value of the Higgs mass.

energies, in particular at the instanton scale. Combining some of the simplest possible extensions of the Standard Model is sufficient to bring down the bound on the Higgs mass down to as little as 10 TeV, while shifting the lifetime to the Page time, the ideal lifetime suggested by search optimization on the landscape [27]. This will be demonstrated throughout the remainder of this chapter.

5.1.2 Metastability bounds in the Standard Model with massive neutrinos

The remaining disparity between the SM bound and observed Higgs mass value is primarily due to a mismatch between the latter and the instability scale μ_I, which is not constrained by vacuum decay via an instanton. If, on the other hand, the instability scale could be observed at a lower energy, the bound resulting from metastability would be greatly improved. Taking seriously the assumption that the near-criticality of the Higgs mass is a result of the vacuum's metastability, this supports SM extensions that cause strong negative contributions to β_λ at energies well below the SM instability scale $\sim 10^{11}$ GeV. In the context of neutrino masses, this occurs naturally by combining light right-handed neutrinos with Yukawa couplings of order one.

As it was argued in section 4.6.2, from the point of view of vacuum stability, the νMSM differs from the SM primarily through the additional Yukawa couplings. These manifest in the running of the couplings, but also through an additional contribution to the effective potential, which is given, e.g., in [80, 81, 87].

Unlike in section 5.1, for the νMSM it makes sense to keep λ and y_t fixed to their SM values at the electroweak scale and instead scan the lifetime by varying $|Y(M)|$. It can then be expected that a notable difference for the mass bound is obtained only if $M \ll \mu_I$, as otherwise the running of λ would be unaffected up to the instability scale and the Higgs mass bound would be unchanged.

The upper bound on the running Higgs mass, $\overline{m}_h$, as a function of the lifetime for different values of M is illustrated in Figure 5.3. In consistency with previous reasoning, stronger Yukawa couplings lead to a steeper decline of λ, which results in a smaller μ_I and thus also a stronger bound on the Higgs mass. Meanwhile a larger neutrino mass implies that their Yukawa couplings become relevant only at higher energies, so their influence on μ_I is weaker.

These results are consistent with experimental bounds on neutrino parameters. While in the νMSM many of the neutrinos' properties depend on the symmetry breaking parts of the Yukawa couplings and the mass matrix, the symmetric version of the Lagrangian (1.20) gives rise to mixing between the active neutrinos with the Dirac fermion $\Psi = N_2 + N_3^c$. The strength of this mixing is determined by the combination $\frac{v}{M}|Y|$ [88]. Although this quantity can not be measured directly, it can be constrained. Current experimental bounds allow for $|Y| \lesssim 0.5$ for $M = 1$ TeV [89], i.e., the full range of parameters investigated in this

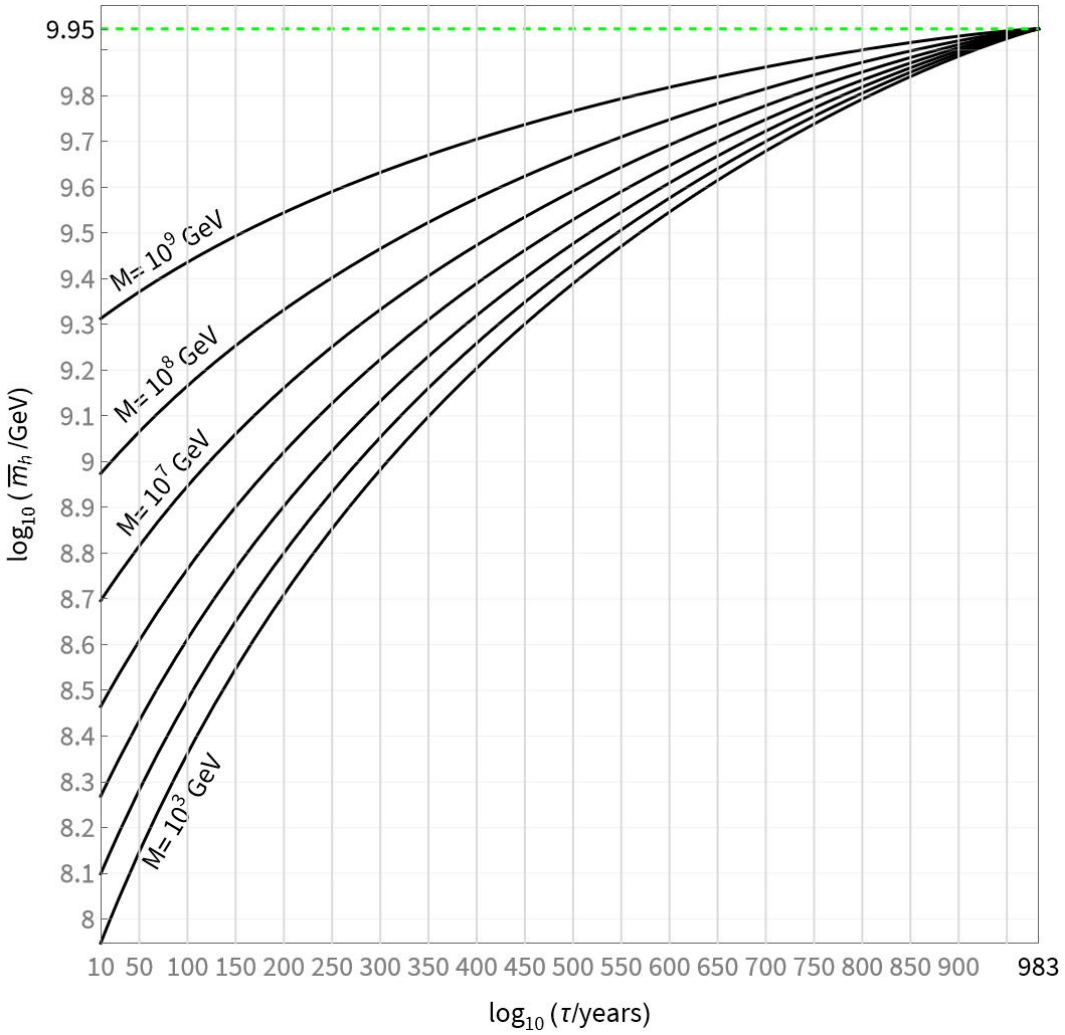

Figure 5.3: The upper bound on the running Higgs mass as a function of the lifetime. Different lifetimes are achieved by varying the neutrino coupling parameter $|Y(M)|$ (per Fig. 4.1), while all other couplings are fixed to their observed values near the electroweak scale. Each curve corresponds to a different value of M. The green dashed line marks the bound obtained for the considered set of parameters in the pure SM.

section.

At this point, it is important to stress once again that the inclusion of right-handed neutrino Yukawa couplings with properties relevant for the metastability bound generally modifies the running of λ in such a way as to shift its minimum to scales beyond the Planck mass. While this on its own would render the most important instantons inaccessible, it is counteracted by gravitational corrections. As described in Sec. 4.6.1, due to their non-logarithmic dependence on the scale, gravitational corrections keep μ_S below the Planck scale, despite the gravitational term being strongly suppressed relative to the Minkowski contribution. This observation is of particular interest as it offers a mechanism capable of significantly lowering the bound on the Higgs mass without relying on too strong Yukawa couplings, and thus hints at how the observed Higgs mass might arise from a metastability bound.

Lastly, there is an important subtlety resulting from the inclusion of neutrinos, or additional fermions in general. For the most interesting scenarios, when $M < \mu_I \sim \overline{m}_h$, the restricted Higgs mass is not that of the SM, but that of the νMSM. These two are related to one another via a threshold correction $\delta m_h^2 = \frac{M^2|Y|^2}{(4\pi)^2}$. Although this term is at least one order of magnitude smaller than $\overline{m}_h^2$ for all parameters considered in this chapter and therefore not important in the context of this bound, this does not necessarily apply tp all setups: The smallness of the correction compared to $\overline{m}_h^2$ can be traced back to the relative smallness of $|Y|$, which on the one hand leads to a small correction, and on the other hand doesn't allow for a fast enough decline of λ to move μ_I close to M. This last point is further enhanced by the threshold correction of λ. If the matching scale M lies close enough to the would-be instability scale, the threshold correction for λ can be large enough for the latter to jump to a negative value without vanishing exactly, spoiling the above analysis. While also this poses no problem for the range of parameters covered in this chapter, it might have consequences for a refined analysis of the model discussed in section 5.1.4 with parameters currently not accessible by the perturbative treatment.

5.1.3 Metastability bounds in a minimal composite Higgs model

One conclusion that could be drawn from the previous example is that, while right-handed neutrinos have the potential to greatly reduce the constraint on the Higgs mass, as seen in Figure 5.3, there are still numerous orders of magnitude between bound and measured value. For the smallest mass permitted by experiments, $M \sim 10^3$ GeV, the shortest possible lifetime of 10^{10} years gives $\overline{m}_h \simeq 10^8$ GeV, which is still many orders of magnitude away from the observed Higgs mass. Within the νMSM, this disparity could only be reduced further by increasing the Yukawa couplings, but this would inevitably render the electroweak vacuum unstable.

If one takes seriously the assumption that the observed value of the Higgs mass is indeed the result of metastability, this result suggests to look further into those SM extensions which can conspire with the right-handed neutrinos in a manner similar to gravity by

stabilizing the vacuum at scales below the instability scale, allowing stronger Yukawa couplings. Following the discussion of section 4.4.3, this is most easily achieved by adding a dimension-six term to the Higgs potential. The simplest models in which such a term occurs naturally are composite Higgs models, the simplest realization of which was studied in section 4.6.3.

For instructional reasons, this section analyzes the influence of Higgs compositeness on the metastability bound without right-handed neutrinos, whereas section 5.1.4 presents the results arising from the superposition of these two SM extensions.

The smallness of the vacuum alignment angle θ_0 is an essential condition for metastability to arise for a composite Higgs, analogous to the hierarchy between the electroweak and the Planck scale in the SM. The critical finding underpinning this discovery is that, once again, in order for the electroweak vacuum to exist, it must be located slightly above or below the instability scale μ_I. Meanwhile, $\lambda(\mu_S)$ must be sufficiently negative to provide a relatively short lifetime. Because λ runs only logarithmically with the scale, this is clearly only feasible if μ_I is several orders of magnitude lower than μ_S.

The simplest case for this occurs if $f \gtrsim \mu_\star$, when the instanton scale is approximately given by $\mu_S \simeq \mu_\star$. Thus, the effect of compositeness is negligible and the hierarchy between μ_I and μ_S is to good approximation given by (5.10). As by assumption $f \gtrsim \mu_\star$, this immediately implies the existence of a large hierarchy between μ_I and $\mu_\star$, and thus $\bar{H}$ and f.

The situation is slightly more involved if is $f \lesssim \mu_\star$, which implies that the dimension-six operator leads to a significant stabilization of the vacuum. This scenario is actually generic for the values of right-handed neutrino Yukawa couplings considered in Sec. 5.1.4, as they generally shift scale μ_* beyond $M_{\rm Pl}$, and thus beyond f as well. Also in this regime metastability demands that λ takes a sufficiently negative value at μ_S, again enforcing a hierarchy between μ_I and μ_S, described approximately by (5.9). Following the arguments of section 4.4.3, the instanton scale μ_S can be expected to lie at best one order of magnitude below f. Combining this insight with the results given in section 5.1, it becomes possible to estimate the upper bound on $\bar{H}$ by (5.5), leading to the good estimate

$$\begin{aligned}\bar{H} &\lesssim \exp\left(-\frac{1}{4}-\frac{\lambda_1(\mu_I)}{\beta_\lambda(\mu_I)}\right)\mu_I \simeq \mu_S\cdot\exp\left(-\frac{|\lambda(\mu_S)|}{|\beta_\lambda(\mu_S)|}-\frac{1}{4}-\frac{\lambda_1(\mu_I)}{\beta_\lambda(\mu_I)}\right)\lesssim \\ &\lesssim f\cdot\exp\left(-\frac{|\lambda(\mu_S)|}{|\beta_\lambda(\mu_S)|}-\frac{1}{4}-\frac{\lambda_1(\mu_I)}{\beta_\lambda(\mu_I)}\right).\end{aligned} \tag{5.11}$$

Taking into account (1.53), this implies an upper bound on the vacuum alignment angle,

$$\theta_0 \lesssim \frac{1}{2\sqrt{2}}\exp\left(-\frac{|\lambda(\mu_S)|}{|\beta_\lambda(\mu_S)|}-\frac{1}{4}-\frac{\lambda_1(\mu_I)}{\beta_\lambda(\mu_I)}\right). \tag{5.12}$$

This upper bound can then be represented as a function of the lifetime, yielding a function that is qualitatively similar to the SM results. For this model, varying f while setting the

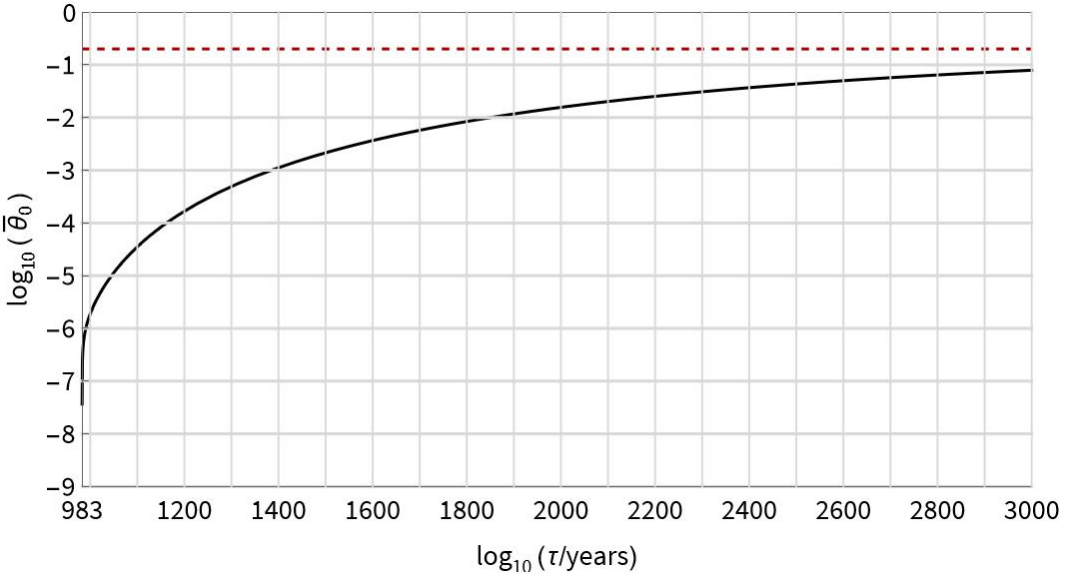

Figure 5.4: The upper bound $\bar{\theta}_0$ on the vacuum alignment angle, given in (5.12), as a function of the lifetime. The red dashed curve indicates the experimental upper bound $\sin\theta_0 \lesssim 0.2$ [22, 23].

SM couplings to their measured values at the electroweak scale is a sensible method to scan different lifetimes. When doing so, (5.11) should be interpreted as a lower limit for f rather than an upper bound for $\bar{H}$, because the dimension-six operator has no effect on the instability scale.

The upper bound (5.12) for θ_0, $\bar{\theta}_0$, can be computed as a function of the lifetime by combining the upper bound (5.5) with a numerically determined μ_I. This relationship is presented in Figure 5.4. As could be expected, a shorter lifetime indeed leads to a tighter bound on θ_0, and hence on the running Higgs mass, in line with earlier findings.

5.1.4 Combining a minimal composite Higgs with symmetry-protected neutrino masses

It's simple to add the influence of compositeness to the upper bound on the running Higgs mass as a function of the vacuum's lifetime once the lifetime has been connected to the neutrino Yukawa couplings. The updated relation is depicted in Figure 5.5, with M = 1 – 5TeV used for concreteness. In keeping with the reasoning given in section 4.4.3, metastability requires m_h to lie persistently at least 2 orders of magnitude below f, which is the natural scale for the Higgs mass in composite models. In line with the description of section 5.1.3, this can alternatively be regarded as restricting θ_0 to be small.

Figure 5.5 confirms that by balancing right-handed neutrinos with the stabilizing effect of a dimension-six operator, it is possible to obtain a much shorter lifetime while also lowering the upper bound on the running Higgs mass to $\simeq$ 10 TeV. Extrapolating these results beyond the applicability of the perturbative treatment, it appears as if lowering f

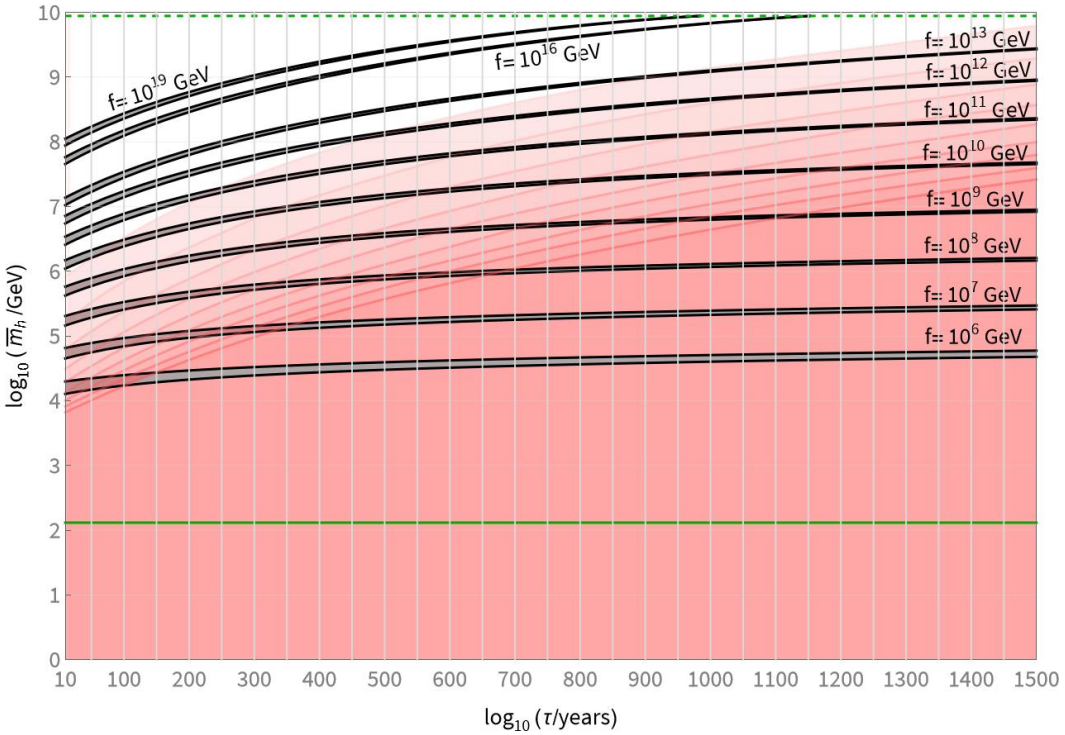

Figure 5.5: The upper bound on the running Higgs mass as a function of the lifetime for different values of f, with the range of f being only restricted by the applicability of our perturbative treatment and not physical reasons. The gray bars represent the interval $M = 1-5$ TeV. The shading in the background again marks areas of different ϵ for $M = 1$ TeV, ranging from 0.1 to 1 in steps of size 0.1.

by one more order of magnitude could allow for an upper bound on the Higgs mass of order 1 TeV. Along with the requirement of a potential barrier separating electroweak and true vacuum, this might be sufficient to explain the observed value of order 10^2 GeV.

Assuming that the stabilization is a result of Higgs compositeness, these predictions also imply a vacuum alignment angle that is substantially lower than existing empirical limitations. Considering that the Higgs mass is protected by the underlying symmetry due to its nature as a pNGB, this also guarantees the absence of any large radiative corrections to its mass, which can be expected to scale as $\delta M_h^2 \propto \sin^2(\theta) f^2$, leading to a Higgs sector with only minimal fine-tuning arising from the limited range of the perturbative treatment and in perfect agreement with all current observational bounds.

5.2 The electroweak vacuum in models with a large hierarchy

The arguments of the previous section seem to support the idea that there could be a shared, fundamental origin for the smallness of the Higgs mass and the metastability of the electroweak vacuum. Strongly simplified, this implies that new physics underlying the Higgs sector does exist, but becomes only relevant at a scale **above** the instability scale, and at least several orders of magnitude above the electroweak scale.

Although particularly interesting from a theoretical perspective, this scenario is also of phenomenological significance - especially in theories with a low-scale seesaw, where the instability scale can be drastically lowered. Thus, even without relying on ideas such as vacuum selection it is reasonable to consider a scenario in which metastability and gauge hierarchy are simultaneously realized. On a technical level, this would imply that the Higgs sector is embedded into some larger theory, which manifests itself only beyond the instability scale. This scenario opens up an interesting perspective on the Higgs potential which will be explored throughout this section.

5.2.1 A radiative origin of the electroweak vacuum

Assuming gauge invariance, the most general Higgs potential is of the form

$$V(\mathbf{H}) = f^4 F\left(\frac{\mathbf{H}^2}{f^2}\right) = -\frac{m^2}{2}\mathbf{H}^2 + \lambda \mathbf{H}^4 + \dots \tag{5.13}$$

where f is some constant of dimension energy, which can be expected to be of order of the scale of new (Higgs) physics Λ_{UV}. Eliminating the Goldstone modes by choosing unitary gauge, the potential can be rewritten as

$$V(H) = f^4 F\left(\frac{H^2}{2f^2}\right) = -\frac{m^2}{4}H^2 + \frac{\lambda}{4}H^4 + \sum_{n=3}^{\infty} \frac{\bar{C_{2n}}}{f^2} H^{2n}, \quad \text{where } \mathbf{H} = \left(0, \frac{H}{\sqrt{2}}\right) \tag{5.14}$$

and the parameters $\bar{C}_{2n}$ are related to the Wilson coefficients C_{2n}.

In this parametrization, the Higgs mass parameter - which is not necessarily identical to the tree level mass due to higher-order corrections - is given by $m^2 = -2F'(0) \cdot f^2$, so that its natural value would be of order f^2.

Following the reasoning in the beginning of this section, this discussion will rely on the following assumptions:

1. λ is negative and small below or at the matching scale Λ_{UV}.
2. The electroweak vacuum spontaneously breaks the gauge symmetry, i.e., $m^2 > 0$.
3. Some mechanism is in place ensuring the weak hierarchy, i.e., $m^2 \ll f^2$.

For the tree-level potential evaluated at the matching scale, the first two assumptions imply the existence of a local maximum[1] at $H = 0$ and subsequently falls off until some value v_{tree} of order f, where it develops a minimum. Assuming that $\bar{C}_6 > 0$ and taking into account that $m^2 \ll f^2$, this minimum is to leading order in $\frac{v_{\text{tree}}}{f}$ given by

$$v_{\text{tree}} \simeq f \cdot \sqrt{\frac{|\lambda|}{6\bar{C}_6}} + O\left(\frac{v_{\text{tree}}^2}{f^2}\right). \tag{5.15}$$

The most notable property of this vacuum is that, despite the smallness of the m^2-parameter, it would provide natural masses to the SM particles. In particular, the tree-level mass of the would-be Higgs boson satisfies $m_h^2 = f^2 \cdot \frac{|\lambda|^2}{3\bar{C}_6} = 2|\lambda| v_{\text{tree}}^2$, while the gauge boson and fermion masses satisfy their standard relations with $v = v_{\text{tree}} \sim f$.

To recover the electroweak vacuum, one has to take into account the running of λ, which is determined by its beta function. In the absence of neutrinos, this function is negative for all energies below $\mu_* \sim 10^{16}$ GeV, where λ reaches a minimum. For relevant neutrino Yukawa couplings, which are necessary for a lowered instability scale, β_λ remains negative until and beyond the Planck scale.

Thus, for energies significantly below the matching scale, the RG running will ultimately render λ positive for small enough energies. Assuming $\Lambda_{UV} < \mu_*$, this happens roughly at

$$\mu_I \approx e^{-\frac{|\lambda(\Lambda_{UV})|}{|\beta_\lambda(\Lambda_{UV})|}} \Lambda_{UV}. \tag{5.16}$$

As this scale is typically several orders of magnitude smaller than Λ_{UV}, the higher-dimension terms of the potential become subdominant in the region of positive λ, i.e., its properties are mostly determined by the quadratic and quartic term,

$$V(H) = -\frac{m^2}{4} H^2 + \frac{\lambda}{4} H^4 + \ldots, \tag{5.17}$$

[1] Note that for $m^2 < 0$, this point would actually be a local minimum.

where λ is now positive. On the first look, this potential seems to have a simple structure. For small values of H, the quadratic term is dominant and thus the potential is decreasing. Meanwhile, for large enough values of H, the quartic term becomes dominant and the potential increases, thus implying the existence of some minimum around the transition between these two regimes. Following the previous section, the existence of this vacuum is ensured through the assumption $m^2 \ll f^2$.

In other words, for potentials with a negative quartic coupling at the matching scale Λ_{UV}, the existence of the false vacuum - and thus, the possibility of metastability - can be understood as a consequence of the electroweak hierarchy. This observation is clearly closely related to the results of the previous section.

To understand the relation between these two results, it is crucial to recall their underlying assumptions. Both are based on the assumption that the quartic coupling is negative at some high energy. Here, this is the matching scale Λ_{UV}, while in section 5.1, this role is taken by the instanton scale μ_I. The crucial difference lies in the interpretation of the electroweak vacuum. In section 5.1, its existence is a necessary condition of the desired metastability. Thus, to consolidate the properties of this vacuum with the negativity of λ necessary for its decay, the hierarchy is necessary. Here, the assumption of metastability has been loosened, only keeping the negativity and smallness of λ at large scales, which could be merely a consequence of the larger theory into which the Higgs sector is embedded in the UV. As this assumption allows for a stable vacuum at some natural scale, it does not necessarily correspond to metastability. However, assuming the smallness of the m^2-parameter, the emergence of an additional, false vacuum is simply a consequence of the RG running of λ and its value at the matching scale.

5.2.2 Example: The SU(4)/Sp(4) composite Higgs

Just as for the arguments of section 5.1, the perspective outlined here can be once again illustrated on the example of the SU(4)/Sp(4) composite Higgs model. Inspired by this model's origin in the idea of naturalness, it is usually investigated under the assumption that the technipion scale lies as close as possible to the electroweak scale to minimize fine-tuning. Under these assumptions, the electroweak vacuum emerges as the unique minimum of the tree-level potential and is stable since $\lambda(\Lambda_f) \geq 0$.

While this last condition is obviously motivated by the SM, it's origin is somewhat more involved in the context of the full UV theory. As was shown in section 1.6, the form of the composite Higgs' potential implies that the value of λ at the matching scale is, at tree level, determined by the coefficients X_t and X_m through

$$\lambda(\Lambda_f) = \frac{1}{96}\big(2X_t(\Lambda_f) - X_m(\Lambda_f)\big), \tag{5.18}$$

where X_t and X_m are given by

$$X_t = C_t y_t^2 - C_g \frac{1}{2}(3g^2 + g'^2) \quad \text{and } X_m = C_m. \tag{5.19}$$

Condition (5.18) on its own would, in principle, allow for negative values of λ at the matching scale, giving rise to the picture outlined in the previous subsection. Taking into account (5.19), it is evident that whether or not this occurs is determined entirely by the parameters C_t, C_g and C_m as well as the matching scale. This picture can be further simplified by demanding a small Higgs mass, which is necessary for the emergence of a familiar electroweak vacuum. In this limit, C_m can be eliminated and thus (5.18) can be simplified to $\lambda \simeq \frac{X_t}{64}$.

Whether or not the resulting Higgs potential showcases the behavior of interest is thus determined by the sign of X_t, which in turn is determined by the ratio of C_t and C_m together with the matching scale. Figure 5.6 depicts the critical ratio indicating the transition from a stable, conventional composite Higgs potential to one with a radiatively generated, metastable electroweak vacuum as a function of the matching scale for multiple values of the Higgs mass.

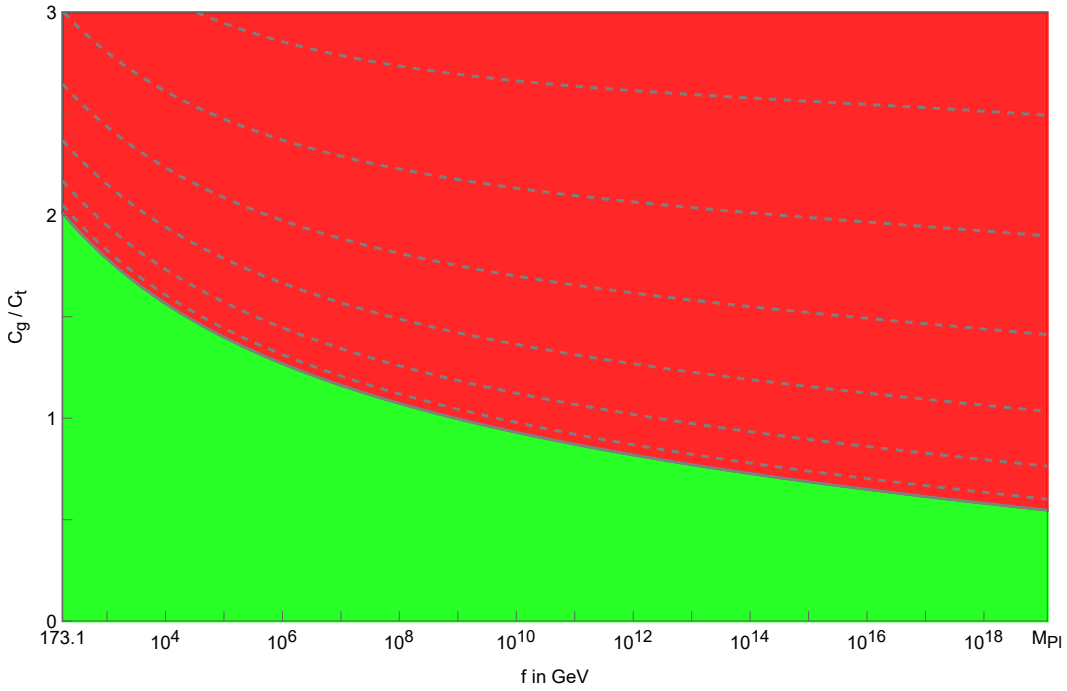

Figure 5.6: The ratio of the loop coefficients $\frac{C_g}{C_t}$ marking the transition from conventional, stable (green) to non-stable, radiatively generated (red) electroweak vacuum as a function of the technipion scale f for $m \simeq 0$. The grey dashed lines describe the transition for $\frac{m^2}{C_t f^2} \in 0.2, 0.4, 0.6, 0.8, 1, 1.2$.

These results imply that for any given $\frac{C_g}{C_t}$, increasing the hierarchy leads to a less stable vacuum through the superposition of three effects. On the one hand, increasing Λ_f changes the values of the couplings that enter X_t. For larger energies, the Yukawa coupling becomes weaker, while the combination $g^2 + g'^2$ becomes larger, and due to their relative sign these effects combine, causing a smaller, and ultimately negative, X_t. This explains the shape of each of the individual curves in Figure 5.1.

If, on the other hand, the Higgs mass is just weakly suppressed relative to its natural value, the approximation $2X_t \simeq X_m$ becomes less reliable, and the deviation manifests as a correction in λ, leading to the upwards shifted curves in Figure 5.1.

Lastly, although not represented in 5.1, the stabilization of the dimension-six term is most efficient for small values of f, and thus, a larger hierarchy.

The remarkable observation is now that this relation is strikingly similar to the one found in 5.1, despite their fundamentally different origins. The latter was obtained entirely within the framework of the SM, and is thus insensitive to the details of the UV theory. Meanwhile, the relation depicted in 5.1 is a consequence of nothing but the matching conditions, which are determined from the UV theory, and mostly independent of the properties of the instanton in the low-energy theory.

5.2.3 Minimal lifetime of the radiatively generated false vacuum

There is one important subtlety to this reasoning, concerning the assumption that λ is not just negative, but also small. λ ultimately becoming positive at low energies, and thus generating the existence of the false vacuum, relies on the top quark's and potentially neutrinos' contribution to its beta function. This also means that μ_I cannot be arbitrarily small, as neither of these particles are appropriate degrees of freedom at all energies - in a consistent treatment, the right-handed neutrinos need to be integrated out below their mass, and the quarks become strongly coupled at the QCD scale, Λ_{QCD}. Thus, for λ to turn positive, it has to do so at some scale at least above the QCD scale, which, following equation 5.16, is only possible if its absolute value at the matching scale is not too large. This translates to a lower bound on the vacuum's lifetime, which is, for most phenomenologically viable models, far smaller than the age of the observed universe.

This reasoning also applies below Λ_{QCD}, where it is well-known that the effects of quark condensation transform the Higgs' Yukawa terms into an additional linear term for the potential, $\Delta V_{\text{lin}} \propto \langle \bar{q}q \rangle H$. In scenarios in which the gauge symmetry is not spontaneously broken through the form of the Higgs potential due to a "wrong" sign of the m^2-parameter this term is responsible for the emergence of a non-vanishing vacuum expectation value as it shifts the potential's minimum away from $H = 0$ [90–92]. If, however, $H = 0$ corresponds to a local maximum and $\lambda < 0$, the only impact of this term is to shift the position of the maximum, but without giving rise to another minimum. Thus, this possibility is not suited to avoid this bound. These arguments furthermore confirm that the only way for such a theory to generate a metastable false vacuum at low energies is indeed through the mechanism described in the last subsection.

Chapter 6

Conclusion

Rather than just providing a passive background for the universe's dynamics to unfold on, the properties of our vacuum are deeply connected to the fields which inhabit it. During my PhD studies I explored two manifestations of these interactions.

One example for this are topological solitons, and in particular the type relevant for the QCD vacuum and at low energies. These configurations are a physical manifestation of a given theory's vacuum structure while also, in many ways, acting as vacuum on their own. In their presence, the spectrum of the theory typically breaks up into three categories. The zero modes reflect the solitons' particle-like behavior, usually representing properties like its position or orientation. The modes corresponding to the discrete part of the spectrum can be understood as the solitons internal dynamics, typically vibrations. Lastly, those corresponding to the continuous spectrum behave asymptotically as free particles, which are bent and deformed through their interaction with the background soliton while propagating through it.

What makes the zero modes and the dynamics they represent special is their universality. Every soliton has one translational zero mode for each dimension of the space in which it exists and one for each additional symmetry. Precisely because of their origin in symmetries, the dynamics represented by the zero modes is of a simple, universal form, which can be fully described by the moduli space and a small number of parameters determining its metric. Thus, the moduli space can alternatively be thought of as an effective theory describing the low-energy dynamics of the soliton.

This effective description captures only the moduli, so that as soon as one is interested in processes involving the remaining modes one has to rely on the full theory. This might appear surprising considering the idea of a soliton as an extended particle, as certain deformations such as "stretching" and "compressing" the soliton appear as universal as translations, suggesting that it should be possible to describe them in a similarly universal way as the moduli. However, as they clearly consist of non-zero modes, this would amount to finding an effective description covering all modes of any soliton in one single framework.

I have shown that such a theory **does** exist and can be obtained through a simple extension of the moduli space.

This theory is based on the introduction of so-called *warp fields*, which can be constructed from all of the theory's modes. Thus, in contrast to conventional effective field theories, the range of this theory's validity is not limited by energy, but rather spatial localization and amplitude. This restriction is not perturbative in nature, but linked to the construction of these fields, and can thus be represented by a clear cut-off.

At large energies, the interplay of our vacuum's content might allow for a drastic change in the behavior of the Higgs field, allowing for configurations of lower energy than that of its current one. The existence of such configurations would imply that the "vacuum" we currently inhabit is not entirely stable and can decay into a state of lower energy as the Higgs field tunnels through the potential barrier protecting its current value.

In the second half of my PhD studies, I investigated this possibility and its consequences with a particular focus on one of its most peculiar aspects. Whether or not our vacuum remains stable at all energies depends strongly on the values of the Higgs' couplings in such a way that even a slight change could either completely stabilize our vacuum or cause it to decay in a time much shorter than the age of the observable universe. Besides its couplings, the only other parameter determining the Higgs' physics is its mass parameter. Interestingly, also this parameter appears, on the first look, to be fine-tuned, giving rise to the so-called hierarchy problem.

Through my work, I have shown that these two apparent tunings are, in fact, **not** independent, as the smallness of the Higgs mass is a necessary condition for metastability. This result rests on the insight that the existence of the electroweak vacuum requires the mass parameter to be smaller than the instability scale by at least one order of magnitude, i.e., the scale where the quartic coupling turns negative due to its RG running, which is necessary for the realization of metastability in the Standard Model. The connection between the instability scale and the natural value of the Higgs mass then follows from the properties of the instanton underlying the decay. The instability scale must be smaller than the so-called *instanton scale*, which characterizes to the dominant instanton. This hierarchy can be linked to the RG running of the quartic coupling, implying that it stretches over multiple orders of magnitude. Furthermore, the equation I derived for the instanton scale implies that it is typically smaller than the natural Higgs value by at least one more order of magnitude.

What makes this result even more intriguing is its potential phenomenological significance. Unless one wishes to assume further fine-tuning, any attempt to solve the hierarchy problem through some mechanism leading to metastability would suggest the conclusion that the Higgs mass should lie at best a few orders of magnitude below the instability scale. Reversely, metastability might offer a plausible explanation for the value of the Higgs mass if it lies sufficiently close to the instability scale. Taking seriously the metastability bound as a solution to the hierarchy problem thus favors Standard Model extensions which drastically

lower the instability scale relative to the Standard Model. The perhaps best-motivated example for such theories are ones in which the neutrino masses are generated through a low-scale seesaw, which allow to decrease the instability scale down into the TeV-range within observation bounds.

Although not in contradiction with observations, the parameters necessary to achieve such a low instability scale would imply a lifetime of the vacuum much smaller than the age of our observable Universe. For them to be feasible, the effect on the stability needs to be at least partially compensated for. This can be easily achieved through new physics manifesting as a dimension-six operator in the potential, and in particular models with two Higgs doublets like the (ν)MSSM or with a (partially) composite Higgs.

In summary, the hypothesis that the hierarchy problem is a consequence of metastability can be linked to a very specific form of Standard Model extension, combining a TeV-scale seesaw with $O(1)$ Yukawa couplings with some extension of the Higgs potential at around 100 TeV.

Despite these significant successes, the underlying result might still be incomplete. Saturating the metastability bound corresponds to the electroweak vacuum emerging as a saddle point without potential barrier. Thus, to avoid vacuum decay through high energetic processes an additional hierarchy is necessary, but its precise extent remains to be determined. Another interesting possibility is that more of the Universe's apparent fine-tunings could be included in this discussion in a similar way. In this context the appearance of the cosmological constant in the lifetime formula is certainly of particular interest.

Appendix A

Conventions and general expressions

A.1 Facts about su(4) and Sp(4)

One of the most famous ideas about physics at very high energies is the idea that the SM's symmetry group might be embedded into some larger group. In the case of the composite model used as go-to example in this thesis, this group is a flavor SU(4).

su(4) denotes the Lie-algebra of SU(4), whose elements can be written as $R = \exp(i\alpha_n T_n)$, with the usual exponential map. In the fundamental matrix representation, unitarity implies that the generators $\{T_n\}_n$ satisfy

$$\mathbb{1} = \left(\mathbb{1} + i\alpha_n T_n + o(\alpha^2)\right) \cdot \left(\mathbb{1} + i\alpha_n T_n + o(\alpha^2)\right)^\dagger = \mathbb{1} + i\alpha_n (T_n^\dagger - T_n) + o(\alpha^2), \tag{A.1}$$

implying that $T_n^\dagger = T_n$. Furthermore, the demand that det(R)= 1 implies that the generators satisfy $\mathrm{tr}(T_n) = 0$. From these conditions, it follows that there exist only $4^2 - 1 = 15$ linear independent generators, which can be chosen as follows:

$$T_1 = \frac{1}{2}\begin{pmatrix}\sigma_1 & 0\\ 0 & 0\end{pmatrix}, \quad T_2 = \frac{1}{2}\begin{pmatrix}\sigma_2 & 0\\ 0 & 0\end{pmatrix}, \quad T_3 = \frac{1}{2}\begin{pmatrix}\sigma_3 & 0\\ 0 & 0\end{pmatrix},$$
$$T_4 = \frac{1}{2}\begin{pmatrix}0 & 0\\ 0 & -\sigma_1^T\end{pmatrix}, \quad T_5 = \frac{1}{2}\begin{pmatrix}0 & 0\\ 0 & -\sigma_2^T\end{pmatrix}, \quad T_6 = \frac{1}{2}\begin{pmatrix}0 & 0\\ 0 & -\sigma_3^T\end{pmatrix},$$
$$T_7 = \frac{1}{2\sqrt{2}}\begin{pmatrix}0 & i\sigma_1\\ -i\sigma_1 & 0\end{pmatrix}, \quad T_8 = \frac{1}{2\sqrt{2}}\begin{pmatrix}0 & i\sigma_2\\ -i\sigma_2 & 0\end{pmatrix}, \quad T_9 = \frac{1}{2\sqrt{2}}\begin{pmatrix}0 & i\sigma_3\\ -i\sigma_3 & 0\end{pmatrix},$$
$$T_{10} = \frac{1}{2\sqrt{2}}\begin{pmatrix}0 & \mathbb{1}\\ \mathbb{1} & 0\end{pmatrix}, \quad T_{11} = \frac{1}{2\sqrt{2}}\begin{pmatrix}0 & \sigma_3\\ \sigma_3 & 0\end{pmatrix}, \quad T_{12} = \frac{1}{2\sqrt{2}}\begin{pmatrix}0 & i\\ -i & 0\end{pmatrix},$$
$$T_{13} = \frac{1}{2\sqrt{2}}\begin{pmatrix}0 & \sigma_1\\ \sigma_1 & 0\end{pmatrix}, \quad T_{14} = \frac{1}{2\sqrt{2}}\begin{pmatrix}0 & \sigma_2\\ \sigma_2 & 0\end{pmatrix}, \quad T_{15} = \frac{1}{2\sqrt{2}}\begin{pmatrix}\mathbb{1} & 0\\ 0 & -\mathbb{1}\end{pmatrix}.$$

Under the flavor SU(4), condensates transform as

$$\Sigma \to U\Sigma U^\dagger = \Sigma + i\alpha_n(T_n\Sigma + \Sigma T_n^\dagger) + O(\alpha^2) \tag{A.2}$$

Thus, the condensate breaks the subgroup spanned by the generators satisfying

$$T_n\Sigma + \Sigma T_n^\dagger \neq 0, \text{ while } T_n\Sigma + \Sigma T_n^\dagger = 0 \tag{A.3}$$

corresponds to the generators of the unbroken subgroup. A powerful approach for the explicit construction of broken and unbroken generators is through the definition of two projection operators, which act on a generator through

$$T_n^{\parallel\Sigma} = \frac{1}{2}(T_n - \Sigma T_n^T\Sigma^\dagger),\ T_n^{\perp\Sigma} = \frac{1}{2}(T_n + \Sigma T_n^T\Sigma^\dagger) \tag{A.4}$$

For any generator T, the images of these projectors satisfy

$$T_n^{\parallel\Sigma}\Sigma + \Sigma(T_n^{\parallel\Sigma})^\dagger = 0\ T_n^{\perp\Sigma}\Sigma - \Sigma(T_n^{\perp\Sigma})^\dagger = 0 \tag{A.5}$$

This has two immediate consequences. First, and most importantly, $\parallel$ projects any element of the Lie algebra su(4) to the unbroken algebra. As a corollary, when $T_n^{\parallel} = T_n$, T_n is a generator of the unbroken symmetry group. Second, the generators of the broken symmetry group, which are linked to the theory's Goldstone bosons, satisfy $T_n^{\perp\Sigma}\Sigma = \Sigma(T_n^{\perp\Sigma})^\dagger$. Given that the condensate transforms under the SU(4) as $\Sigma \to R\Sigma R$, this can be used to significantly simplify calculations.

There are three condensates of phenomenolgical interest:

$$\sigma_H = \begin{pmatrix} 0 & \mathbb{1}_{2\times2} \\ -\mathbb{1}_{2\times2} & 0 \end{pmatrix},\quad \Sigma_A = \begin{pmatrix} i\sigma^2 & 0 \\ 0 & i\sigma^2 \end{pmatrix},\quad \Sigma_B = \begin{pmatrix} i\sigma^2 & 0 \\ 0 & -i\sigma^2 \end{pmatrix}, \Sigma_H = \begin{pmatrix} 0 & \mathbb{1}_{2\times2} \\ \mathbb{1}_{2\times2} & 0 \end{pmatrix} \tag{A.6}$$

It is easy to see that the generators of the custodial symmetry group of the condensate Σ_H satisfy the defining equation of the symplectic group sp(4). As Σ_H and Σ_B are related to one another through SU(4) transformations, it is more efficient to find the broken and unbroken generators for a general condensate of the form

$$\sigma_\theta = \begin{pmatrix} \cos(\theta)i\sigma^2 & \sin(\theta)\mathbb{1}_{2\times2} \\ -\sin(\theta)\mathbb{1}_{2\times2} & -\cos(\theta)i\sigma^2 \end{pmatrix}, \tag{A.7}$$

where $\theta = 0$ corresponds to the Σ_B condensate, and $\theta = \frac{\pi}{2}$ to Σ_H. Applying the projectors (A.4) to the full set of SU(4) generators, it is straightforward to obtain a complete set of linearly independent generators:

$$T_1^{\parallel\Sigma_\theta} = \frac{1}{2}\begin{pmatrix} 0 & \mathbb{1}_{2\times2} \\ \mathbb{1}_{2\times2} & 0 \end{pmatrix}, \quad T_2^{\parallel\Sigma_\theta} = \frac{1}{2}\begin{pmatrix} 0 & i\sigma^1 \\ -i\sigma^1 & 0 \end{pmatrix}, \quad T_3^{\parallel\Sigma_\theta} = \frac{1}{2}\begin{pmatrix} \sin(\theta)\mathbb{1}_{2\times2} & \cos(\theta)i\sigma^2 \\ -\cos(\theta)i\sigma^2 & -\sin(\theta)\mathbb{1}_{2\times2} \end{pmatrix},$$

$$T_4^{\parallel\Sigma_\theta} = \frac{1}{2}\begin{pmatrix} 0 & i\sigma^3 \\ -i\sigma^3 & 0 \end{pmatrix}, \quad T_5^{\parallel\Sigma_\theta} = \frac{1}{2}\begin{pmatrix} \sigma^1 & 0 \\ 0 & -\sigma^1 \end{pmatrix}, \quad T_6^{\parallel\Sigma_\theta} = \frac{1}{2}\begin{pmatrix} \cos(\theta)\sigma^1 & \sin(\theta)\sigma^3 \\ \sin(\theta)\sigma^3 & \cos(\theta)\sigma^1 \end{pmatrix},$$

$$T_7^{\parallel\Sigma_\theta} = \frac{1}{2\sqrt{2}}\begin{pmatrix} \sigma^3 & 0 \\ 0 & -\sigma^3 \end{pmatrix}, \quad T_8^{\parallel\Sigma_\theta} = \frac{1}{2\sqrt{2}}\begin{pmatrix} \cos(\theta)\sigma^3 & -\sin(\theta)\sigma^1 \\ -\sin(\theta)\sigma^1 & \cos(\theta)\sigma^3 \end{pmatrix},$$

$$T_9^{\parallel\Sigma_\theta} = \frac{1}{2\sqrt{2}}\begin{pmatrix} \cos(\theta)\sigma^2 & -i\sin(\theta)\mathbb{1}_{2\times2} \\ i\sin(\theta)\mathbb{1}_{2\times2} & -\cos(\theta)\sigma^2 \end{pmatrix}, \quad T_{10}^{\parallel\Sigma_\theta} = \frac{1}{2\sqrt{2}}\begin{pmatrix} \sigma^2 & 0 \\ 0 & \sigma^2 \end{pmatrix},$$

$$T_1^{\perp\Sigma_\theta} = \frac{1}{2\sqrt{2}}\begin{pmatrix} \sin(\theta)\sigma^1 & -\cos(\theta)\sigma^3 \\ -\cos(\theta)\sigma^3 & \sin(\theta)\sigma^1 \end{pmatrix}, \quad T_2^{\perp\Sigma_\theta} = \frac{1}{2\sqrt{2}}\begin{pmatrix} \sin(\theta)\sigma^2 & i\cos(\theta)\mathbb{1}_{2\times2} \\ -i\cos(\theta)\mathbb{1}_{2\times2} & -\sin(\theta)\sigma^2 \end{pmatrix},$$

$$T_3^{\perp\Sigma_\theta} = \frac{1}{2\sqrt{2}}\begin{pmatrix} \sin(\theta)\sigma^3 & \cos(\theta)\sigma^1 \\ \cos(\theta)\sigma^1 & \sin(\theta)\sigma^3 \end{pmatrix}, \quad T_4^{\perp\Sigma_\theta} = \frac{1}{2\sqrt{2}}\begin{pmatrix} 0 & \sigma^2 \\ \sigma^2 & 0 \end{pmatrix},$$

$$T_5^{\perp\Sigma_\theta} = \frac{1}{2\sqrt{2}}\begin{pmatrix} \cos(\theta)\mathbb{1}_{2\times2} & -\sin(\theta)i\sigma^2 \\ \sin(\theta)i\sigma^2 & -\cos(\theta)\mathbb{1}_{2\times2} \end{pmatrix}.$$

A.2 Beta functions

The beta function of the quartic coupling λ at 3-loop order is given by

$$
\begin{aligned}
\beta_\lambda = \frac{1}{(4\pi)^2}\Bigg[& 24\lambda^2 - 6y_\mathrm{t}^4 - 6y_\mathrm{b}^4 - 2y_\tau^4 + \frac{3}{8}\left(2g^4 + \left(g^2+g'^2\right)^2\right) - \\
& - \lambda\left(9g^2 + 3g'^2 - 12y_\mathrm{t}^2 - 12y_\mathrm{b}^2 - 4y_\tau^2\right) + |Y|^2\left(4\lambda - 2|Y|^2\right)\Bigg] \\
+ \frac{1}{(4\pi)^4}\Bigg[& \frac{1}{48}\left(915g^6 - 289g^4g'^2 - 559g^2g'^4 - 379g'^6\right) + 30y_\mathrm{t}^6 + 30y_\mathrm{b}^6 + 10y_\tau^6 - \\
& - y_\mathrm{t}^4\left(\frac{8}{3}g'^2 + 32g_s^2 + 3\lambda + 6y_\mathrm{b}^2\right) - y_\mathrm{b}^4\left(\frac{4}{3}g'^2 + 32g_s^2 + 3\lambda + 6y_\mathrm{t}^2\right) - y_\tau^4\left(4g'^2 + 3\lambda\right) \\
& + \lambda\left(-\frac{73}{8}g^4 + \frac{39}{4}g^2g'^2 + \frac{629}{24}g'^4 + 108g^2\lambda + 36g'^2\lambda - 312\lambda^2\right) \\
& + y_\mathrm{t}^2\left(-\frac{9}{4}g^4 + \frac{21}{2}g^2g'^2 - \frac{19}{4}g'^4 + \lambda\left(\frac{45}{2}g^2 + \frac{85}{6}g'^2 + 80g_s^2 - 144\lambda - 42y_\mathrm{b}^2\right)\right) \\
& + y_\mathrm{b}^2\left(-\frac{9}{4}g^4 + \frac{9}{2}g^2g'^2 - \frac{5}{4}g'^4 + \lambda\left(\frac{45}{2}g^2 + \frac{25}{6}g'^2 + 80g_s^2 - 144\lambda - 42y_\mathrm{t}^2\right)\right) \\
& + y_\tau^2\left(-\frac{3}{4}g^4 + \frac{11}{2}g^2g'^2 - \frac{25}{4}g'^4 + \lambda\left(\frac{15}{2}g^2 + \frac{75}{6}g'^2 - 48\lambda\right)\right) \\
& + |Y|^2\left(-96\lambda^2 + \lambda(5g'^2 + 15g^2 - 2|Y|^2) - \frac{3}{2}g^4 + 20|Y|^4\right)\Bigg] \\
+ \frac{1}{(4\pi)^6}\Bigg[& \lambda^3\left(12022.7\lambda + 1746y_\mathrm{t}^2 - 774.904g^2 - 258.3g'^2\right) \\
& + \lambda y_\mathrm{t}^2\left(3536.52y_\mathrm{t}^2 + 321.54g_s^2 - 719.078g^2 - 212.896g'^2\right) \\
& + \lambda^2\left(-1580.56g^4 - 1030.734g'^4 - 1055.466g^2g'^2\right) \\
& + \lambda y_\mathrm{t}^4\left(-446.764y_\mathrm{t}^2 - 1325.732g_s^2 - 10.94g^2 - 70.05g'^2\right) \\
& + \lambda y_\mathrm{t}^2\big(713.936g_s^4 - 639.328g^4 - 415.888g'^4 + \\
& \qquad + 30.288g_s^2g^2 + 58.18g_s^2g'^2 + 18.716g^2g'^2\big) \\
& + \lambda g^4\left(-114.288g_s^2 + 1730.966g^2 + 265.46g'^2\right) + \\
& + \lambda g'^4\left(-46.562g_s^2 + 343.072g^2 + 260.814g'^2\right) \\
& + y_\mathrm{t}^6\left(-486.298y_\mathrm{t}^2 + 500.988g_s^2 + 146.276g^2 + 113.1g'^2\right) \\
& + y_\mathrm{t}^4\left(-100.402g_s^4 + 31.768g^4 + 88.6g'^4 + 26.698g_s^2g^2 + 58.566g_s^2g'^2 - 234.52g^2g'^2\right) \\
& + y_\mathrm{t}^2g_s^2\left(32.928g^4 + 3.644g'^4 + 37.954g^2g'^2\right) + y_\mathrm{t}^2g^4\left(125g^2 + 43.470g'^2\right) \\
& + y_\mathrm{t}^2g'^4\left(58.318g^2 + 102.936g'^2\right) + \\
& + g_s^2\left(15.072g^6 + 7.138g'^6 + 5.024g^4g'^2 + 6.138g^2g'^4\right) \\
& - 228.182g^8 - 23.272g'^8 - 126.296g^6g'^2 + 36.112g^4g'^4 - 14.288g^2g'^6\Bigg] + \mathcal{O}\left(\frac{m_h^2}{\Lambda_f^2}\right).
\end{aligned}
\tag{A.8}
$$

For the top Yukawa coupling y_t, one finds, also at 3-loop order,

$$\begin{aligned}
\beta_{y_t} = {} & \frac{y_t}{(4\pi)^2}\left[-\frac{9}{4}g^2 - \frac{17}{12}g'^2 - 8g_s^2 + \frac{9}{2}y_t^2 + |Y|^2 \right] \\
& + \frac{y_t}{(4\pi)^4}\left[-\frac{23}{4}g^4 - \frac{3}{4}g^2g'^2 + \frac{1187}{216}g'^4 + 9g^2g_s^2 + \frac{19}{9}g'^2g_s^2 - 108g_s^4 + \right. \\
& \qquad + y_t^2\left(\frac{225}{16}g^2 + \frac{131}{16} + 36g_s^2\right) \\
& \qquad \left. + 6\left(\lambda^2 - 2y_t^4 - 2\lambda y_t^2\right) + |Y|^2\left(-\frac{9}{8}y_t^2 - \frac{9}{4}|Y|^2 + \frac{5}{8}g'^2 + \frac{15}{8}g^2\right)\right] \\
& + \frac{y_t}{(4\pi)^6}\left[y_t^4\left(58.6028y_t^2 + 198\lambda - 157g_s^2 - \frac{1593}{16}g^2 - \frac{2437}{48}g'^2\right)\right. \\
& \qquad + \lambda y_t^2\left(\frac{15}{4}\lambda + 16g_s^2 - \frac{135}{2}g^2 - \frac{127}{6}g'^2\right) \\
& \qquad + y_t^2\big(363.764g_s^4 + 16.990g^4 - 67.839g'^4 + \\
& \qquad\quad + 48.370g_s^2g^2 + 30.123g_s^2g'^2 + 58.048g^2g'^2\big) \\
& \qquad + \lambda^2\left(-36\lambda + 45g^2 + 15g'^2\right) + \lambda\left(-\frac{171}{16}g^4 - \frac{1089}{144}g'^4 + \frac{39}{8}g^2g'^2\right) \\
& \qquad - 619.35g_s^6 + 169.829g^6 + 74.074g'^6 + 73.654g_s^4g^2 - 25.16g_s^4g'^2 \\
& \qquad - 21.072g_s^2g^4 - 61.997g_s^2g'^4 - \frac{107}{4}g_s^2g^2g'^2 - \\
& \qquad \left. - 7.905g^4g'^2 - 12.339g^2g'^4\right] + \mathcal{O}\left(\frac{m_h^2}{\Lambda_f^2}\right).
\end{aligned} \tag{A.9}$$

The beta functions of the gauge couplings g', g and g_s are respectively given by

$$\begin{aligned}
\beta_{g'} = {} & \frac{g'^3}{(4\pi)^2}\frac{41}{6} + \frac{g'^3}{(4\pi)^4}\left[\frac{199}{18}g'^2 + \frac{9}{2}g^2 + \frac{44}{3}g_s^2 - \frac{17}{6}y_t^2 - \frac{1}{2}|Y|^2\right] \\
& + \frac{g'^3}{(4\pi)^6}\left[y_t^2\left(\frac{315}{16}y_t^2 - \frac{29}{5}g_s^2 - \frac{785}{32}g^2 - \frac{2827}{288}g'^2\right) + \lambda\left(-3\lambda + \frac{3}{2}g^2 + \frac{3}{2}g'^2\right)\right. \\
& \left. + 99g_s^4 + \frac{1315}{64}g^4 - \frac{388613}{5184}g'^4 - \frac{25}{9}g_s^2g^2 - \frac{137}{27}g_s^2g'^2 + \frac{205}{96}g^2g'^2\right];
\end{aligned} \tag{A.10}$$

$$\begin{aligned}
\beta_g = {} & -\frac{g^3}{(4\pi)^2}\frac{19}{6} + \frac{g^3}{(4\pi)^4}\left[\frac{3}{2}g'^2 + \frac{35}{6}g^2 + 12g_s^2 - \frac{3}{2}y_t^2 - \frac{1}{2}|Y|^2\right] \\
& + \frac{g^3}{(4\pi)^6}\left[y_t^2\left(\frac{147}{16}y_t^2 - 7g_s^2 - \frac{729}{32}g^2 - \frac{593}{96}g'^2\right) + \lambda\left(-3\lambda + \frac{3}{2}g^2 + \frac{1}{2}g'^2\right)\right. \\
& \left. + 81g_s^4 + \frac{324953}{1728}g^4 - \frac{5597}{576}g'^4 + 39g_s^2g^2 - \frac{1}{3}g_s^2g'^2 + \frac{291}{32}g^2g'^2\right]
\end{aligned} \tag{A.11}$$

and

$$\begin{aligned}\beta_{g_s} = &-\frac{g_s^3}{(4\pi)^2}\cdot 7 + \frac{g_s^3}{(4\pi)^4}\left[\frac{11}{6}g_s^2 + \frac{9}{2}g^2 - 26g_s^2 - 2y_\mathrm{t}^2\right] \\ &+ \frac{g_s^3}{(4\pi)^6}\Bigg[y_\mathrm{t}^2\left(15y_\mathrm{t}^2 - 40g_s^2 - 93/8g^2 - 101/24g'^2\right) \\ &+ \frac{65}{2}g_s^4 + \frac{109}{8}g^4 - \frac{2615}{216}g'^4 + 21g_s^2g^2 + \frac{77}{9}g_s^2g'^2 - \frac{1}{8}g^2g'^2\Bigg]. \end{aligned} \tag{A.12}$$

These are at 3-loop order, except for β_{g_s} which includes the dominant 4-loop term. For the neutrinos' Yukawa couplings, the beta function at 2-loop order is

$$\begin{aligned}\beta_{Y_i} = &\frac{Y_i}{(4\pi)^2}\left[\frac{5}{2}|Y|^2 + 3y_\mathrm{t}^2 - \frac{3}{4}g'^2 - \frac{9}{4}g^2\right] \\ &+ \frac{Y_i}{(4\pi)^4}\Bigg[\frac{3}{2}|Y|^4 - \frac{9}{4}|Y|^2\left(3y_\mathrm{t}^2 + |Y|^2\right) - \frac{9}{4}\left(3y_\mathrm{t}^4 + |Y|^4\right) + \frac{3}{2}\lambda^2 - 64\lambda|Y|^2 + \frac{|Y|^2}{16}\left(93g'^2 + 135g^2\right) \\ &+ \frac{5}{2}\left(y_\mathrm{t}^2\left(\frac{17}{12}g'^2 + \frac{9}{4}g^2 + 8g_s^2\right) + \frac{3}{4}|Y|^2\left(\frac{1}{3}g'^2 + g^2\right)\right) + \frac{7}{48}g'^4 - \frac{9}{4}g^2g'^2 - \frac{23}{4}g^4\Bigg] + \mathcal{O}\left(\frac{m_h^2}{\Lambda_f^2}\right). \end{aligned} \tag{A.13}$$

The running of the Wilson coefficient C_6 at 1-loop order is determined by

$$\beta_{C_6} = \frac{C_6}{(4\pi)^2}\left[-\frac{9}{2}\left(3g^2 + g'^2\right) + 108\lambda + 18y_\mathrm{t}^2\right]. \tag{A.14}$$

Lastly, the running mass m_h^2 satisfies

$$\frac{\mathrm{d}m_h^2}{\mathrm{d}\ln\mu} = \frac{3m_h^2}{8\pi^2}\left[2\lambda + y_\mathrm{t}^2 - \frac{3}{4}g^2 - \frac{3}{20}g'^2 + \mathcal{O}\left(\frac{m_h^2}{\Lambda_f^2}\right)\right]. \tag{A.15}$$

Bibliography

[1] T. Steingasser, "On the domain of moduli fields," JHEP **05**, 153 (2020) doi:10.1007/JHEP05(2020)153 [arXiv:2001.09943 [hep-th]].

[2] J. Khoury and T. Steingasser, "Gauge hierarchy from electroweak vacuum metastability," Phys. Rev. D **105**, no.5, 055031 (2022) doi:10.1103/PhysRevD.105.055031 [arXiv:2108.09315 [hep-ph]].

[3] M. D. Schwartz, "Quantum Field Theory and the Standard Model," Cambridge University Press, 2014

[4] G. y. Huang and S. Zhou, "Precise Values of Running Quark and Lepton Masses in the Standard Model," Phys. Rev. D **103**, no.1, 016010 (2021) doi:10.1103/PhysRevD.103.016010 [arXiv:2009.04851 [hep-ph]].

[5] M. Sher, "Electroweak Higgs Potentials and Vacuum Stability," Phys. Rept. **179**, 273 (1989). doi:10.1016/0370-1573(89)90061-6

[6] D. Buttazzo, G. Degrassi, P. P. Giardino, G. F. Giudice, F. Sala, A. Salvio and A. Strumia, "Investigating the near-criticality of the Higgs boson," JHEP **1312**, 089 (2013) doi:10.1007/JHEP12(2013)089 [arXiv:1307.3536 [hep-ph]].

[7] A. Andreassen, W. Frost and M. D. Schwartz, "Scale Invariant Instantons and the Complete Lifetime of the Standard Model," Phys. Rev. D **97**, no. 5, 056006 (2018) [arXiv:1707.08124 [hep-ph]].

[8] N. Arkani-Hamed, S. Dimopoulos and G. R. Dvali, "The Hierarchy problem and new dimensions at a millimeter," Phys. Lett. B **429**, 263-272 (1998) doi:10.1016/S0370-2693(98)00466-3 [arXiv:hep-ph/9803315 [hep-ph]].

[9] C. P. Burgess, "Introduction to Effective Field Theory,", Cambridge University Press 2020 doi:10.1017/9781139048040

[10] A. Deur, S. J. Brodsky and G. F. de Teramond, "The QCD Running Coupling," Nucl. Phys. **90**, 1 (2016) doi:10.1016/j.ppnp.2016.04.003 [arXiv:1604.08082 [hep-ph]].

[11] S. Scherer and M. R. Schindler, "A Primer for Chiral Perturbation Theory," Lect. Notes Phys. **830**, pp.1-338 (2012) doi:10.1007/978-3-642-19254-8

[12] I. Zahed and G. E. Brown, "The Skyrme Model," Phys. Rept. **142**, 1-102 (1986) doi:10.1016/0370-1573(86)90142-0

[13] J. Schechter and H. Weigel, "The Skyrme model for baryons," [arXiv:hep-ph/9907554 [hep-ph]].

[14] M. Shaposhnikov, "A Possible symmetry of the nuMSM," Nucl. Phys. B **763**, 49-59 (2007) doi:10.1016/j.nuclphysb.2006.11.003 [arXiv:hep-ph/0605047 [hep-ph]].

[15] F. Bezrukov, M. Y. Kalmykov, B. A. Kniehl and M. Shaposhnikov, "Higgs Boson Mass and New Physics," JHEP **10**, 140 (2012) doi:10.1007/JHEP10(2012)140 [arXiv:1205.2893 [hep-ph]].

[16] T. Asaka and M. Shaposhnikov, "The νMSM, dark matter and baryon asymmetry of the universe," Phys. Lett. B **620**, 17-26 (2005) [arXiv:hep-ph/0505013 [hep-ph]].

[17] T. Asaka, S. Blanchet and M. Shaposhnikov, "The nuMSM, dark matter and neutrino masses," Phys. Lett. B **631**, 151-156 (2005) doi:10.1016/j.physletb.2005.09.070 [arXiv:hep-ph/0503065 [hep-ph]].

[18] M. Shaposhnikov, "The nuMSM, leptonic asymmetries, and properties of singlet fermions," JHEP **08**, 008 (2008) doi:10.1088/1126-6708/2008/08/008 [arXiv:0804.4542 [hep-ph]].

[19] L. Canetti, M. Drewes, T. Frossard and M. Shaposhnikov, "Dark Matter, Baryogenesis and Neutrino Oscillations from Right Handed Neutrinos," Phys. Rev. D **87**, 093006 (2013) doi:10.1103/PhysRevD.87.093006 [arXiv:1208.4607 [hep-ph]].

[20] J. Ghiglieri and M. Laine, "Sterile neutrino dark matter via coinciding resonances," JCAP **07**, 012 (2020) doi:10.1088/1475-7516/2020/07/012 [arXiv:2004.10766 [hep-ph]].

[21] G. Cacciapaglia and F. Sannino, "Fundamental Composite (Goldstone) Higgs Dynamics," JHEP **04**, 111 (2014) doi:10.1007/JHEP04(2014)111 [arXiv:1402.0233 [hep-ph]].

[22] G. Cacciapaglia, C. Pica and F. Sannino, "Fundamental Composite Dynamics: A Review," Phys. Rept. **877**, 1-70 (2020) doi:10.1016/j.physrep.2020.07.002 [arXiv:2002.04914 [hep-ph]].

[23] D. Buarque Franzosi, G. Cacciapaglia and A. Deandrea, "Sigma-assisted low scale composite Goldstone–Higgs," Eur. Phys. J. C **80**, no.1, 28 (2020) doi:10.1140/epjc/s10052-019-7572-z [arXiv:1809.09146 [hep-ph]].

[24] G. F. Giudice, "The Dawn of the Post-Naturalness Era," doi:10.1142/9789813238053_0013 [arXiv:1710.07663 [physics.hist-ph]].

[25] I. M. Bloch, C. Csáki, M. Geller and T. Volansky, "Crunching away the cosmological constant problem: dynamical selection of a small Λ," JHEP **12**, 191 (2020) doi:10.1007/JHEP12(2020)191 [arXiv:1912.08840 [hep-ph]].

[26] G. F. Giudice, M. McCullough and T. You, "Self-organised localisation," JHEP **10**, 093 (2021) doi:10.1007/JHEP10(2021)093 [arXiv:2105.08617 [hep-ph]].

[27] J. Khoury and O. Parrikar, "Search Optimization, Funnel Topography, and Dynamical Criticality on the String Landscape," JCAP **12**, 014 (2019) doi:10.1088/1475-7516/2019/12/014 [arXiv:1907.07693 [hep-th]].

[28] J. Khoury, "Accessibility Measure for Eternal Inflation: Dynamical Criticality and Higgs Metastability," JCAP **06**, 009 (2021) doi:10.1088/1475-7516/2021/06/009 [arXiv:1912.06706 [hep-th]].

[29] G. Kartvelishvili, J. Khoury and A. Sharma, "The Self-Organized Critical Multiverse," JCAP **02**, 028 (2021) doi:10.1088/1475-7516/2021/02/028 [arXiv:2003.12594 [hep-th]].

[30] J. Khoury and S. S. C. Wong, "Early-Time Measure in Eternal Inflation," [arXiv:2106.12590 [hep-th]].

[31] P. J. Steinhardt, "Natural inflation," Contribution to the "Nuffield Workshop on the Very Early Universe", p. 251, UPR-0198T.

[32] A. Vilenkin, "The Birth of Inflationary Universes," Phys. Rev. D **27**, 2848 (1983). doi:10.1103/PhysRevD.27.2848

[33] A. D. Linde, "Eternal chaotic inflation," Mod. Phys. Lett. A **1**, 81 (1986). doi:10.1142/S0217732386000129

[34] A. D. Linde, "Eternally Existing Selfreproducing Chaotic Inflationary Universe," Phys. Lett. B **175**, 395-400 (1986). doi:10.1016/0370-2693(86)90611-8

[35] A. A. Starobinsky, "Stochastic de Sitter (inflationary) stage in the early universe," Lect. Notes Phys. **246**, 107-126 (1986). doi:10.1007/3-540-16452-9_6

[36] S. Weinberg, "Anthropic Bound on the Cosmological Constant," Phys. Rev. Lett. **59**, 2607 (1987) doi:10.1103/PhysRevLett.59.2607

[37] V. Agrawal, S. M. Barr, J. F. Donoghue and D. Seckel, "Viable range of the mass scale of the standard model," Phys. Rev. D **57**, 5480-5492 (1998) doi:10.1103/PhysRevD.57.5480 [arXiv:hep-ph/9707380 [hep-ph]].

[38] J. Garriga, D. Schwartz-Perlov, A. Vilenkin and S. Winitzki, "Probabilities in the inflationary multiverse," JCAP **0601**, 017 (2006) doi:10.1088/1475-7516/2006/01/017 [hep-th/0509184].

[39] F. Denef, M. R. Douglas, B. Greene and C. Zukowski, "Computational complexity of the landscape II - Cosmological considerations," Annals Phys. **392**, 93 (2018) [arXiv:1706.06430 [hep-th]].

[40] G. Dvali, "S-Matrix and Anomaly of de Sitter," Symmetry **13**, no.1, 3 (2020) doi:10.3390/sym13010003 [arXiv:2012.02133 [hep-th]].

[41] M. Geller, Y. Hochberg and E. Kuflik, "Inflating to the Weak Scale," Phys. Rev. Lett. **122**, no.19, 191802 (2019) doi:10.1103/PhysRevLett.122.191802 [arXiv:1809.07338 [hep-ph]].

[42] R. Jackiw, *Quantum meaning of classical field theory*, *Review of Modern Physics* **49** (1977), 681

[43] R. Rajaraman. *Solitons and Instantons: An Introduction to Solitons and Instantons in Quantum Field Theory*. North-Holland (1982).

[44] M. Shifman. *Advanced topics in Quantum Field Theory*. Cambridge University Press (2012).

[45] N. Manton, P. Sutcliffe. *Topological Solitons*. Cambridge monographs on mathematical physics (2004).

[46] J. Goldstone, R. Jackiw, *Quantization of nonlinear waves*, *Physical Review D* **11** (1975), 1486

[47] G. S. Adkins, C. R. Nappi, E. Witten, *Static Properties of Nucleons in the Skyrme Model*, *Nuclear Physics B* **228** (1983), 552

[48] J. Schechter, H. Weigel, *The Skyrme Model for Baryons*. (1999) [arXiv:hep-ph/9907554v1]

[49] A. Jevicki, *Treatment of zero-frequency modes in perturbation expansion about classical field configuratios*, *Nuclear Physics B* **117** (1976), 365

[50] R. F. Dashen, E. Hasslacher, A. Neveu, *Physical Review D* **10**, 4114 (1974)

[51] J.L. Gervais, A. Jevicki, B. Sakita, *Phys. Rev. D* **12**, 1038 (1975)

[52] J.L. Gervais, A. Jevicki, B. Sakita, *Phys. Rep* **23**, 281 (1976)

[53] M. Creutz, *Quantum mechanics of extended objects in relativistic field theory*, *Physical Review D* **12** (1975), 3126

[54] J. Baacke, H. J. Rothe, *On the Quantization of Moving Extended Objects in One Space Dimension*, *Nuclear Physics B* **118** (1977), 371

[55] N. D. Lambert and P. C. West, New J. Phys. **4**, 7 (2002) doi:10.1088/1367-2630/4/1/307 [arXiv:hep-th/0012121 [hep-th]].

[56] I. Low, A. V. Manohar, *Spontaneously Broken Spacetime Symmetries and Goldstone's Theorem*, *Physics Review Letters* **88** (2002), 101602 [hep-th/0110285]

[57] H.Watanabe, H.Murayama, *The effective Lagrangian for nonrelativistic systems*, *Physics Review X* **3** (2014), 031057 [hep-th/1402.7066]

[58] H.Watanabe, H.Murayama, *Phys. Rev. Lett.* **110** (2013), 181601, [cond-mat.other/1302.4800]

[59] I. Kharuk, A. Shkerin, *Solving puzzles of spontaneously broken spacetime symmetries*, *Phys. Rev. D* **98** (2018), 125016

[60] H. B. Nielsen, S. Chadha, *On How to Count Goldstone Bosons*, *Nuclear Physics B* **105** (1976), 445

[61] N. D. Lambert, P. C. West, *Goldstone-soliton interactions and brane world neutrinos*, *New Journal of Physics* **4**, (2002) [hep-th/0012121]

[62] E. Mottola, "Zero modes of the 't Hooft-Polyakov monopole," Phys. Lett. B **79**, 242 (1978) [erratum: Phys. Lett. B **80**, 433 (1979)] doi:10.1016/0370-2693(79)91212-7

[63] G. S. Adkins, C. R. Nappi and E. Witten, Nucl. Phys. B **228**, 552 (1983) doi:10.1016/0550-3213(83)90559-X

[64] J. L. Gervais, A. Jevicki and B. Sakita, Phys. Rev. D **12**, 1038 (1975) doi:10.1103/PhysRevD.12.1038

[65] J. L. Gervais, A. Jevicki and B. Sakita, Phys. Rept. **23**, 281-293 (1976) doi:10.1016/0370-1573(76)90049-1

[66] G. Dvali, M. Shifman, *Tilting the Brane, or Some Cosmological Consequences of the Brane Universe*, *Phys.Rept.* **320**, (1999) [hep-th/9904021v1]

[67] H. B. Nielsen, P. Olesen, *Vortex-line models for dual strings. Nuclear Physics B*, **61** (1973)

[68] A. J. Hanson, T. Regge, C. Teitelboim. *Constrained Hamiltonian Systems.* Academia Nazionale Dei Lincei (1976)

[69] G. Scharf Finite Quantum Electrodynamics: The Causal Approach, Third Edition Dover Books on Physics (2014)

[70] A. Andreassen, D. Farhi, W. Frost and M. D. Schwartz, "Direct Approach to Quantum Tunneling," Phys. Rev. Lett. **117**, no.23, 231601 (2016) doi:10.1103/PhysRevLett.117.231601 [arXiv:1602.01102 [hep-th]].

[71] A. Andreassen, D. Farhi, W. Frost and M. D. Schwartz, "Precision decay rate calculations in quantum field theory," Phys. Rev. D **95**, no.8, 085011 (2017) doi:10.1103/PhysRevD.95.085011 [arXiv:1604.06090 [hep-th]].

[72] S. R. Coleman, V. Glaser and A. Martin, "Action Minima Among Solutions to a Class of Euclidean Scalar Field Equations," Commun. Math. Phys. **58**, 211-221 (1978) doi:10.1007/BF01609421

[73] J. R. Espinosa, "Vacuum Decay in the Standard Model: Analytical Results with Running and Gravity," JCAP **06**, 052 (2020) doi:10.1088/1475-7516/2020/06/052 [arXiv:2003.06219 [hep-ph]].

[74] G. Isidori, V. S. Rychkov, A. Strumia and N. Tetradis, "Gravitational corrections to standard model vacuum decay," Phys. Rev. D **77**, 025034 (2008) doi:10.1103/PhysRevD.77.025034 [arXiv:0712.0242 [hep-ph]].

[75] A. Salvio, A. Strumia, N. Tetradis and A. Urbano, "On gravitational and thermal corrections to vacuum decay," JHEP **09**, 054 (2016) doi:10.1007/JHEP09(2016)054 [arXiv:1608.02555 [hep-ph]].

[76] A. Celis, J. Fuentes-Martin, A. Vicente and J. Virto, "DsixTools: The Standard Model Effective Field Theory Toolkit," Eur. Phys. J. C **77**, no.6, 405 (2017) doi:10.1140/epjc/s10052-017-4967-6 [arXiv:1704.04504 [hep-ph]].

[77] S. Chigusa, T. Moroi and Y. Shoji, "Decay Rate of Electroweak Vacuum in the Standard Model and Beyond," Phys. Rev. D **97**, no.11, 116012 (2018) doi:10.1103/PhysRevD.97.116012 [arXiv:1803.03902 [hep-ph]].

[78] I. Garg, S. Goswami, K. N. Vishnudath and N. Khan, "Electroweak vacuum stability in presence of singlet scalar dark matter in TeV scale seesaw models," Phys. Rev. D **96**, no.5, 055020 (2017) doi:10.1103/PhysRevD.96.055020 [arXiv:1706.08851 [hep-ph]].

[79] S. Khan, S. Goswami and S. Roy, "Vacuum Stability constraints on the minimal singlet TeV Seesaw Model," Phys. Rev. D **89**, no.7, 073021 (2014) doi:10.1103/PhysRevD.89.073021 [arXiv:1212.3694 [hep-ph]].

[80] L. Delle Rose, C. Marzo and A. Urbano, "On the stability of the electroweak vacuum in the presence of low-scale seesaw models," JHEP **12**, 050 (2015) doi:10.1007/JHEP12(2015)050 [arXiv:1506.03360 [hep-ph]].

[81] S. Mandal, R. Srivastava and J. W. F. Valle, "Consistency of the dynamical high-scale type-I seesaw mechanism," Phys. Rev. D **101**, no.11, 115030 (2020) doi:10.1103/PhysRevD.101.115030 [arXiv:1903.03631 [hep-ph]].

[82] Y. F. Pirogov and O. V. Zenin, "Two loop renormalization group restrictions on the standard model and the fourth chiral family," Eur. Phys. J. C **10**, 629-638 (1999) doi:10.1007/s100520050602 [arXiv:hep-ph/9808396 [hep-ph]].

[83] S. Antusch, J. Kersten, M. Lindner and M. Ratz, "Neutrino mass matrix running for nondegenerate seesaw scales," Phys. Lett. B **538**, 87-95 (2002) doi:10.1016/S0370-2693(02)01960-3 [arXiv:hep-ph/0203233 [hep-ph]].

[84] S. Antusch, J. Kersten, M. Lindner, M. Ratz and M. A. Schmidt, "Running neutrino mass parameters in see-saw scenarios," JHEP **03**, 024 (2005) [arXiv:hep-ph/0501272 [hep-ph]].

[85] A. Andreassen, W. Frost and M. D. Schwartz, "Consistent Use of the Standard Model Effective Potential," Phys. Rev. Lett. **113**, no. 24, 241801 (2014) [arXiv:1408.0292 [hep-ph]].

[86] A. Rajantie and S. Stopyra, "Standard Model vacuum decay with gravity," Phys. Rev. D **95**, no.2, 025008 (2017) [arXiv:1606.00849 [hep-th]].

[87] J. A. Casas, V. Di Clemente, A. Ibarra and M. Quiros, "Massive neutrinos and the Higgs mass window," Phys. Rev. D **62**, 053005 (2000) doi:10.1103/PhysRevD.62.053005 [arXiv:hep-ph/9904295 [hep-ph]].

[88] P. Agrawal, M. Bauer, J. Beacham, A. Berlin, A. Boyarsky, S. Cebrian, X. Cid-Vidal, D. d'Enterria, A. De Roeck and M. Drewes, *et al.* "Feebly-Interacting Particles:FIPs 2020 Workshop Report," [arXiv:2102.12143 [hep-ph]].

[89] M. Chrzaszcz, M. Drewes, T. E. Gonzalo, J. Harz, S. Krishnamurthy and C. Weniger, "A frequentist analysis of three right-handed neutrinos with GAMBIT," Eur. Phys. J. C **80**, no.6, 569 (2020) doi:10.1140/epjc/s10052-020-8073-9 [arXiv:1908.02302 [hep-ph]].

[90] S. Samuel, "The Standard model in its other phase," Nucl. Phys. B **597**, 70-88 (2001) doi:10.1016/S0550-3213(00)00741-0 [arXiv:hep-ph/9910559 [hep-ph]].

[91] N. Arkani-Hamed, S. Dimopoulos and S. Kachru, "Predictive landscapes and new physics at a TeV," [arXiv:hep-th/0501082 [hep-th]].

[92] J. Kubo, K. S. Lim and M. Lindner, "Electroweak Symmetry Breaking via QCD," Phys. Rev. Lett. **113**, 091604 (2014) doi:10.1103/PhysRevLett.113.091604 [arXiv:1403.4262 [hep-ph]].

Danksagung

I owe special gratitude to Justin Khoury for guiding me to my current field of research, and without whose support, interest and encouragement my intellectual development would not have been the same. The same holds true for Dieter Lüst, who I could consistently rely on even years after being technically supervised by him. This includes, for both of them, invaluable support with my ongoing attempt to pursue an academic career.

If this attempt succeeds in the way I hope it will, it will also do so thanks to additional assistance by Ivo Sachs, Alan Guth and David Kaiser, who managed to have an enormous impact through small gestures of genuine kindness and support which helped me create a way forward.